

NANOPARTICLE-STABILIZED CO<sub>2</sub> FOAMS TO IMPROVE CONVENTIONAL  
CO<sub>2</sub> EOR PROCESS AT BATI RAMAN FIELD

A THESIS SUBMITTED TO  
THE GRADUATE SCHOOL OF NATURAL AND APPLIED SCIENCES  
OF  
MIDDLE EAST TECHNICAL UNIVERSITY

BY

SAIBE ESRA SAFRAN

IN PARTIAL FULFILLMENT OF THE REQUIREMENTS  
FOR  
THE DEGREE OF DOCTOR OF PHILOSOPHY  
IN  
PETROLEUM AND NATURAL GAS ENGINEERING

SEPTEMBER 2019



Approval of the thesis:

**NANOPARTICLE-STABILIZED CO2 FOAMS TO IMPROVE  
CONVENTIONAL CO2 EOR PROCESS AT BATI RAMAN FIELD**

submitted by **SAIBE ESRA SAFRAN** in partial fulfillment of the requirements for the degree of **Doctor of Philosophy in Petroleum and Natural Gas Engineering Department, Middle East Technical University** by,

Prof. Dr. Halil Kalıpçılar  
Dean, Graduate School of **Natural and Applied Sciences**

\_\_\_\_\_

Assoc. Prof. Dr. Çağlar Sınayuç  
Head of Department, **Petroleum and Natural Gas Eng.**

\_\_\_\_\_

Prof. Dr. Mustafa Verşan Kök  
Supervisor, **Petroleum and Natural Gas Eng., METU**

\_\_\_\_\_

**Examining Committee Members:**

Assoc. Prof. Dr. Çağlar Sınayuç  
Petroleum and Natural Gas Eng., METU

\_\_\_\_\_

Prof. Dr. Mustafa Verşan Kök  
Petroleum and Natural Gas Eng., METU

\_\_\_\_\_

Prof. Dr. Mahmut Parlaktuna  
Petroleum and Natural Gas Eng., METU

\_\_\_\_\_

Assoc. Prof. Dr. Gürşat Altun  
Petroleum and Natural Gas Eng., ITU

\_\_\_\_\_

Assoc. Prof. Dr. Emre Artun  
Petroleum and Natural Gas Eng., METU NCC

\_\_\_\_\_

Date: 04.09.2019

**I hereby declare that all information in this document has been obtained and presented in accordance with academic rules and ethical conduct. I also declare that, as required by these rules and conduct, I have fully cited and referenced all material and results that are not original to this work.**

Name, Surname: Saibe Esra Safran

Signature:

## **ABSTRACT**

### **NANOPARTICLE-STABILIZED CO<sub>2</sub> FOAMS TO IMPROVE CONVENTIONAL CO<sub>2</sub> EOR PROCESS AT BATI RAMAN FIELD**

Safran, Saibe Esra  
Doctor of Philosophy, Petroleum and Natural Gas Engineering  
Supervisor: Prof. Dr. Mustafa Verşan K k

September 2019, 111 pages

Because of the natural fractured characteristic of the B. Raman field which is the largest field of Turkey, already existing CO<sub>2</sub> injection system does not work at desired efficiency. Thus, the main purpose of this project is to control CO<sub>2</sub> mobility in the reservoir by creating nanoparticle stabilized CO<sub>2</sub> foam using the property of nanoparticles to place at the gas-water interface permanently and to achieve additional oil recovery at B. Raman.

For this purpose, first nanoparticle dispersion stabilization and foamability were evaluated. Dealing with the nanoparticle due to their high surface energy is not easy as bulk material. They have high tendency to agglomerate and/or flocculate. Different type of nanosilica was considered. Effect of the nanoparticle concentration, salinity, temperature and pH on the foamability and dispersion stabilization were examined. This studies showed that half hydrophobicity, salt addition and increased concentration have positive effect on the foamability but salinity above 1% generated flocculation. Also, even if the 50 % hydrophobic nanosilica called H30 has better foamability, it could not be stabilized. The particle size of the silica in H30 dispersion was not small enough to flow through the B. Raman core sample. The effect of the

pressure, phase ratio and flow rate on the foam formation were also studied. Better foam was observed at the observation cell when CO<sub>2</sub>: nanodispersion phase ratio was 1. Also, it was found that the pressure should be above 1100 psi where CO<sub>2</sub> was in the supercritical phase to create foam with current core flooding system. The phase envelop of the Dodan gas was created by using PVTsim program. XRF test results before and after flooding showed that not any adsorption occurred into core sample. Then, the oil recovery test was conducted with suitable nanoparticles which were PEG and CC301. First, CO<sub>2</sub> injection and then WAG were applied to the core sample to express B. Raman field case and obtained extra production after CO<sub>2</sub> injection with WAG application. NWAG (nanoparticle dispersion alternating gas) at 650 psi and foam at 1200 psi was tested, later. The results indicated that foam application was successful if appropriate conditions existed. On the other hand, not a significant production was obtained with NWAG application. Interfacial measurements were also studied between both nanodispersion-CO<sub>2</sub> and nanodispersion-oil. Nanoparticles were not changing IFT markedly even if they were located at the interface of the water and CO<sub>2</sub> as the surfactant. However, a significant decrease of the IFT was obtained between water and oil in the presence of nanoparticles

Keywords: Nanoparticle, Foam, CO<sub>2</sub> injection, Oil recovery, Batı Raman, EOR

## ÖZ

### **BATI RAMAN SAHASINDAKİ CO<sub>2</sub> EOR PROSESİNİ NANOPARÇACIK İLE STABİL EDİLMİŞ CO<sub>2</sub> KÖPÜĞÜ KULLANARAK İYİLEŞTİRME**

Safran, Saibe Esra  
Doktora, Petrol ve Doğal Gaz Mühendisliği  
Tez Danışmanı: Prof. Dr. Mustafa Verşan Kök

Eylül 2019, 111 sayfa

Türkiye'nin en büyük petrol sahası olan B.Raman'ın doğal çatlaklı yapısından kaynaklı, halihazırda var olan CO<sub>2</sub> enjeksiyon sistemi istenilen verimde çalışmamaktadır. Bu sebeple, çalışmanın amacı, nanoparçacıkların gaz-su arayüzeyine kalıcı tutunabilmeleri özelliklerini kullanarak, nanoparçacık ile stabil edilmiş CO<sub>2</sub> köpüğü ile CO<sub>2</sub>'in mobilitesini kontrol etmek ve B. Raman'da ilave petrol kurtarımı sağlamaktır.

Bu amaçla, öncelikle, nanoparçacık dispersiyonunun stabilitesi ve köpük yapma yetisi değerlendirilmiştir. Farklı yapıda nanoparçacık ile çalışılmıştır. Köpük yapma yetisi ve dispersiyon stabilizasyonu üzerine nanoparçacık konsantrasyonunun, tuzluluğun, sıcaklığın ve pH'nın etkisi incelenmiştir. Bu çalışma, yarı hidrofobik özelliğin, tuz eklemesinin ve konsantrasyon artışının köpüklenme üzerine pozitif etki ettiğini göstermiştir. Ayrıca, H30 olarak adlandırılan ve %50 hidrofobik özelliğe sahip nanosilikanın en iyi köpük yaptığı tespit edilmesine karşın dispersiyonu stabil hale getirilememiştir. H30 içeren dispersiyonda silikanın parçacık boyutu B.Raman karotu içinde akabilecek kadar küçük değildir. Basınç, faz oranı ve toplam akış hızının köpük oluşumu üzerine etkileri de çalışılmıştır. CO<sub>2</sub>:nanodispersiyon faz oranınının 1 olduğu noktada en iyi köpük elde edilmiştir. Ayrıca, mevcut karot öteleme sisteminde köpük

oluřturabilmek için basıncın karbondioksitin superkritik fazda olduđu 1100 psi'ın üzerinde olması gerektiđi görülmüřtür. Dodan gazının faz diagramı PVTsim programı kullanılarak oluřturulmuřtur. Öteleme öncesi ve sonrasında XRF cihazı ile dispersiyonda silika konsantrasyonu test edilmiř ve karot içerisinde bir adsorbsiyonun olmadığı sonucuna varılmıřtır. Sonrasında, uygun olan PEG ve CC301 dispersiyonları ile petrol kurtarım testleri yapılmıřtır. Köpük enjeksiyonu öncesi, B. Raman saha kořullarını en iyi řekilde yaratabilmek için önce CO<sub>2</sub> sonra WAG uygulaması yapılmıřtır ve WAG uygulaması ile CO<sub>2</sub> enjeksiyonu sonrasında ilave petrol üretimi elde edilmiřtir. Son olarak 650 psi'da NWAG(nanoparçacık dispersiyonu ve gazın ardıřık basımı) ve 1200 psi da köpük uygulanmıřtır. Sonuçlar, eđer uygun ortam mevcut ise köpük uygulamasının başarılı olduđunu göstermiřtir. Diđer taraftan, NWAG uygulaması ile belirgin bir üretim yapılamamıřtır. Nanodispersiyon-CO<sub>2</sub> ve nanodispersiyon - petrol arasındaki ara yüzey gerilimleri de ölçülmüřtür. Nanoparçacıklar, su – gaz ara yüzeyine tutunmalarına karřın, sürfaktantlar gibi IFT deđerlerinde önemli bir düşüře neden olmamıřlardır. Buna karřın, nanoparçacık varlıđında, su – petrol ara yüzey geriliminde düşüř elde edilmiřtir.

Anahtar Kelimeler: Nanoparçacık, Köpük, CO<sub>2</sub> enjeksiyonu, Petrol kurtarımı, Batı Raman, Geliřtirilmiř petrol kurtarımı

To my lovely daughter, Eliz

## ACKNOWLEDGEMENTS

This study financed by Turkish Petroleum Corporation.

I would first like to show my sincere gratitude to my thesis advisor Dr. Mustafa Verşan KÖK for the continuous support and sharing expertise. He steered me in the right direction whenever he thought I needed it during this study.

Besides my advisor, I would like to thank the rest of my thesis committee, Dr. Mahmut PARLAKTUNA and Dr. Gürşat ALTUN for their insightful comments and guidance.

I would also express my warm thanks to the whole member of the Reservoir Technology Department of the Turkish Petroleum Corporation R&D Center especially to Uğur KARABAKAL and Can ERCAN. During my research, they were always with me and shared their pearls of wisdom.

Moreover, I am thankful to Mustafa OYMAEL and İrem Yaşar BAYRAM for their supports during experimental studies.

I must also express my very profound gratitude to my family: my husband, my little angel and my friends for the unceasing encouragement and spiritual support.

Finally, many thanks to one and all, who directly or indirectly, have lent their hand in this study.

## TABLE OF CONTENTS

ABSTRACT .....	v
ÖZ .....	vii
ACKNOWLEDGEMENTS .....	x
TABLE OF CONTENTS .....	xi
LIST OF TABLES .....	xv
LIST OF FIGURES .....	xvi
LIST OF ABBREVIATIONS .....	xix
LIST OF SYMBOLS .....	xxi
CHAPTERS	
1. INTRODUCTION .....	1
2. LITERATURE REVIEW .....	3
2.1. CARBON DIOXIDE ENHANCED OIL RECOVERY .....	3
2.1.1. History of CO <sub>2</sub> EOR .....	4
2.1.2. Properties of CO <sub>2</sub> .....	4
2.1.3. Mechanism .....	5
2.1.3.1. Oil swelling and viscosity reduction in oil .....	5
2.1.3.2. Reduction of the interfacial tension between oil and water .....	6
2.1.3.3. Solution gas drive .....	6
2.1.3.4. Extraction and vaporization of the light oil component .....	6
2.1.3.5. Effect of the weak acid .....	6
2.1.4. Techniques of CO <sub>2</sub> Injection Process .....	6
2.1.4.1. Continuous Miscible and Immiscible CO <sub>2</sub> Flooding .....	7

2.1.4.2. Cyclic CO <sub>2</sub> Flooding.....	8
2.1.4.3. Water Alternating Gas (WAG).....	8
2.1.4.4. CO <sub>2</sub> Foam .....	10
2.1.5. Worldwide CO <sub>2</sub> Flood Projects .....	10
2.2. FOAM .....	11
2.2.1. Surfactant Stabilized CO <sub>2</sub> Foam.....	13
2.2.2. Particle Stabilized CO <sub>2</sub> Foam in Oil and Gas Industry .....	14
2.3. BATH RAMAN FIELD .....	19
3. STATEMENT OF THE PROBLEM .....	23
4. MATERIALS AND METHODS .....	25
4.1. MATERIALS.....	25
4.1.1. Nanoparticles.....	25
4.1.2. Reservoir Fluids .....	26
4.1.3. Core Samples.....	27
4.2. EXPERIMENTAL SETUP AND PROCEDURE .....	27
4.2.1. Rock Samples Preparation and Routine Core Analysis .....	27
4.2.2. Zetasizer .....	29
4.2.3. Core Flood System .....	29
4.2.4. Interfacial Tension (IFT) .....	30
4.2.5. X-Ray Fluorescence Spectroscopy (XRF).....	32
4.2.6. Scanning Electron Microscope/ Energy Dispersive Spectrometry (SEM/EDS) .....	32
5. RESULTS AND DISCUSSION .....	35

5.1. NANOSILICA DISPERSION STABILIZATION, FOAMABILITY AND PARAMETERS EFFECT .....	35
5.1.1. Stabilization and Foamability .....	35
5.1.2. Effect of the Salinity .....	38
5.1.3. Effect of the Concentration.....	38
5.1.4. Effect of the Temperature .....	39
5.1.5. Effect of the pH.....	39
5.2. NANOSILICA DISPERSION STABILIZATION, FOAMABILITY AND PARAMETERS EFFECT .....	44
5.3. PVT SIMULATION.....	47
5.4. FOAM GENERATION FLOOD TEST .....	49
5.5. OIL RECOVERY .....	61
5.5.1. Oil Recovery with CC301 Dispersion .....	61
5.5.2. Oil Recovery with PEG Dispersion .....	64
5.6. IFT MEASUREMENT.....	70
5.6.1. IFT between Nanodispersion-CO <sub>2</sub> .....	70
5.6.2. IFT between Nanodispersion-Oil.....	72
6. CONCLUSION AND RECOMMENDATION.....	73
REFERENCES.....	77
A. Nanoparticle Data Sheet .....	91
B. Test Report of the B.Raman Formation Water and Dodan Gas .....	97
C. Test Report of Nanoparticle Size Distribution .....	99
D. Test Report of the XRF.....	105
E. Oil Recovery Test Results .....	106

CURRICULUM VITAE..... 111

## LIST OF TABLES

### TABLES

Table 2.1. Number of the worldwide CO <sub>2</sub> EOR applications (Koottungal, 2012) ....	10
Table 2.2. Examples of foam in the oil and gas Industry (Shramm, 1994) .....	15
Table 4.1. Selected nanoparticles and their properties.....	25
Table 4.2. Test results of B. Raman formation water .....	26
Table 4.3. Test results of B. Raman oil.....	27
Table 4.4. Test results of Dodan gas .....	27
Table 4.5. Experimental conditions of IFT .....	31
Table 4.6. SEM/EDS experimental conditions .....	33
Table 5.1. Prepared dispersions for early foam test .....	35
Table 5.2. Particle size distribution of the dispersions.....	37
Table 5.3. Particle size distribution analysis results before and after pH adjustment	43
Table 5.4. Properties of B.Raman field core sample.....	44
Table 5.5. Properties of the core sample .....	45
Table 5.6. Results of the XRF analysis .....	45
Table 5.7. Particle size distribution analysis results before and after pH adjustment	58
Table 5.8. The properties and the picture of the core sample .....	61
Table 5.9. Oil recoveries of each step for all experiments.....	66
Table 5.10. IFT between gas-liquid .....	70
Table 5.11. IFT between liquid-oil .....	72

## LIST OF FIGURES

### FIGURES

Figure 2.1. Phase diagram of CO <sub>2</sub> (Picha, 2007) .....	5
Figure 2.2. The process of miscible CO <sub>2</sub> EOR process (Verma, 2015).....	8
Figure 2.3. Illustration of a foam structure (Schramm, 1994).....	12
Figure 2.4. The shape of bubbles related to formation methods (Weaire, 1999) .....	13
Figure 2.5. Foam flow through pores (Talebian, 2014).....	14
Figure 2.6. Estimated B. Raman field borders.....	19
Figure 2.7. Contour map of the B. Raman field .....	20
Figure 2.8. Flow diagram of the CO <sub>2</sub> injection system.....	21
Figure 2.9. B. Raman production history .....	22
Figure 4.1. Porosimeter and permeameter test system .....	28
Figure 4.2. Core flood test system .....	30
Figure 4.3. IFT test system .....	31
Figure 4.4. XRF spectroscopy .....	32
Figure 4.5. SEM/EDS system.....	33
Figure 5.1. Dispersion A) before B) after the early foamability test.....	36
Figure 5.2. Foams after 16 hours of the early foam test .....	37
Figure 5.3. The effect of the NaCl concentration on the foam generated by 1% H30 dispersion A) before B) after C) 1 hour later.....	38
Figure 5.4. The effect of the NaCl concentration on the foam generated by 0.5% H30 dispersion A) before B) after .....	39
Figure 5.5. Dispersion stabilization A) at 25 °C B) two days after at 25 °C) at 65 °C D) 2 days after at 65 °C .....	40
Figure 5.6. H30 dispersion after 2 days at 65 °C.....	40
Figure 5.7. Zeta potential during acid titration .....	41
Figure 5.8. Zeta potential during base titration.....	41

Figure 5.9. B. Raman pore throat size distribution (Karabakal, 2008) .....	42
Figure 5.10. The effect of the pH on the foam generated by 1 % H30 dispersion A) before B) after .....	43
Figure 5.11. Pressure differences during dispersion flooding.....	46
Figure 5.12. Phase diagram of the Dodan gas.....	48
Figure 5.13. Phase diagram of the pure CO <sub>2</sub> .....	48
Figure 5.14. Flow diagram of the core flooding system for foam generation test.....	49
Figure 5.15. Pressure differences during simultaneous injection of the formation water and CO <sub>2</sub> at 650 psi 65 °C .....	50
Figure 5.16. Pressure differences during simultaneous injection of the formation water and CO <sub>2</sub> at 1200 psi 65 °C .....	51
Figure 5.17. Pressure differences during simultaneous injection of the PEG and CO <sub>2</sub> at 650 psi 65 °C.....	54
Figure 5.18. Pressure differences during simultaneous injection of the PEG and CO <sub>2</sub> at 1200 psi 65 °C.....	55
Figure 5.19. Pressure differences during simultaneous injection of the CC301 and CO <sub>2</sub> at 1200 psi 65 °C .....	56
Figure 5.20. Pressure differences during simultaneous injection of the H30 and CO <sub>2</sub> at 1200 psi 65 °C.....	57
Figure 5.21. Sapphire observation cell image A) during the simultaneous injection of CO <sub>2</sub> and formation water B) during the simultaneous injection of CO <sub>2</sub> and CC301 dispersion .....	59
Figure 5.22. Foam image A) during the simultaneous injection of CO <sub>2</sub> and H30 B) when covered the observation cell C) when foam go out the system to the atmospheric condition.....	59
Figure 5.23. Results of the SEM/EDS A) picture of the silica particles B) chemical analysis.....	60
Figure 5.24. Flow diagram of the core flooding system for oil recovery test.....	62
Figure 5.25. The image of the production after centrifuge which was obtained when foam was applied.....	64

Figure 5.26. Oil recoveries in each step of the CC301 experiment.....	67
Figure 5.27. Oil recoveries in each step of the PEG experiment.....	68
Figure 5.28. Oil recoveries in total recovery for both CC301 and PEG experiment.	69
Figure 5.29. Temperature effect on the IFT .....	71
Figure 5.30. Nanosilica effect on IFT .....	71

## LIST OF ABBREVIATIONS

### ABBREVIATIONS

AERO	: 100 % hydrophobic nanosilica dispersion
B.Raman	: Batı Raman
CC301	: 100 % hydrophilic nanosilica dispersion
CO <sub>2</sub>	: carbon dioxide
EOR	: enhanced oil recovery
H30	: 50 % hydrophobic nanosilica in powder form
HP	: high pressure
HSE	: health and safety
HT	: high temperature
IFT	: interfacial tension
IOR	: improved oil recovery
MERLAB	: Middle East Technical University Central Laboratory
MMP	: minimum miscibility pressure
N20	: 100 % Hydrophilic nanosilica in powder form
Nano	: nanoparticle
NaCl	: sodium chloride
NaOH	: sodium hydroxide
NWAG	: nanodispersion alternating gas
OOIP	: original oil in place
PECNP	: polyelectrolyte complex nanoparticles
PEG	: polyethylene glycol coated nanosilica dispersion
PV	: pore volume
PVTSim	: pressure volume temperature simulation program
Si	: silica
SWAG	: simultaneous water and gas
UNAM	: National Nanotechnology Research Center

USA : the United States of America  
WAG : water alternating gas  
XRF : x-ray florescence  
ENG : engineering

## LIST OF SYMBOLS

### SYMBOLS

$C_{\text{NaCl}}$	: NaCl concentration, % wt.
$C_{\text{nano}}$	: nanoparticle concentration, % wt.
$d$	: diameter, cm
$k$	: effective permeability of reservoir rock, darcy
$k_{\text{air}}$	: air permeability, millidarcy
$k_{\text{w}}$	: water permeability, millidarcy
$L$	: length, cm
$M$	: mobility ratio
$N_{\text{ca}}$	: capillary number
$P$	: pressure, psi
$P_{\text{c}}$	: critical pressure, psi
$Q_{\text{total}}$	: total flow rate, cc/min
$R$	: particle radius, m
$T_{\text{c}}$	: critical temperature, °C
$V_{\text{p}}$	: pore volume, cc
$W_{\text{r}}$	: adsorption energy, kT

### GREEK SYMBOLS

$\Phi$	: porosity, %
$\rho_{\text{g}}$	: grain density, g/cc
$v$	: velocity, m/sec
$\mu$	: fluid viscosity, cP
$\sigma$	: interfacial tension, mN/m
$\theta$	: contact angle, °
$\gamma$	: surface tension, mN/m
$\Delta P$	: pressure difference



## CHAPTER 1

### INTRODUCTION

Batı Raman (B. Raman) is the biggest oil field of Turkey but it is not easy to produce oil from this field due to its nature. B. Raman has natural fractured carbonate reservoir with the low permeable matrix. Also, it has 12 API heavy oil and low pressure which is below 1000 psi (Issever, 1993). It is almost impossible to produce petroleum by originating from all these conditions, with the primary production method. As the Department of Energy and Natural Gas Resources of Turkey declared, above 90% of the oil still waiting to be produced (MAPEG, 2018). Therefore, many kind of improved oil recovery (IOR) and enhanced oil recovery (EOR) methods were tried in this field. Carbon dioxide (CO<sub>2</sub>) injection is one of these methods and more productive one. CO<sub>2</sub> injection is accepted by the whole world for oil production and is the most widely used method. However, due to its low density and viscosity, sweep efficiency cannot be effective especially if you have fractured reservoir (Verma, 2015). Because the fluids always choose the easiest way and early breakthrough occurs when high permeable zone exists. Therefore, mobility control of the CO<sub>2</sub> is crucial to increase oil production. In such a case, the increase of CO<sub>2</sub> density can be a solution. Scientists have studied on this subject for several years. The studied techniques to increase the density of the CO<sub>2</sub> also have some weakness, restriction or limitation for the reservoir.

Nanotechnology is an emerging technology of the last decades. Even if it has not been used effectively the oil and gas industry, for now, there has been a lot of progress in the last 10 years. One of areas that this technology can be used is the mobility control of the CO<sub>2</sub>. Nanoparticle can be used to create CO<sub>2</sub> foam which is denser than the gas form of CO<sub>2</sub>. This solid particles are at nanometer scale and has high surface energy. Because of this property, nanoparticles can adsorb at the interface of the water and gas

and can provide long term stabilization, even more, this adsorption can be permanent (Sheng, 2013). Then, this denser nanoparticle stabilized CO<sub>2</sub> foam can penetrate the matrix and contact with the more oil to sweep.

Increasing the productivity of the CO<sub>2</sub> injection system at B. Raman with nanoparticle stabilized CO<sub>2</sub> foam is the main goal of this study. For this purpose, first, the nanoparticle dispersion stabilization was studied, extensively. The parameters effect which were concentration, salinity, temperature and pH on the foam generation and dispersion stabilization were examined. Afterward, the system was checked if plugging due to solid particles occurs. Then, nanoparticle stabilized CO<sub>2</sub> foam was generated using core flooding system with appropriate nanosilica dispersions. Also, the effect of the pressure, flow rate and phase ratio were studied. Later, oil recovery test was evaluated to obtain extra oil production with the application of CO<sub>2</sub> injection, water alternating gas (WAG), nanodispersion alternating gas (NWAG) and foam applications. Interfacial tension (IFT) measurement between nanodispersion-CO<sub>2</sub> and nanodispersion-oil was also determined.

## CHAPTER 2

### LITERATURE REVIEW

#### 2.1. CARBON DIOXIDE ENHANCED OIL RECOVERY

According to the Department of Energy and Natural Gas Resources of Turkey, the amount of recoverable oil in Turkey is approx. 20% of the original oil in place (OOIP) (MAPEG, 2018). Also, two third of the worldwide oil is still waiting to be produced as the Department of Energy the United States of America (USA) declared (Tunio, 2011). Therefore, improved oil recovery (IOR) and enhanced oil recovery (EOR) methods applications were needed to produce more. IOR signifies any improvement of oil recoveries (Thomas, 2008). However, EOR is seen as a tertiary recovery process or in other word, an increase in oil recovery after primary or secondary recovery by improving mobility ratio and increasing capillary number. The capillary number is defined as the ratio of viscous to capillary forces.

$$N_{ca} = \frac{\text{Viscous Forces}}{\text{Capillary Forces}} = \frac{v\mu}{\sigma\cos\theta} \quad (2.1)$$

where  $v$  and  $\mu$ , are the velocity and viscosity. Also, the interfacial tension and the contact angle between the oil-water interfaces are defined as  $\sigma$  and  $\theta$ . Furthermore,  $M$  is the mobility ratio of the displacing fluid to the displaced fluid and  $k$  is the relative or effective permeability (Elwy, 2012).

$$M = \frac{(k/\mu)_{\text{displacing}}}{(k/\mu)_{\text{displaced}}} \quad (2.2)$$

Despite, technical and economic challenges hampers oil companies, EOR methods application has been enlarging since the researchers focus on this subject for long years. Approx. 3% of the worldwide produced oil obtains from EOR methods (Taber,

1997). CO<sub>2</sub> injection is a proven, potential and well-known EOR process and going to be detailed since it's the main title of this study.

### **2.1.1. History of CO<sub>2</sub> EOR**

Gas injection is one of the oldest methods used by engineers to improve oil recovery for more than 60 years. Usage of CO<sub>2</sub> as a method of EOR has been mentioned as early as 1916 in the literature, but it was dismissed as a laboratory curiosity. The first patent of CO<sub>2</sub> as injection gas for oil recovery was taken in 1952 by Whorton et al. (1952). Then, in 1964, the first pilot field test was performed at the Mead Strawn Field to figure out if CO<sub>2</sub> injection process increases oil production (Holm, 1971). After these improvements, the real commercial CO<sub>2</sub> injection project was started at the Kelly-Snyder Field in the United States (Langston, 1988). Since that day, its usage has increased significantly.

### **2.1.2. Properties of CO<sub>2</sub>**

The physical properties of carbon dioxide are crucial parameters to understand the CO<sub>2</sub> EOR process, exactly. At atmospheric temperature and pressure, CO<sub>2</sub> is a colorless, odorless, inert, and non-combustible gas and about 1.5 times heavier than air. The molecular weight of CO<sub>2</sub> is 44.01 g/mol and at 0 °C and 1.013 bar, its specific gravity, and density are 1.529 and 1.95 kg/m<sup>3</sup>, respectively. Figure 2.1 demonstrates the phase diagram of the CO<sub>2</sub> clearly (Picha, 2007).

It can be figured out from Figure 2.1, critical properties of CO<sub>2</sub> are;

Critical Temperature (T<sub>c</sub>): 31.05 °C

Critical Pressure (P<sub>c</sub>): 72.9 atm ≈ 73.9 bar ≈ 1071 psi

At above critical pressures and temperatures, CO<sub>2</sub> is in the supercritical state and behaves more like a liquid. It forms a phase in which density is close to that of a liquid and its viscosity stays low as 0.05 – 0.08 cp. This denser form of CO<sub>2</sub> can extract hydrocarbon components from oil more easily than gas form CO<sub>2</sub> (Jarrell, 2002). Even

though the low CO<sub>2</sub> viscosity is not beneficial to sweep efficiency, the oil viscosity is also going to decrease when CO<sub>2</sub> dissolved in oil, which in turn helps increase oil production. (Verma, 2015).

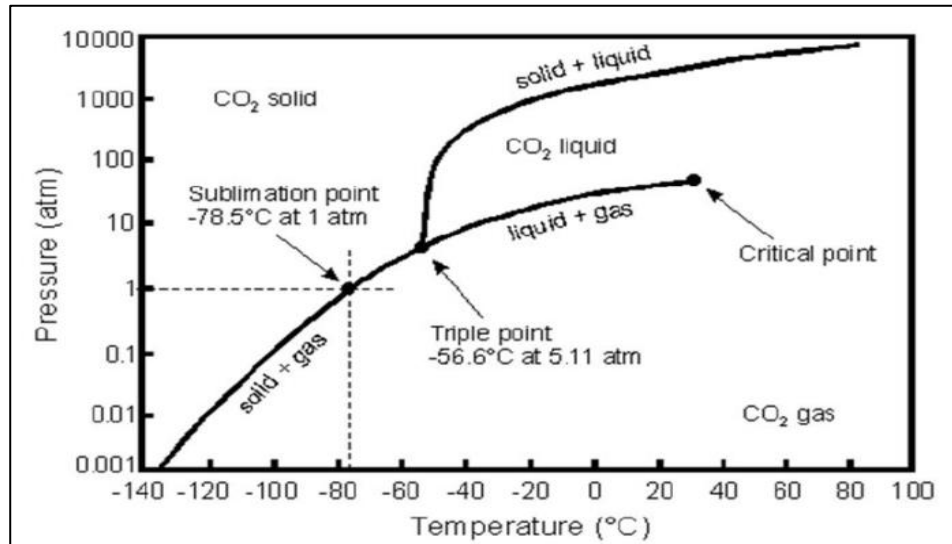


Figure 2.1. Phase diagram of CO<sub>2</sub> (Picha, 2007)

### 2.1.3. Mechanism

The mechanisms of CO<sub>2</sub> EOR can be mainly attributed to a reduction of the interfacial tension between oil and water, reduction of mobility ratio, extraction and vaporization of the light oil component, oil swelling and viscosity reduction in oil, effect of a weak acid and solution gas drive (Haynes, 1990; Gozalpour, 2005; H.Feng 2016).

#### 2.1.3.1. Oil swelling and viscosity reduction in oil

After an injection to the reservoir, the volume of the reservoir oil can be expanded due to dissolution. This swelling effect increases the oil mobility ratio, and the oil can flow easier from the reservoir to the production well. Additionally, the dissolved CO<sub>2</sub> can reduce the oil viscosity and again increase the oil mobility. Studies show that the more percentage of viscosity reduction can be achieved for heavy oils. That is why CO<sub>2</sub> flooding is choosing as an EOR technique mostly for high viscous oil.

### **2.1.3.2. Reduction of the interfacial tension between oil and water**

When CO<sub>2</sub> is injected into the reservoir, CO<sub>2</sub> will reduce the interfacial tension of oil and water. This decrease promotes the reservoir oil flow mechanism positively and concludes with high oil production.

### **2.1.3.3. Solution gas drive**

During the injection process, after CO<sub>2</sub> breakthrough, the pressure of the reservoir can be decline to or below the saturation pressure. Then the dissolved CO<sub>2</sub> in the crude oil is going to be separated from the oil and forms gas drive which supplies extra energy for the displacement of oil. This drive mechanism seems to be an important mechanism, however; early gas breakthrough can decrease the miscibility effect.

### **2.1.3.4. Extraction and vaporization of the light oil component**

CO<sub>2</sub> can extract and vaporize the light oil component from the reservoir oil when the pressure is higher than a certain value. This value depends on the oil properties. This mechanism is mostly correlated with light oil recovery.

### **2.1.3.5. Effect of the weak acid**

When CO<sub>2</sub> and water come together, they form carbonic acid and this acid can give a reaction with the carbonate rocks and corrode it which can increase the rock permeability. Also, this acid may help to clear the inorganic scale and to increase oil production.

## **2.1.4. Techniques of CO<sub>2</sub> Injection Process**

There are some techniques to inject CO<sub>2</sub> to the reservoir for increasing oil recovery and the advantages and disadvantages of the techniques will be evaluated in this section.

#### **2.1.4.1. Continuous Miscible and Immiscible CO<sub>2</sub> Flooding**

CO<sub>2</sub> EOR processes can be classified as immiscible or miscible, depending on reservoir pressure, temperature, injected gas composition and oil properties. These two processes have a different mechanism which is going to be detailed. According to literature, the miscible process is preferred more because higher recoveries can be achieved (Martin, 1992).

The pressure at which miscibility starts to occur is called the minimum miscibility pressure (MMP). MMP is also described as the pressure at which more than 80 % of OOIP is recovered at CO<sub>2</sub> breakthrough (Holm & Josendal, 1974). There are some mechanisms which explain how miscible process is given an extra recovery. Primarily, CO<sub>2</sub> does not actually dissolve in the oil at the first contact in the reservoir. But then, at the multiple contact process, the intermediate and higher molecular weight hydrocarbons from the reservoir oil vaporize into the CO<sub>2</sub> which is called as vaporization gas drive process and part of the injected CO<sub>2</sub> dissolves into the oil which is called as condensation gas drive process (Merchant, 2010; Verma 2015). When miscibility is generated, the new mixture of CO<sub>2</sub> and reservoir oil can flow together because of the low interfacial tension and low viscosity and then oil recovery can be improved. The miscible CO<sub>2</sub> EOR process is shown in Figure 2.2. If the reservoir pressure is lower than MMP, CO<sub>2</sub> is only partially dissolved in the reservoir oil so CO<sub>2</sub> and oil will not generate a single phase and will not be miscible. This process is defined as the immiscible CO<sub>2</sub> process. Even if not exact dissolution may occur, the injected part of the CO<sub>2</sub> can cause oil swelling and viscosity reduction to improve oil recovery. Also, CO<sub>2</sub> can act as an artificial gas cap, giving extra force to the reservoir oil. Additionally, CO<sub>2</sub> may extract the light oil components which cause a reduction of density and viscosity and helps the oil production as well.

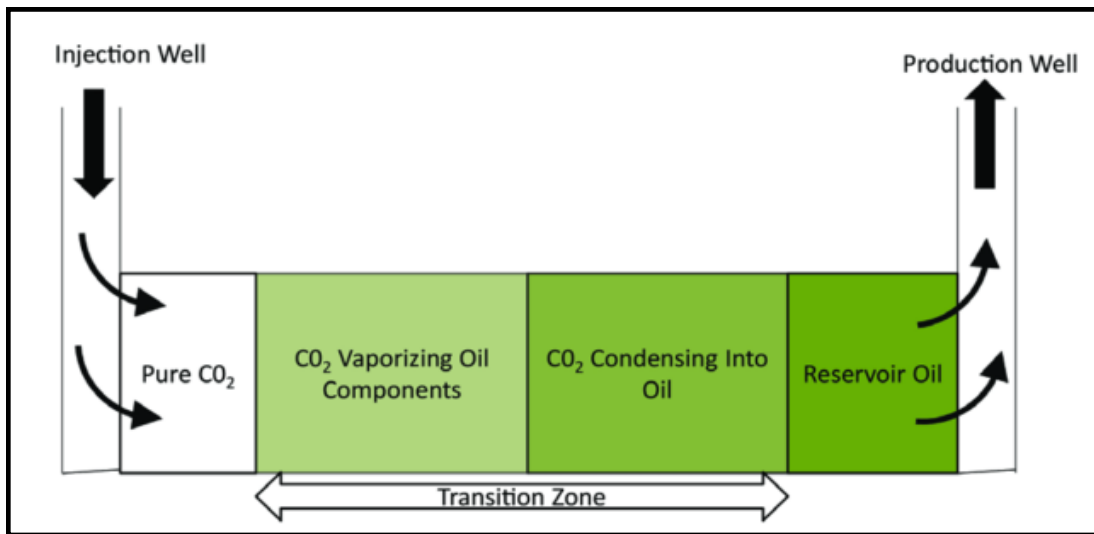


Figure 2.2. The process of miscible CO<sub>2</sub> EOR process (Verma, 2015)

#### 2.1.4.2. Cyclic CO<sub>2</sub> Flooding

The cyclic CO<sub>2</sub> injection has been successfully applied to increase oil recovery during the past four decades and called the huff-n-puff process. In this injection system mainly involves 3 steps; injection phase, shut-in phase and production phase (Thomas 1990). The mechanisms during these steps can be count as oil swelling, viscosity and interfacial tension reduction, dissolved gas drive and vaporization of lighter oil components (Abedini, 2014). Moreover, generated carbonic acids when applied CO<sub>2</sub> can improve the rock permeability related the ions in the brine (Mohamed, 2011).

The projects which were done to figure out the performance of cyclic injection process indicated that efficiency of this process was higher in the presence of gravity segregation, gas cap, higher residual oil saturation, long soaking period and large CO<sub>2</sub> slug size (Wolcott, 1995; Abedini, 2014).

#### 2.1.4.3. Water Alternating Gas (WAG)

The main problem with both miscible and immiscible gas injection is poor volumetric sweep efficiency due to unfavorable mobility ratio of gas. Because of the low viscosity

and density of the CO<sub>2</sub>, fingering and channeling through matrix may occur. Therefore, the main aim of the WAG system is to fill the channels with water and increase sweep efficiency (Dong, 2005; Verma, 2015; Nasir, 2009).

The first WAG operation was reported in Canada in 1957 and since that day, it has been commonly used as a worldwide EOR technique (Caudle, 1958; Jiang, 2012).

The WAG process involves two hydrocarbon recovery techniques in it as waterflooding and gas injection. Since it's a combination, it has the advantages of these two kinds of injections. The method of the WAG process is injecting a slug of CO<sub>2</sub> in cycles alternating with equal volumes of water. The water is using here to control the mobility and to generate front stability. Christensen, J. R (1998) was reported a review of 60 field cases where WAG was applied and concluded the study that this process was successful and could obtain up to 20% extra oil recovery. The corrosion is the major problem of the WAG injection system. Also, the other issues during WAG injection are gradual oil response, gravity segregation and infectivity loss (Nasir, 2009).

The types of WAG injection can be classified in terms of injection property as miscible, immiscible, simultaneous, hybrid, foam assisted (Skauge, 2003). If water and gas are injected at the same time, then this process is called simultaneous water and gas injection (SWAG). The mixing of CO<sub>2</sub> and water can be either in the well or surface. The objective of the system is to enhance the profile control in comparison with WAG and continuous injection. In other words, this process can reduce the capillary entrapment of oil and supply ahead of mobility control of gas relative to WAG (Nasir, 2009). The study which was practice by the P. Heidari et al. (2013) to make a comparison between WAG and SWAG injection indicated that SWAG can increase the speed of oil production compare to WAG injection.

One of the other types of WAG is Tapered/hybrid WAG. The main objective of this process is to enhance CO<sub>2</sub> utilization because the design of the system increases the performance of the flood and preclude the early breakthrough of the CO<sub>2</sub> so can obtain higher recovery (Verma, 2015). In Hybrid WAG, a large volume of the CO<sub>2</sub> is continuously injected to about 20% to 40% PV pore volume followed by a small number of slugs of water and gas. The early production, higher injectivity, reduced water blocking, higher recovery, and CO<sub>2</sub> utilization can be counted as the advantages of this system relative to the WAG process (Hadlow, 1992).

#### 2.1.4.4. CO<sub>2</sub> Foam

One of the techniques to overcome the low density of the CO<sub>2</sub> is the foam. If foam form of the gas can be created, then this new dense form can control the mobility. Explanation of foam and solid particles usage for foam stability is the main subject of this study and going to be detailed in CHAPTER 3.

#### 2.1.5. Worldwide CO<sub>2</sub> Flood Projects

Since positive outputs were taken from the CO<sub>2</sub> floods trials in the USA, CO<sub>2</sub> floods have been implemented outside of the USA such as Canada, Hungary, Turkey, Trinidad, and Brazil.

Table 2.1. Number of the worldwide CO<sub>2</sub> EOR applications (Koottungal, 2012)

<b>Country</b>	<b>Number of Miscible CO<sub>2</sub> Projects</b>	<b>Number of Immiscible CO<sub>2</sub> Projects</b>	<b>Total number of CO<sub>2</sub> Projects</b>
USA	112	9	121
Canada	6	0	6
Brazil	2	1	3
Trinidad	0	5	5
Turkey	0	1	1
<b>Total</b>	<b>120</b>	<b>16</b>	<b>136</b>

Miscible CO<sub>2</sub> injection is much more prevalent than an immiscible system, as it appears from *Table 2.1*. Turkey has only one project which has been applied to the Bati

Raman (B.Raman) field. In this EOR technic, the problem is about the CO<sub>2</sub> supply. USA has an adequate natural source of CO<sub>2</sub> and that is why they have more projects than other countries.

## 2.2. FOAM

Foams can be formed by an instantaneous increase in the contact area between water and air. In simple term, if a liquid and a gas come together and then a shear is applied, the gas phase is going to be bubbles dispersed in the liquid which are so-called foams as shown in Figure 2.3. The gas phases are drifted away by a film of liquid described as lamella as seen from the figure. Also, the plateau border has defined a connection of three lamellas at an angle of 120°. They are non-equilibrium systems and a very special kind of colloidal dispersions. All dispersion is listed below and foams commonly belong to the first group (Bikerman, 1973).

- Gases dispersed in the liquids (foam, gas emulsion)
- Liquids dispersed in the gases ( mists, fogs, liquid aerosols)
- Gases dispersed in solids (solid foam)
- Solids dispersed in gases (fumes, smokes, solid aerosols)
- Liquids dispersed in liquids (emulsions)
- Liquids dispersed in solids (some gels)
- Solids dispersed in liquids ( suspensions, sols)
- Solid dispersed in solids

First of all, it should be indicated that pure liquids cannot create foam because of their high surface tension (72 mNm<sup>-1</sup>). Gas bubbles will go up and fly off. For this reason, a surface active material should present to stabilization of bubbles such as surfactants, and solid particles etc. (Pugh, 1996; Stocco, 2013). These materials will accumulate at the liquid-gas interface and stabilize the foam.

The liquid designates the types of the foam which are wet and dry (The range is 1% - 30 %). On the other hand, gas content is used to specify the foam quality by the engineers. The small spherical bubbles separated by the thick layers of liquid called as wet (liquid fraction larger than 20%), while the thin layer of foam consisting of larger bubbles is referred to dry foam. (Sheng, 2013; Stevenson, 2012).

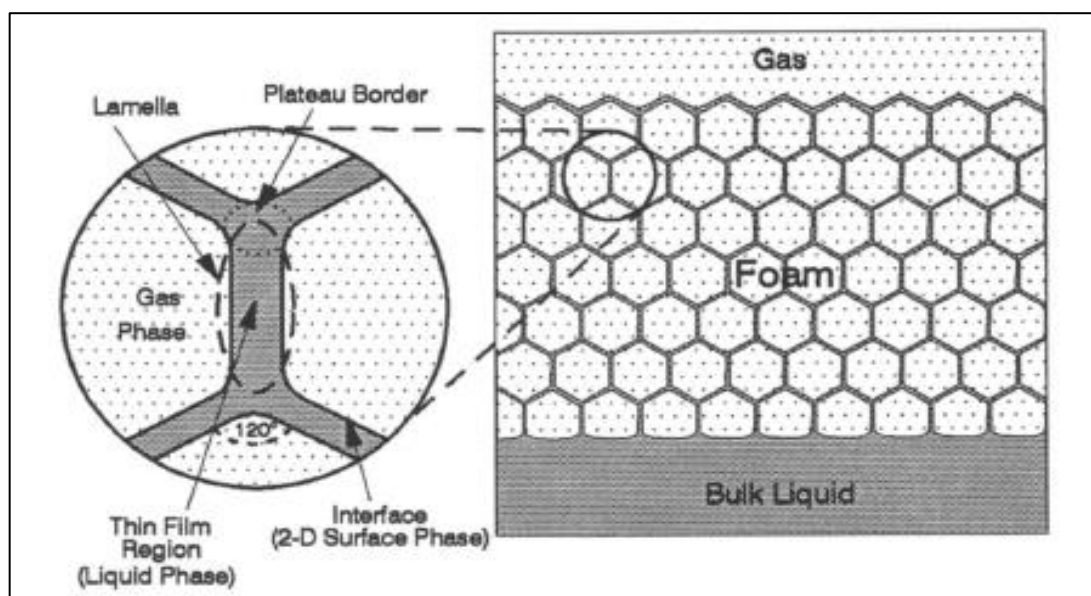


Figure 2.3. Illustration of a foam structure (Schramm, 1994)

The various shape of the bubbles is formed when different generation methods apply. All formation processes have two basic mechanisms: i) capturing gas bubbles from ambient air because of the turbulence of the liquid phase and ii) applying air bubbles by the chemical or physical way (Karakashev, 2012). Figure 2.4 gives the detailed of the shape of bubbles as results of formation methods. The faster process for gas bubbles formation flows through a porous plug. The only issue is the low controllability of this procedure.

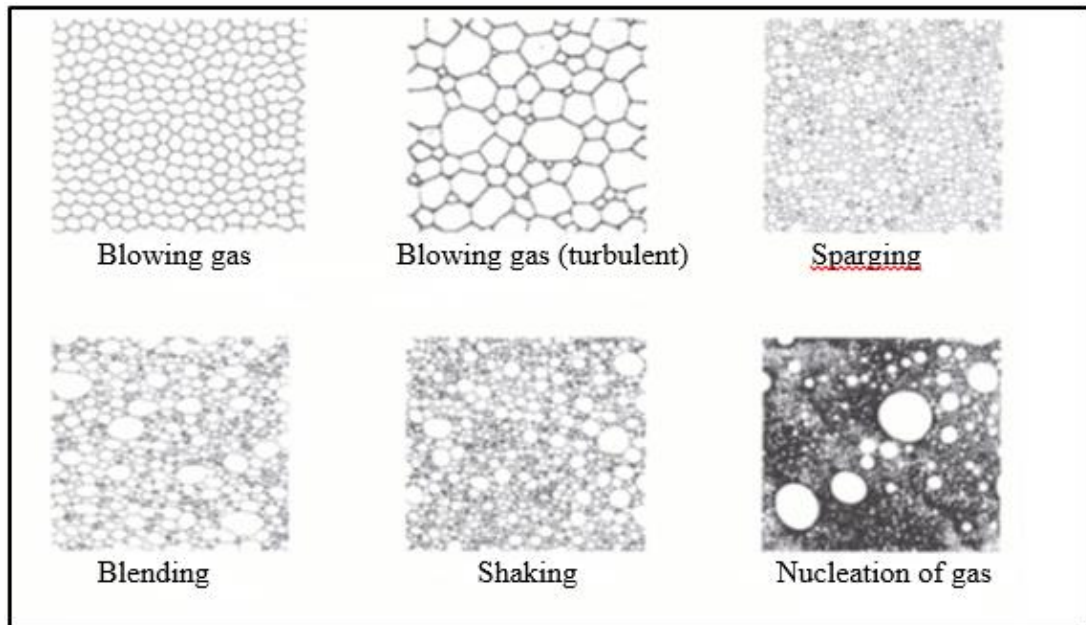


Figure 2.4. The shape of bubbles related to formation methods (Weaire, 1999)

### 2.2.1. Surfactant Stabilized CO<sub>2</sub> Foam

As mentioned before, CO<sub>2</sub> suffers from its poor sweep efficiency due to low density and viscosity. Since the years of CO<sub>2</sub> EOR invention, big progress was made by the scientist. If foam form of the gas can be created, then this new dense form can overcome the mobility control problem. Surfactants are surface active agents. These chemicals accumulate at the gas-liquid interface which ended up the decrease in interfacial tension and generates stabilization of the foam. Thus, this stabilized foam can penetrate both low permeable and high permeable zones which give better recovery as shown in Figure 2.5. However, this method has some potential weaknesses; long term stability, adsorption at the rock surface e.g. There are several laboratory and field studies mostly related to foamability, foam stability and retention of the surfactant in the last four decades. (Chou, 1992; Harpole, 1994; Pugh, 1996; Schramm, 1994; 2000; 2005; Liu, 2005; Zuta, 2009; Adkins, 2009; Andrianov, 2011; Heetschap, 2015; Kanokkarn, 2017; Wang, 2019; Sun, 2019; Zeng, 2019)

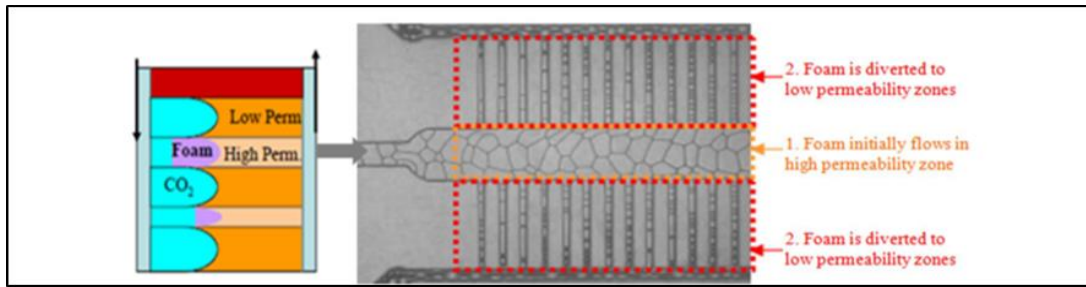


Figure 2.5. Foam flow through pores (Talebian, 2014)

### 2.2.2. Particle Stabilized CO<sub>2</sub> Foam in Oil and Gas Industry

Although many industries generate foam as a purpose, it can be also unwanted for some of the petroleum and chemical industries. The studies for this kind of foams are about breaking them off. Examples of desirable and undesirable foams in the oil and gas industry are shown in Table 2.2.

In this study, particle stabilized foam to control CO<sub>2</sub> mobility in the reservoir will be examined. As mentioned before sections, CO<sub>2</sub> injection is a proven and potential EOR process but, the inherently poor volumetric sweep efficiency resulting from low viscosity and density of CO<sub>2</sub> is its critical weakness. Because of this, gravity segregation and viscous fingering and channeling through high permeable layers may occur. Therefore, the need for mobility control of the CO<sub>2</sub> in the reservoir is highly desirable. To overcome surfactant foam stability and retention problems, new studies are focused on the nanoparticle stabilized CO<sub>2</sub> foam. Similar to surfactants, particles also place at the gas-liquid interface but do not change the IFT and contrary to surfactant, solid particles adsorb permanently (Sheng, 2013). The adsorption energy ( $W_f$ ) depends on the contact angle ( $\theta$ ), particle radius ( $R$ ) and surface tension of the CO<sub>2</sub> and the aqueous phase ( $\gamma$ ). (Dong, 2003; Hunter, 2008; Kruglyakov, 2011; Yu, 2012; Yekeen, 2018)

$$W = \gamma_{\text{CO}_2\text{-water}} R^2 \pi (-|\cos \theta|)^2 \quad (2.1)$$

Much higher energy needs to take out the particles from the adsorbed interface. Also, nanoparticle retention on the rock surface could be kept minimal (Zhang, 2015;

Aroonsri, 2013). Many studies demonstrated that the nanoparticle stabilized foams were a stable long time, on the other hand, surfactants can only stabilize a few hours (Binks, 2000; 2002; 2005; Sun, 2014; Yu, 2012a; Li 2016; Yekeen, 2018). Adhesion energy, electrostatic repulsion and van der Waals attraction between particles are the key parameters of the stability. The other supremacy of the nanoparticle is its durability against harsh reservoir conditions and may be produced from low-cost materials such as silica (Golomb, 2006; Aroonsri, 2013).

Table 2.2. *Examples of foam in the oil and gas Industry (Shramm, 1994)*

<b>Undesirable Foams</b>	<b>Desirable Foams</b>
Producing oil well and well-head foams	Foam drilling
Oil flotation process front	Foam fracturing liquid
Distillation and fractionation tower foams	Foam acidizing fluid
Fuel oil and jet fuel tank foam	Blocking and diverting foams
	Gas mobility control foams

Back in times, the first papers about nanoparticle stabilized foams were the studies of Dickson et al. (2004), Adkins et al (2007) and Martinez et al. (2008). They all declared that it was possible to create stable foam by using nanoparticles and this foam could last long. Scientists were first focused to create CO<sub>2</sub> foam and effect of the parameters on stability. Stability of CO<sub>2</sub> foam related to particles size, concentration, hydrophobicity, phase ratio, type of the particle, pressure, temperature and rock structure has been presented in several papers. Yu et al. (2012a) were investigated the particle concentration, pressure, temperature and surfactant impact during CO<sub>2</sub> foam generation at static condition. The study showed that above the supercritical point of the CO<sub>2</sub>, even low nanosilica concentration (4000-6000 ppm) it was possible to create CO<sub>2</sub> foam and surfactant adding affected positively. The same group also worked with the dynamic process for generating foam and examined total flow rate and phase ratio relation (Yu, 2012b). Singh and Mohanty (2017) treated nanoparticle for high temperature (HT) and high pressure (HP) reservoirs. Zhu et al. (2017), Eide et al. (2018) and Bashir et al. (2018) also had the works on the nanoparticle stabilize CO<sub>2</sub>

foam application for tough reservoirs. At the end of the study, they saw that nanoparticle stabilized foam have some issue if you injected below 200 md permeability core sample. One of the key parameters is hydrophobicity of the nanoparticle for foam stability. The studies indicated that more stable foam could be achieved when half hydrophobic nanoparticle was used (Stocco, 2013; Zang, 2010). Similar results were obtained by Worthen et al. (2012a; 2012b) and Rognmo et al. (2018). Worthen et al. worked with hydrophilic, half hydrophobic and PEG coated nanosilica and indicated that 50 % hydrophobicity gave the best stable foam. The results of the Rognmo et al. study pointed at the different type of nanosilica particles gave different results. Furthermore, the measured pressure gradient showed that silica nanoparticle stabilized CO<sub>2</sub>-foam remain stable even though surfactant couldn't stabilize the foam as expected from the earliest projects. Yu et al. (2014) observed that the hydrophobic nanosilica created higher mobility reduction in porous media. Espinosa et al. (2010) were demonstrated the particle size effect on foam. According to authors, very low concentration (0.05 %) of the nanoparticles is enough to create foam but if the particle size was larger, this time, higher concentration (0.5 %) might need. Mohd et al. (2014) concluded their project with the same result as even %0.5 concentration could generate foam. They also obtained that increased salinity supported foaming but excessive concentration led to aggregation. The effect of sodium chloride and calcium chloride on the generation of the stable foam was also studied by San et al. (2016). They found that foam was denser with increased sodium chloride and calcium chloride.

Xue et al. (2016) presented a new model for stabilized CO<sub>2</sub> foam. The polymer was also added to surfactant and nanoparticle mixture to heighten continuous phase and surface viscosity which was caused the low lamellae drainage rates and inhibited coalescence. The studies which were done by Ermani et al. (2015; 2017a; 2017b) proved that the nanoparticles adding into surfactant solution gave more stable CO<sub>2</sub> foam. This group also compared foams of the nanoparticle-surfactant and polymer-surfactant mixture. The findings revealed that nanoparticle- surfactant foams are much

stable. Furthermore, they tested this nanoparticle stabilized CO<sub>2</sub> foam as a fluid of hydraulic fracturing. Yusuf et al. (2013) also work with the nanosilica-surfactant mixture to create foam. The study indicated that the adsorption of the non-ionic surfactant (TX100) on the nanosilica particles depends on the silica concentration. Same studies had made by Farhadi et al. (2016) and Zhang et al. (2015). Ibrahim and Nasr-El-Din (2018) used a viscoelastic surfactant to increase the mobility of the foam for EOR.

Different nanoparticles also were evaluated as a CO<sub>2</sub> foam stabilizer instead of nanosilica by the researchers. Kalyanaraman et al. (2015) compared the polyelectrolytes and polyelectrolyte complex nanoparticles (PECNP) with surfactant about their oil recovery efficiency. The study indicated higher recovery could be obtained when PECNP-surfactant CO<sub>2</sub> foam applied. A similar study has been done by the Nazari et al. (2018). Also, results suggested that the best stable foam did not mean the highest oil recovery. Alargova et. al. (2004) used polymer microrods to stabilize aqueous foams in the absence of surfactant for the conditions which the common surfactant was not effective. In another study, micrometer-sized, sterically stabilized PS latex particles were used by Fujii et. al. (2006) to prepare highly stable aqueous foams. Fly ash performance for foam generation was also evaluated by the scientist. Lee et al. (2015) were one of them but they found that the fly ash could not be used as a stabilizer, alone. Contrary, the results of the Eftekhari et al. (2015) work showed that even very small amount of nano fly ash gave a more stable and stronger foam.

The second type of studies was about the foam flow through core samples and oil recovery increment. Nanoparticle stabilized CO<sub>2</sub> foam flow through a sandstone core sample at 1200 psi where CO<sub>2</sub> was in supercritical phase was studied by Mo et al. (2012). The same group also analyzed the other type of rocks potential for oil recovery increment which was limestone and dolomite (Mo, 2014). Higher oil recovery by foam was achieved when the sandstone core sample was used. Aminzadeh et. al.

(2012) saturated core samples with nanoparticle dispersion and brine then injected CO<sub>2</sub> into a saturated core and achieved increased sweep efficiency when nanoparticle was placed. Evaluation of the performance of the nanosilica and nanoclay on CO<sub>2</sub> foam stability and improvement of oil recovery inside a microfluidic device was conducted by Guo and Aryana (2016). This study results showed that CO<sub>2</sub> foams with increased stability by using nanoparticle gave a significantly increase oil recovery. AlYousef et al. (2017) had increased oil recovery when nanoparticle was placed into a surfactant mixture. Yu et al. (2013) also assessed the oil recovery increment and obtained higher recovery when applied low permeable reservoir as expected. The effect of pressure and temperature on the oil recovery by using nanoparticle stabilized CO<sub>2</sub> foam was studied by Fu (2018) et. al. The results suggested that oil recovery was increasing with increased pressure and decreased temperature. When applied foam, additional % 17 IOIP after waterflood was obtained by Nguyeng et al. (2014). Rahmani (2018) developed nanosilica CO<sub>2</sub> foam to oil recovery for fractured and unfractured carbonate reservoir. Aroonsri et al. (2013) also compare the foam in the fractured and unfractured sandstone core samples with a focus on the role of shear rate. The results indicated that in both conditions, a critical shear rate existed and the lower critical shear rate was achieved at low permeability.

Extensive researches have been conducted to generate CO<sub>2</sub> foam and the effect of parameters on foam stability, but not enough researches have been done about CO<sub>2</sub> foam used for EOR. Also, the studies are mostly for sandstone and very little work can be found for carbonate reservoirs. Furthermore, there is none of the study in the literature at the field where CO<sub>2</sub> injection has already been applied. The all studies related to EOR aimed to examine the oil recovery after waterflood, only. Therefore, the objective of this work is to show any increased efficiency of the conventional CO<sub>2</sub> injection system at B. Raman field by using nanoparticle stabilized CO<sub>2</sub> foam.

### 2.3. BATI RAMAN FIELD

The B. Raman field located in the southeastern part of Turkey was discovered in 1961. The field is about 20 km long and 5 km wide (Figure 2.6), known as the largest oil field in Turkey, and having about 1.85 billion barrels of OOIP. Oil is produced from the Garzan Formation which is fractured, vuggy and heterogeneous limestone. The formation thickness is 210 ft and the average depth is 1300 m. The counter map of the field is shown in Figure 2.7. The average reservoir porosity is %18 and the matrix permeability is ranging from 10 to 100 md. On the hand, the effective porosity is in between 200 to 500 md due to fractures and vugs.



Figure 2.6. Estimated B. Raman field borders

The reservoir contains about 12 API heavy oil, and the viscosity ranging from 450 to 1000 cp at reservoir conditions. Reservoir fluids have low solution gas. The original reservoir pressure was 1800 psi but after 30 million stock tank barrel production, the pressure dropped to around 400 psi between the years of 1961 to 1989 (Issever, 1993). Therefore, the high production decline was observed. Dodan field is about 55 miles away from B.Raman field. Estimated total reserve is 383 Bscf and contains almost 90 % vol. CO<sub>2</sub>. Hydrogen Sulphur (almost 3500 ppm) and the trace amount of nitrogen and hydrocarbons also place in the gas composition (Sahin, 2010). The Dodan facility supplies 60 MMscfd gas. CO<sub>2</sub> injection as the huff-n-puff process at B. Raman was first introduced in 1986. Even though the incremental production was obtained, during injection, it was figured out that the effective mechanism was the gas drive. Therefore, the project was converted to continuous CO<sub>2</sub> injection.

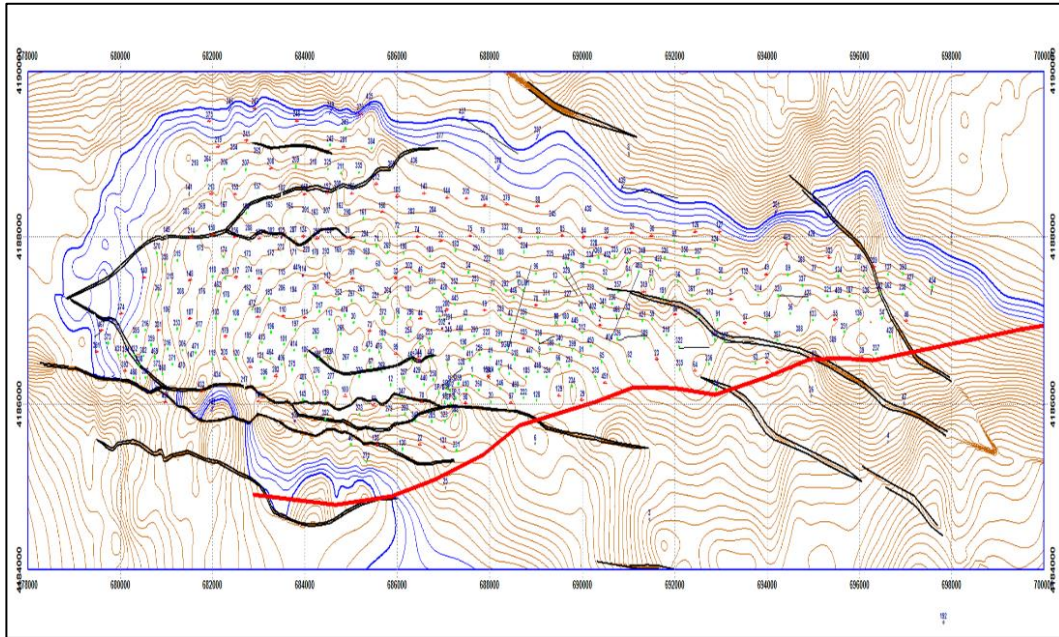


Figure 2.7. Contour map of the B. Raman field

The pressure of the reservoir is well below the miscibility pressure of the CO<sub>2</sub> so the injection at the B.Raman field is called as immiscible CO<sub>2</sub> injection. Since CO<sub>2</sub> injection process was exhibited significant performance, Turkish Petroleum Corporation decided to enlarge the process to all of the fields.

The process starts with the evaporation stage of the liquid CO<sub>2</sub>. After that, two phase separators are using to remove water. Then, the hydrogen Sulphur content in gas is lessening with acid gas removal solvent. Finally, triethylene glycol is using to dehydrate the gas. The CO<sub>2</sub> injection flow diagram is shown in Figure 2.8. At the beginning of the project, produced gas was released to the atmosphere but then, CO<sub>2</sub> was captured and reinjected to decrease consumption and to ensure environmental safety.

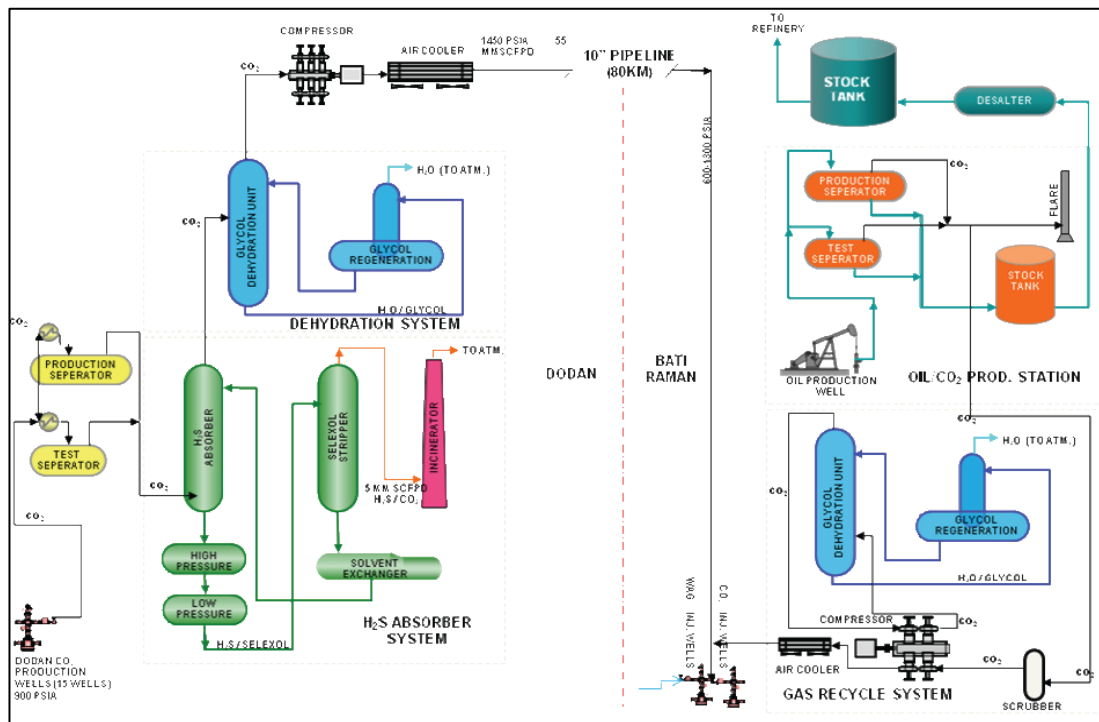


Figure 2.8. Flow diagram of the CO<sub>2</sub> injection system

Estimated recovery increase was 10% but it observed as half of this value to date. Because the B. Raman field is naturally fractured reservoir as mentioned before which causes the early breakthrough of the CO<sub>2</sub>. Therefore, low sweep efficiency was obtained. The polymer gel applied to the field to blockage of the fractures in the years of 2002 to 2004 (Karaoğuz, 2004). Also, surfactant foam was tested at the laboratory to control the mobility of the CO<sub>2</sub>. Although these methods gave high sweep efficiency, methods did not seem feasible. Consequently, conventional WAG has been applied since 2005 to control the mobility of the CO<sub>2</sub> (Sahin 2007). The all these production history was graphed in Figure 2.9. The production history of the CO<sub>2</sub> injection process was reported periodically (Kantar, 1985; Karaoğuz, 1989; Issever, 1993; Sahin, 2007; 2010; 2012).

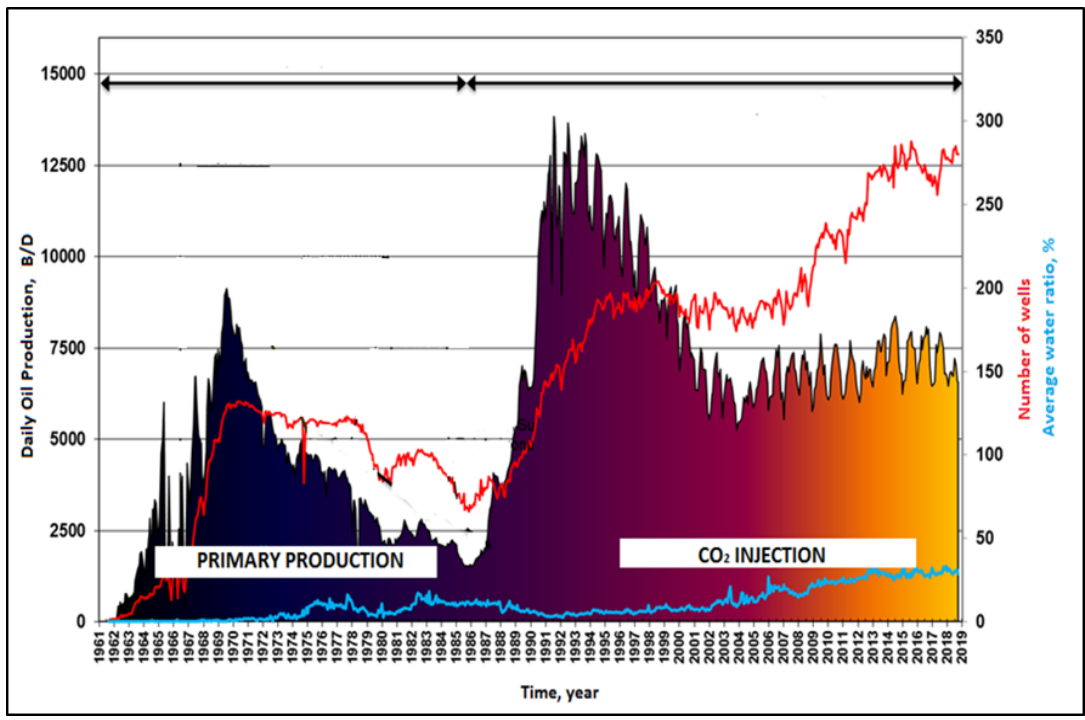


Figure 2.9. B. Raman production history

## CHAPTER 3

### STATEMENT OF THE PROBLEM

There is not enough study in the literature about CO<sub>2</sub> foam used in EOR. The existing studies are mostly for sandstone reservoir. On the other hand, B. Raman has a carbonate rock. Additionally, there is no study at the field where CO<sub>2</sub> injection has already been applied. The studies in the literature aim to examine any production increase when foam applies after water flooding. However; this study shows the any increased efficiency of the conventional CO<sub>2</sub> injection system.

Therefore, the aim of this study is creating nanoparticle stabilized CO<sub>2</sub> foam at the reservoir condition to increase the sweep efficiency of the CO<sub>2</sub> injection system at B. Raman Field. Nanoparticles can adsorb at the interface of the gas and water and can give permanent stabilization. When this stable foam is generated, this denser form will contact with oil over more and give incremental oil recovery

In parallel with this purpose, first nanoparticle dispersion stabilization will be focused on. Different type of nanosilica will be considered. These particles have a tendency to agglomerate and precipitate. It is important to stabilize nanoparticle dispersion before all studies to not plug the pore matrix. After making sure that the dispersions are stable and do not block the matrix, foam formation tests will be begun. In this experiment, nanodispersion and the CO<sub>2</sub> will be injected to the core flooding system simultaneously and foam formation will be checked using the increase in pressure differences and observation cell. Effect of the pressure, phase ratio and total flow rate on foam generation will be examined to get the optimum condition. After conditions are noted, then the oil recovery test will be conducted with suitable nanoparticles. IFT measurement will be also studied for better understanding.



## CHAPTER 4

### MATERIALS AND METHODS

#### 4.1. MATERIALS

##### 4.1.1. Nanoparticles

Five different types of nanosilica were supplied from the chemical companies. These nanosilicas were detailed in Table 4.1. Detailed properties were given in APPENDIX A.

Table 4.1. *Selected nanoparticles and their properties*

<b>Nanoparticle</b>	<b>Named as</b>	<b>Properties</b>	<b>Physical Form</b>
Silica	PEG	Polyethylene glycol coated, 100 % hydrophilic	Dispersion
	CC301	100 % Hydrophilic	Dispersion
	N20	100 % Hydrophilic	Powder
	H30	Dimethylsiloxo coated, 50 % Hydrophobic	Powder
	AERO	100 % Hydrophobic	Dispersion

The different procedure was examined for the nanosilicas in powder form to disperse in the aqueous phase. The N20 was directly put in the water and stirred at high speed for 5 min to disperse because it's 100% hydrophilic. Then put into a sonic bath for an hour. On the other hand, H30 needs extra steps for dispersion preparation due to its partially hydrophobic properties and a procedure which were determined by DiCarlo et al. (2015) was used for this purpose. This time, nanosilica was first dispersed in ethanol, mixed then centrifuged and decanted the supernatant. This step was repeated until ethanol was removed. Then the particles were redispersed in water and sonicated

1 hour after high speed stirrer. The nanosilica in dispersion form were only diluted to the desired concentration and sonicated.

Health and Safety (HSE) procedures were crucial when dealing with nanoparticles. These particles can go into the body using the skin pores easily and can be harmful due to their very small origin. Also, again because of their particle size, the nanoparticles can be inhaled and can cause lung damage. Because of all, while working on these little particles, the disposable lab coat which covers the whole body was used. Additionally, two layer lab gloves and appropriate mask were worn. Moreover, after the weighing of the nanoparticles for dispersion preparation, the ventilation was turned on to clean the air and spills were cleaned with water if any.

#### 4.1.2. Reservoir Fluids

The formation water and the oil was brought from B. Raman field and used for the tests. The main component of the B. Raman formation water which was analyzed by using ICP-OES and the properties of the B. Raman oil were demonstrated in Table 4.2 and Table 4.3, respectively. Detailed analysis results of the water and Dodan gas were given in APPENDIX B.

Pure CO<sub>2</sub> (99.9 %) was used for the foam generation tests as a CO<sub>2</sub> source because of the large quantities of the run. However, for the recovery test, Dodan gas was applied to make a better demonstration of the reservoir. The main components of the Dodan gas were given at the below table (Table 4.4).

Table 4.2. Test results of B. Raman formation water

<b>Analysis</b>	<b>Result</b>
pH, 25 °C	6.51
Specific Gravity, 15.6 °C	1.070
Total Salinity (Sodium chloride, NaCl), mg/l	92 647
Conductivity, 25 °C, µS/cm	127 800

Table 4.3. Test results of B. Raman oil

<b>Analysis</b>	<b>Result</b>
Density, 25 °C, g/cm <sup>3</sup>	0.987071
Density, 65 °C, g/cm <sup>3</sup>	0.957537
API Gravity, 60 °F	10.82
Kinematic Viscosity, 65 °C,	625.02

Table 4.4. Test results of Dodan gas

<b>Analysis</b>	<b>Result</b>
Carbon dioxide, % mol	86.878
Nitrogen, % mol	3.562
Methane, % mol	7.315
Hydrogen Sulphur, ppm	483.1

### **4.1.3. Core Samples**

All core samples belong to the B. Raman field which means they are the carbonate rock. 1.5 inch core plugs were used for the flooding tests. On the other hand, for recovery tests, 4.5 inch core sample was placed to the core holder. Properties of the samples which were analyzed by using porosimeter and permeameter were located on their own flood graph or under their own title in CHAPTER 5 because various core plug samples were used due to the high number of the run.

## **4.2. EXPERIMENTAL SETUP AND PROCEDURE**

### **4.2.1. Rock Samples Preparation and Routine Core Analysis**

Firstly, all of the plug samples were cleaned from hydrocarbon contents by using a Soxhlet toluene extraction system. Afterward, the samples were immersed in an alcohol bath and placed in a vacuumed-oven system to clean any possible salt remaining in the pores of the samples due to drilling fluid and formation water. Then they were dried in a temperature-controlled oven at 70°C and, finally, their weights and physical dimensions were measured.

Porosity values of core plug samples were measured by using a helium gas expansion porosimeter and the principle of “Boyle’s Law”. Plug samples were individually placed in the matrix cap connected to the porosimeter. Helium, at a known pressure of 100 psig from a reference cell of the known volume was allowed to expand into the matrix cap and into the available pore spaces. The volume of expansion was recorded and used to calculate the grain volume using the principle of Boyle’s law. Bulk volumes of the samples were determined by measuring the length and diameter of the samples and then applying appropriate mathematical formulas.

For permeability measurements, clean and dry plug samples were placed in the “Hassler” type core holder of the “steady-state” air permeameter. The stabilized flow rate of dried air through the core sample was monitored and differential pressure across the plug sample was measured and used in conjunction with the measured sample length and cross-sectional area to calculate air permeability using “Darcy’s Law”. Calculated air permeability ( $k_{air}$ ) values were corrected by “Klinkenberg Correction” to obtain equivalent liquid permeability ( $k_w$ ). Systems were shown in Figure 4.1

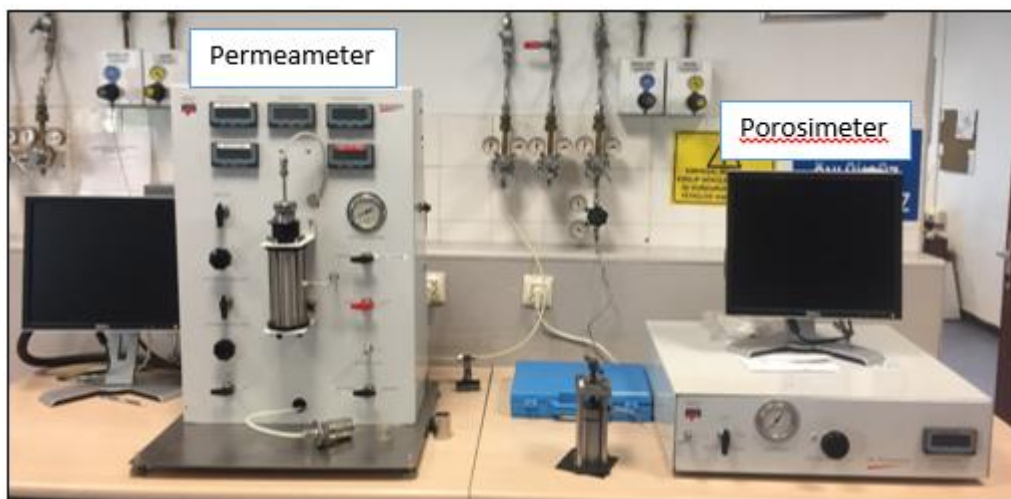


Figure 4.1. Porosimeter and permeameter test system

#### **4.2.2. Zetasizer**

Zetasizer system was used to measure size distribution from less than a nanometer to several microns and zeta potential of the particles. This system was performed to determine the stability of the nanoparticles in the dispersion. The tests were carried out by the laboratory of the National Nanotechnology Research Center (NNRC) and METU Central Laboratory. For bigger particles, Master Sizer was used.

When nanoparticles are dispersed in a liquid, opposite charged ions binds to the surface of the nanoparticles and create a thin layer, called as ‘Stern Layer’. This layer causes a second diffuse outer layer, consisted of loosely associated ions, known as “diffusive ion layer”. This double layer of ions travels with the nanoparticle as it diffuses throughout the solution. The layers are called ‘the electrical double layer’ together. When the nanoparticles are put in a liquid, a boundary appears between the ions in the diffuse layer that move with the particle and ions that remain with the bulk dispersant. The electrical potential at this “slipping plane” boundary is known as the ‘Zeta Potential’ of the particle and has values ranging from +100 mV to -100 mV. The value of the zeta potential defines the colloidal stability of the nanoparticles. Nanoparticles with Zeta Potential values higher than +30 mV or lower than -30 mV typically have the best stability.

#### **4.2.3. Core Flood System**

All flood tests were performed with a ‘core flood system’. This system allows to reach 10000 psi fluid and confining pressure and 150°C temperature. The system includes gas, liquid and oil accumulator and a core holder (for 1.5 inch plugs) with the connected lines in an oven. An extra core holder was used for nanosilica dispersions. Also, a sapphire cell was inserted into the system to observe the foam during foam generation flooding test. Core holder for 4.5 inch core sample is at outside the oven and has own heating shells. This core holder was used during oil recovery tests. In all runs, core samples were placed vertically in the core holder and the flood was applied

at the bottom of the cores. Upstream and the downstream pressures and the differences between them were recorded by the pressure sensors. A dual pump which is capacity is 100 cc fluids and maximum 25cc/min flow rate was used. Confining pressure was applied by using another pump. The pressure was kept constant with a back pressure regulator. All system (pumps, valve etc.) is controlled with software and this software records all data. The system is shown in Figure 4.2.



*Figure 4.2. Core flood test system*

#### **4.2.4. Interfacial Tension (IFT)**

This test was performed to figure out interfacial tension between fluids. *Table 4.5* demonstrates the experimental condition of the IFT.

The test was conducted with IFT700 system which was displayed in Figure 4.3 and allow us to reach 10000 psi pressure and 175 °C temperature. The measurement range is 0.1-72 mN/m. The cell and drop fluids are placed into their own accumulators and heated up to the desired temperature. When the system reached the steady state then a drop is generated by using the drop fluid with a needle. While the drop wants to go up, the IFT between drop fluid and cell fluid precludes this motion. The camera which

is inserted to the test system is used to picture drop. The shape of this drop is analyzed to measure IFT. ‘Rising Drop Method’ is used if the fluids are oil and water and ‘Pendant Drop Method’ is selected for water and gas.



Figure 4.3. IFT test system

Table 4.5. Experimental conditions of IFT

Drop Fluid	Bulk Fluid	Pressure psi	Temperature °C
CO <sub>2</sub> (g)	%1 NaCl çözeltisi	600	25
	%1 NaCl çözeltisi + %1 Nanosilica dispersion	600	65
B.Raman Oil	%1 Nanosilica Dispersion	600	25
			65

#### 4.2.5. X-Ray Fluorescence Spectroscopy (XRF)

XRF was used to figure out the composition of the silica in the dispersions after and before the flooding tests. In this system, first, a source produces X-rays. The elements emit the radiation which is unique for each element and by measuring the energy of the emitted radiation, qualitative and quantitative results can be obtained. Figure 4.4 demonstrates the image of the XRF spectroscopy.



*Figure 4.4.* XRF spectroscopy

#### 4.2.6. Scanning Electron Microscope/ Energy Dispersive Spectrometry (SEM/EDS)

A scanning electron microscope (SEM) is used to obtain surface topography and composition. The microscope creates images by scanning the sample surface with a high-energy beam of electrons. As the electrons interact with the sample, they produce secondary electrons, backscattered electrons, and X-rays are produced when electrons hit the surface. Then, signals are detected by the detectors to create images and this image is displayed by the computer. The SEM /EDS system which is shown in Figure 4.5 was used to picture of the foam in the core sample pores. For this purpose, the piece part of the selected core samples was placed on the sample carrier and dried in an oven

at 600 °C for 2 hours. The dried fragment was coated with 200 Å thick gold by using EMS-550X Coating Device. Then, IXRF-EDS-2004 system was used to analyze under the condition which was shown in *Table 4.6*.



*Figure 4.5. SEM/EDS system*

*Table 4.6. SEM/EDS experimental conditions*

SEM accelerator voltage	15 kV
SEM beam current	1 $\mu$ A
EDS analysis program	SQ
EDS correction program	ZAF



## CHAPTER 5

### RESULTS AND DISCUSSION

#### 5.1. NANOSILICA DISPERSION STABILIZATION, FOAMABILITY AND PARAMETERS EFFECT

##### 5.1.1. Stabilization and Foamability

Nanosilica types and the dispersion preparation procedure were touched on CHAPTER 4. Adhering to this procedure, dispersions were prepared for the early foamability test by using pure water and used dispersions were provided in *Table 5.1*. For this basic test, the dispersion was placed in the glass tubes and shaken hard and fast for a minute. It was expected that nanoparticles placed at the interface of the air and the water and create foam. The purpose of this test was seeing the foam generation and life of the foam to select suitable nanosilica.

Table 5.1. *Prepared dispersions for early foam test*

Case No	Nanoparticle	Nanoparticle Concentration	NaCl Concentration
1	PEG	1%	-
2	CC301	1%	-
3	AERO	1%	-
4	N20	1%	-
5	H30	0.5%	-
6	H30	1%	-
7	H30	1%	1%

As mentioned in CHAPTER 2, half hydrophobic nanosilica proved itself as a better stabilizer of the foam. In light of this information, different concentration of the H30 and the salinity effects on the H30 foam were also examined. Designation of the dispersions before and after the early foamability test was in Figure 5.1.

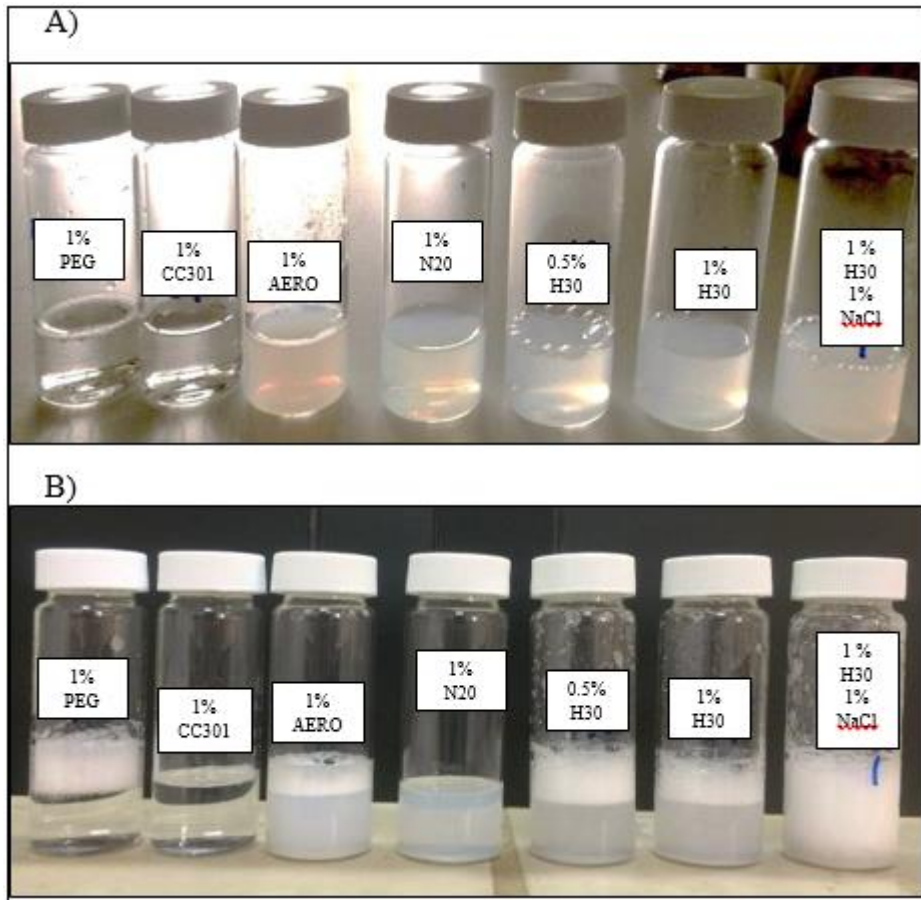


Figure 5.1. Dispersion A) before B) after the early foamability test

As observed from the figure, N20 couldn't generate foam. On the contrary, the utmost foam was obtained with H30, as proof of the literature. This test also indicated that NaCl promoted foam formation as expected. After that stage, the dispersion was put aside to watch foams half-life as a proof of stability. Figure 5.2 represented the picture of the foams after 16 hours which was the half-life of the H30 dispersions. This result was much higher than the half-life of the surfactant foam which could be describe in minute or a few hours (Wang, 2017). The foam which was created with AERO dispersion was collapsed too fast. The half-life of the PEG and CC301 was around 10 h.

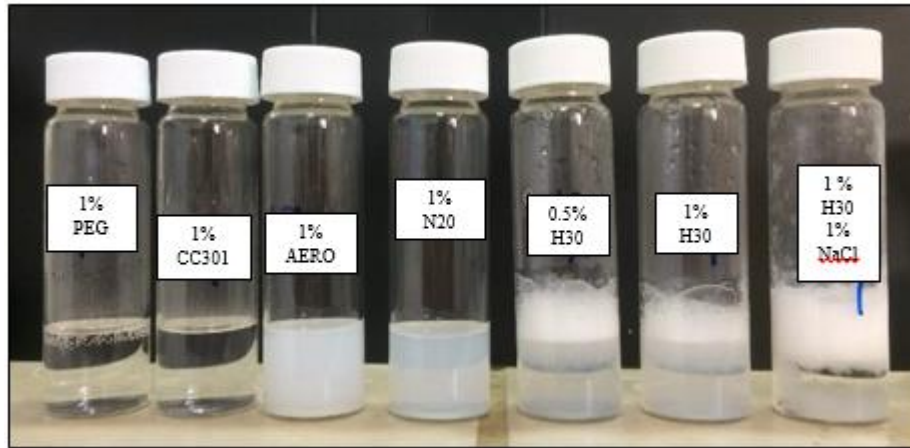


Figure 5.2. Foams after 16 hours of the early foam test

After the foamability test, N20 and AERO were eliminated. Then, before the final decision of nanodispersion selection for flood tests, the particle size of nanoparticles in dispersions was analyzed to figure out if the dispersions were stable or not. The dispersions, content %1 nanoparticle and %1 NaCl, by using PEG, CC301 and H30 and also %2 H30 was prepared to this end. The test was conducted by the Middle East Technical University Central Laboratory (MERLAB). The average results showed in Table 5.2 and the analyses report were given in APPENDIX C. As could be seen from the table, H30 dispersions were not stable because its particle size was higher than expected which point out agglomeration.

Table 5.2. Particle size distribution of the dispersions

	PEG	CC301	H30	
<b>Dispersion</b>	1% Nanosilica+ 1% NaCl	1% Nanosilica+ 1% NaCl	1% Nanosilica+ 1% NaCl	2% Nanosilica
<b>Average Particle Size</b>	10.1 nm	9.6 nm	48.6 $\mu\text{m}$	5.8 $\mu\text{m}$

### 5.1.2. Effect of the Salinity

After seeing the positive effect of the NaCl, its different concentrations were tested. %1 H3O dispersion with 1%, 2% and 5% concentrated NaCl solutions were prepared and again shaken a minute hardly. The foam was obtained for all concentration of NaCl content but the particle agglomeration was visible with respect to the increased concentration of NaCl as observed from Figure 5.3. According to literature, NaCl content greater than 1.5% generates flocculation of the nanosilica particles (Metin, 2011). Also, the critical salt concentration was higher for small diameter nanoparticles (Azadgoleh, 2014).

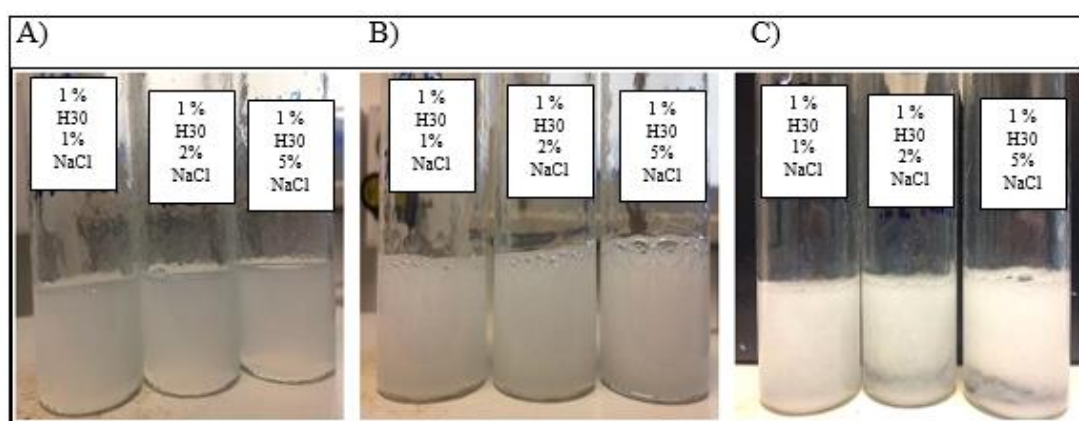


Figure 5.3. The effect of the NaCl concentration on the foam generated by 1% H3O dispersion A) before B) after C) 1 hour later

### 5.1.3. Effect of the Concentration

The same test also was conducted with 0.5% H3O dispersion to compare the effect of the H3O concentration on foamability. The results suggested that the higher the concentration, the better the foamability (Figure 5.4). In that case, the cost of the nanoparticle should be thought and it was important to select the optimum concentration.

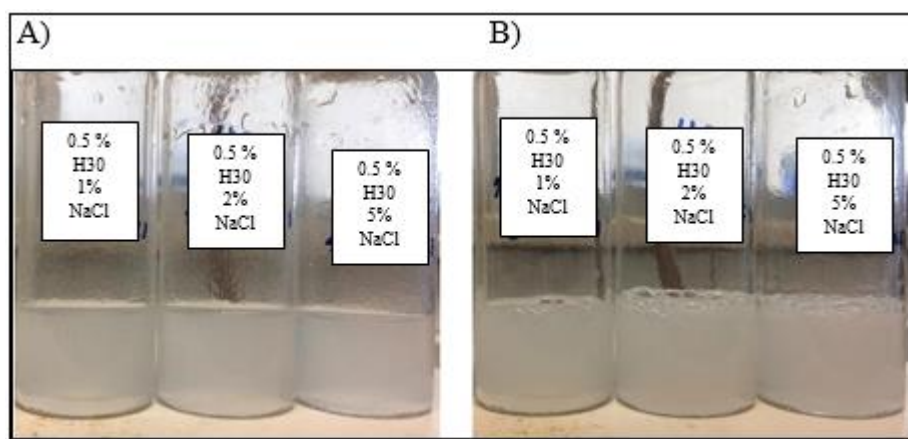


Figure 5.4. The effect of the NaCl concentration on the foam generated by 0.5% H30 dispersion A) before B) after

#### 5.1.4. Effect of the Temperature

This time, the dispersion was prepared and just waited at 25 °C and 65 °C which was B.Raman reservoir temperature to see if flocculation or/and agglomeration was occurring or not. Figure 5.5 explained the dispersion stabilization when dispersions were exposed 25 °C and 65 °C for two days. It was not possible to see clearly from the figure that the H30 dispersion was not stable at 65°C after 2 days. The figure of the detailed photo of the H30 dispersion was placed below additionally for this reason (Figure 5.6). The other dispersions seemed stable even at 65 °C.

#### 5.1.5. Effect of the pH

PH adjustment is one of the methods to stabilize nanoparticle dispersions. Therefore, zeta potential test by titrating acid and base was carried out at the laboratory of the National Nanotechnology Research Center (UNAM). The graphs were in Figure 5.7 and Figure 5.8. As explained in CHAPTER 4, nanoparticles with Zeta Potential values higher than +30 mV or lower than -30 mV have the best stability. Therefore, as figures indicated, dispersions should be stable at the pH above 9. For this reason, 1% H30 dispersions' pH was measured and adjusted 10 with sodium hydroxide (NaOH). After that, the particle size distribution analysis was performed again. All results were shown in *Table 5.3*.

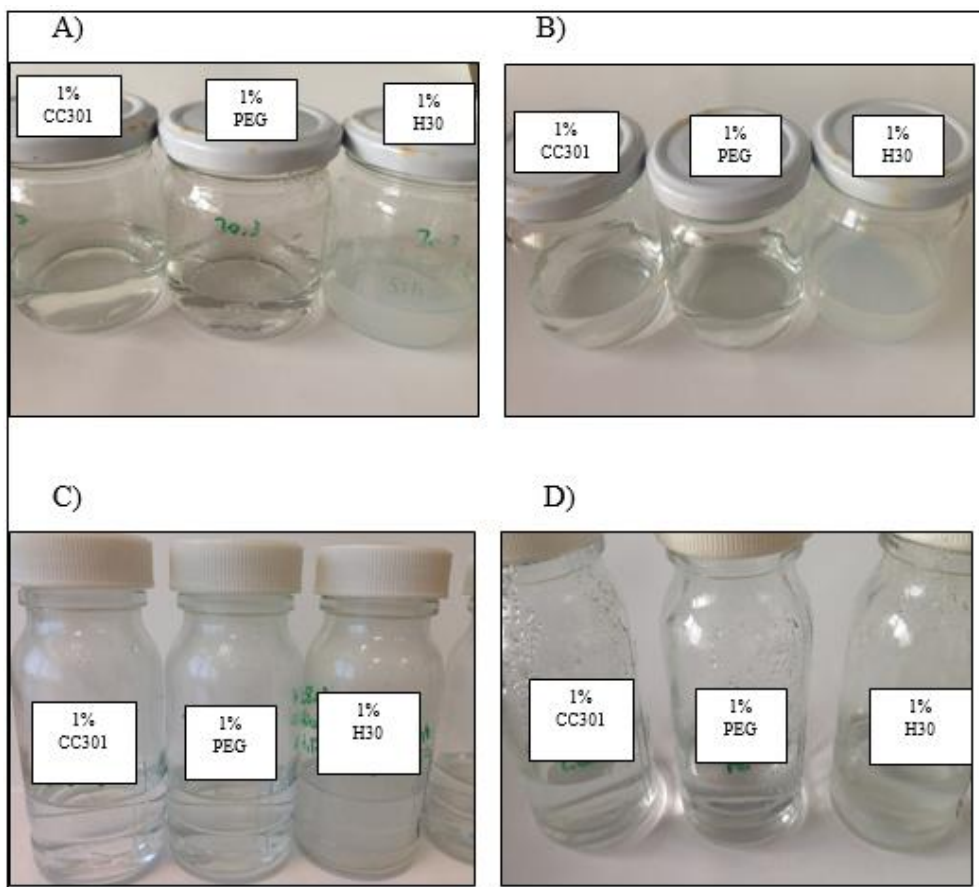


Figure 5.5. Dispersion stabilization A) at 25 °C B) two days after at 25 °C C) at 65 °C D) 2 days after at 65 °C

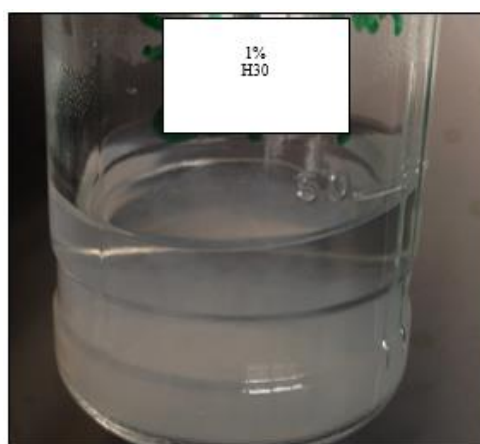


Figure 5.6. H30 dispersion after 2 days at 65 °C

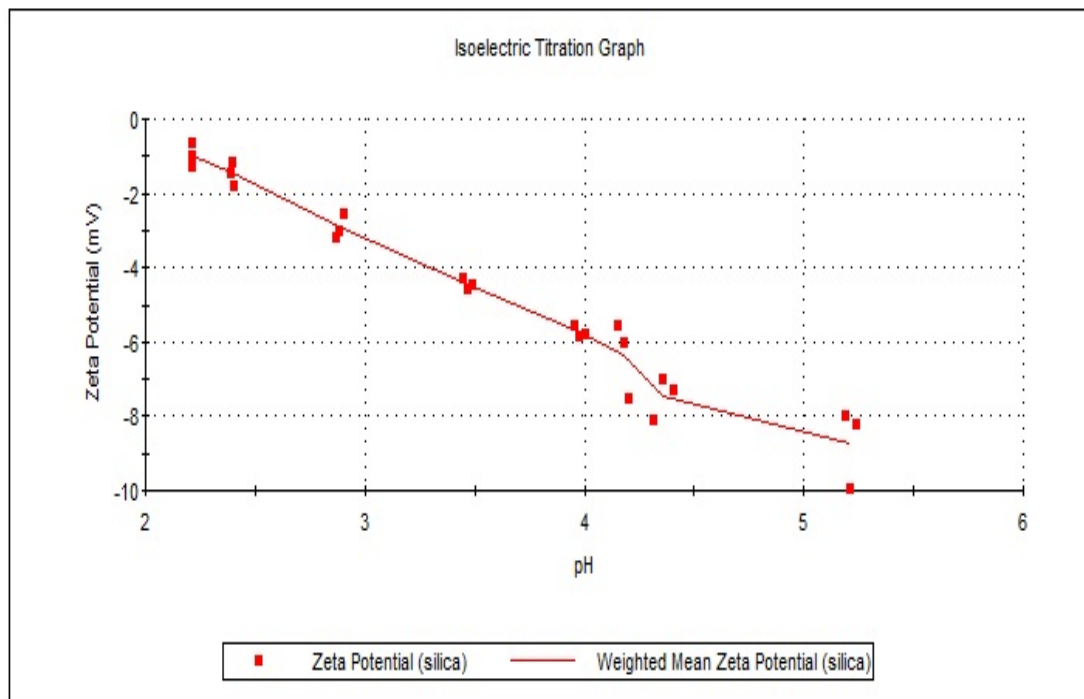


Figure 5.7. Zeta potential during acid titration

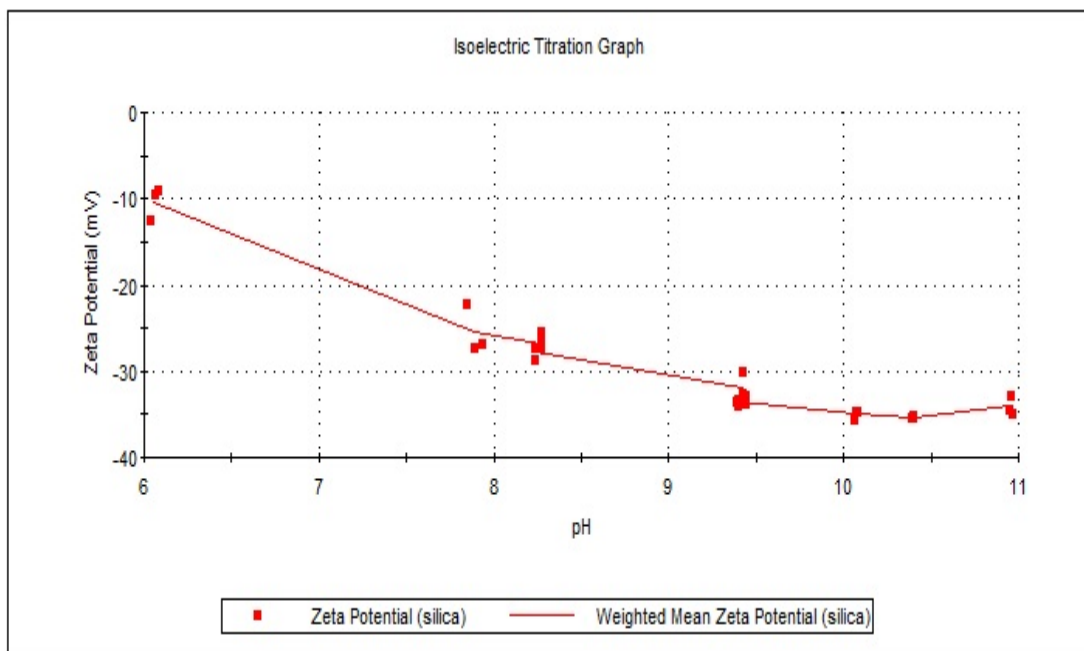


Figure 5.8. Zeta potential during base titration

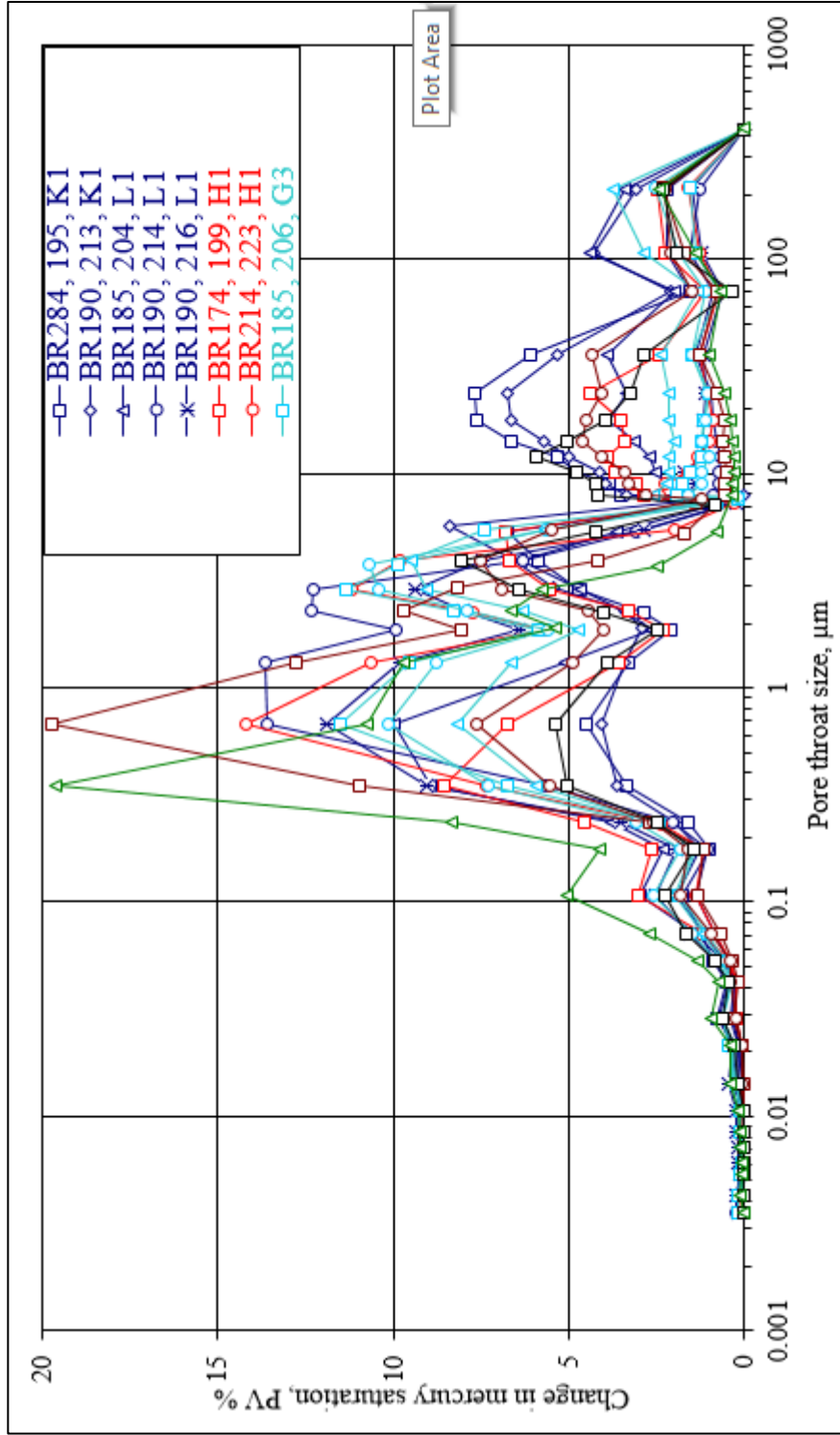


Figure 5.9. B. Raman pore throat size distribution (Karabakal, 2008)

Table 5.3. Particle size distribution analysis results before and after pH adjustment

Dispersion	pH, 25°C	Average Particle Size
% 1 H30 + 1% NaCl	6.09	48.6 μm
	10.02	122.7 nm

The result at pH 10 showed that the dispersion was stabled. The particle size was enough small for B. Raman matrix as shown in *Figure 5.9*. It was proper for the flooding test if the particles in the dispersion were below 200 nm.

After this result, early foam tests at pH 9-10-11 were performed again to see foamability of the dispersion. As *Figure 5.10* indicated, high pH has a negative impact on foam formation. In other words, the foam couldn't be seen when pH was increased. Therefore, it inferred that pH adjustment was not appropriate for this study, even though the positive results in the particle size analysis were achieved.

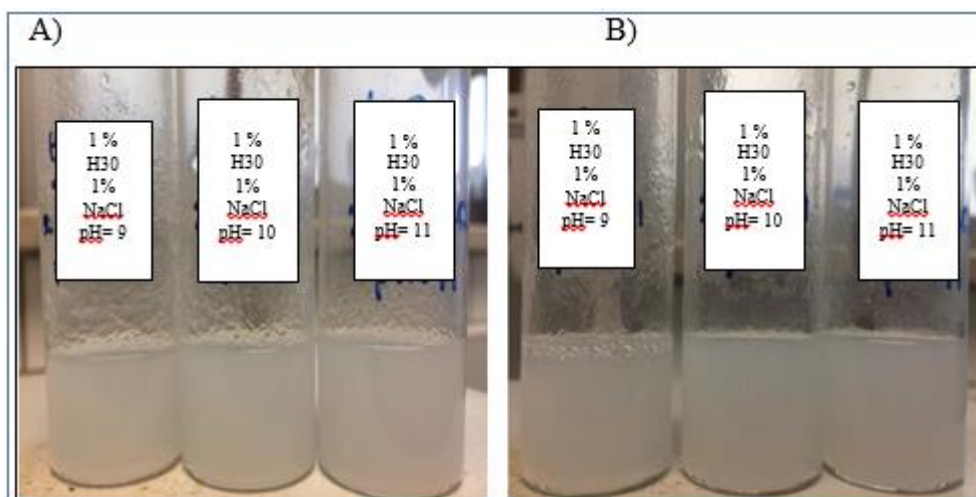


Figure 5.10. The effect of the pH on the foam generated by 1 % H30 dispersion A) before B) after

## 5.2. NANOSILICA DISPERSION STABILIZATION, FOAMABILITY AND PARAMETERS EFFECT

This test was performed for two objectives; 1) if there was any plugging due to the instability of the nanoparticle dispersions and 2) if any adsorption on the rock was occurring during dispersion flooding. For this purpose, first, the 1.5 inch carbonate core from B. Raman field was selected and analyzed by using permeameter and porosimeter. Then, the core was inserted to the core holder in the core flood system for flooding test. 1 % concentrated nanosilica dispersions for PEG, CC301 and H30 were prepared and placed into the accumulator. First core was saturated with B.Raman formation water then dispersions was flooded through the core sample each in turn to figure out whether or not nanosilica had an effect on core permeability. Flood test was performed by injection about 10 PV nanosilica dispersions at 600 psi and room temperature (~25 °C) and all pressure drops were recorded. Core sample information and the test results graph were shown in *Table 5.4* and *Figure 5.11*, respectively.

Table 5.4. *Properties of B.Raman field core sample*

PARAMETER	RESULT
Length (L), cm	6.7
Diameter (d), cm	3.78
Pore Volume ( $V_p$ ), cc	15.56
Grain Density ( $\rho_g$ ), g/cc	2.71
Porosity ( $\Phi$ ), %	20.8
Permeability ( $k_{air}$ ), md	105.43

As clearly depicted in *Figure 5.11*, the pressure drop was increased by increasing the injection of H30 dispersion which indicated a permeability decrease. On the other hand, other dispersions (PEG and CC301 dispersions) had a stable pressure drop as expected. These results were compatible with the results of B. Raman pore throat size distribution and dispersion stabilization studies. Because of all this, it was decided not to use H30 for further analyses due to the stability problem. This nanoparticle can be suitable for high permeable reservoirs but not for B. Raman field which have low permeability.

Additionally, the concentration of the silica in nanosilica dispersion was attempted to analyze before and after flooding for again proving if there was any adsorption in the matrix. XRF spectroscopy was used for this purpose. It was obvious that H30 dispersion plugged the system, so PEG dispersion was selected to analyze which had the same particle size as CC301. 0.6 % PEG dispersion was prepared. The core was saturated with formation water then the dispersion was flooded through the core. The properties of the core sample were listed in *Table 5.5*. First, 5 PV dispersion was flooded and then the output tube was changed and an extra 5 PV was injected. After that, the silica content of the fluid inside the output tube was analyzed by XRF. The results were given in *Table 5.6* and detailed analysis report was in APPENDIX D. A confusing results were obtained. The output included a little higher silica. This result was thought to be due evaporation of the output fluids during analysis and standard deviation of the spectroscope. It could be said that no adsorption occurred during dispersion flooding with PEG.

Table 5.5. *Properties of the core sample*

PARAMETER	RESULT
Length (L), cm	5.22
Diameter (d), cm	3.80
Pore Volume( $V_p$ ), cc	4.3
Grain Density ( $\rho_g$ ), g/cc	2.68
Porosity ( $\Phi$ ), %	7.26
Permeability ( $k_{air}$ ), md	13.52

Table 5.6. *Results of the XRF analysis*

ELEMENT	CONCENTRATION, wt %	
	Before Flooding	After Flooding
Si	0.579	0.599

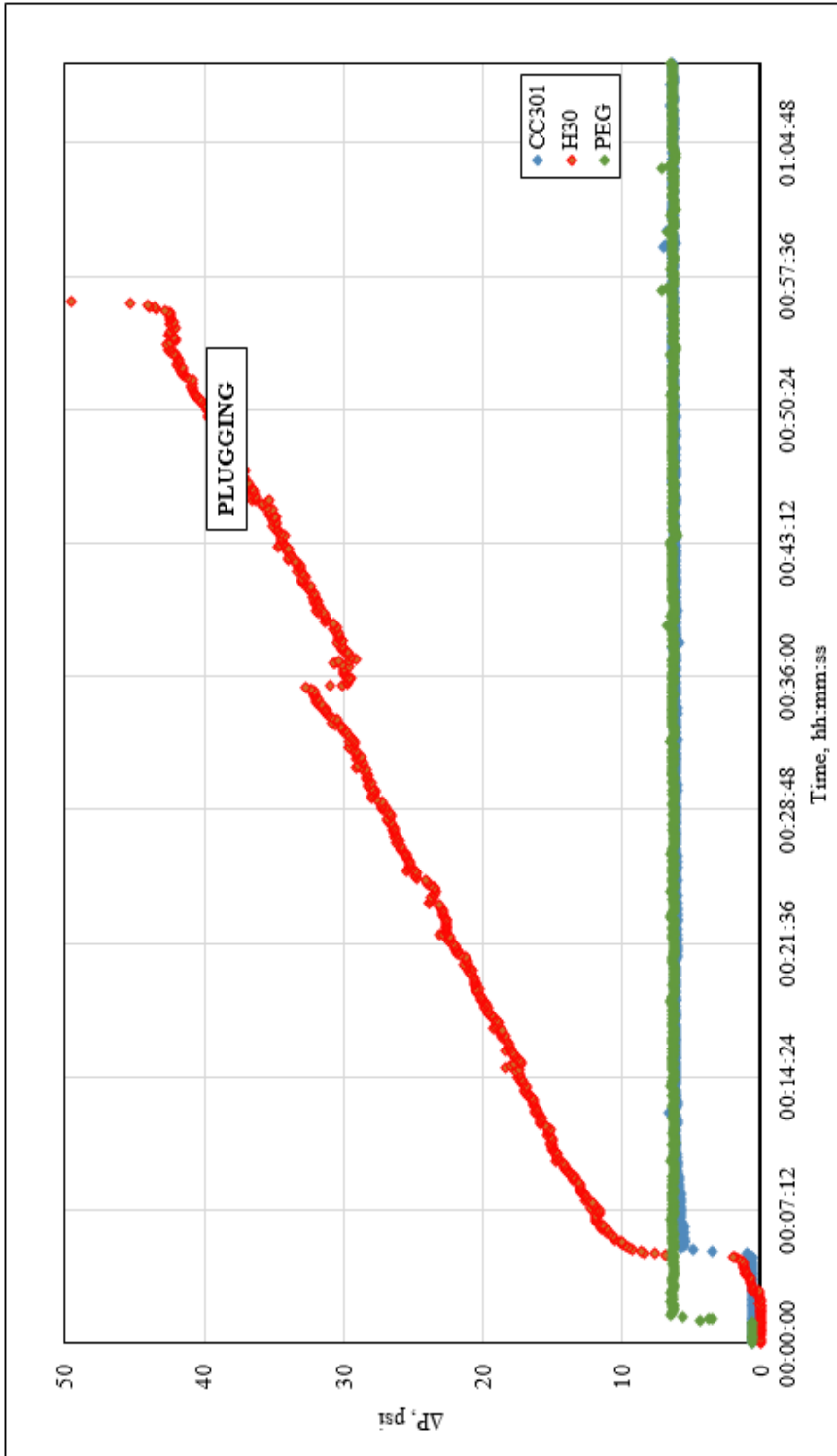


Figure 5.11. Pressure differences during dispersion flooding

### 5.3. PVT SIMULATION

Before starting foam generation tests, Dodan gas's phase diagram was drawn by using Calsep's PVTsim Compositional Simulator. Because the critical pressure and temperature of the gases were crucial parameters for the generation of foam. In the supercritical region, the fluid acts as both a liquid and a gas. In other saying, it supercritical fluids have liquid-like densities and gas-like diffusivities, particularly. In our study, both gas and supercritical phase of CO<sub>2</sub> were used by changing pressure. was aimed to get a better interaction between CO<sub>2</sub> and nanodispersion when CO<sub>2</sub> at its supercritical phase. Therefore, PVTsim program and equation of Peng-Robinson (PR) were used to control the critical point of the Dodan gas.

Pure (99.9%) CO<sub>2</sub> was also studied to see the differences. The graphs were pictured in Figure 5.12 and Figure 5.13. The composition of the Dodan gas was detailed in CHAPTER 4 and this composition was inserted to the simulation program. Different vapor to liquid volume ratio was applied and the critical point found as 1030 psi and 82 °F. If the pure Dodan gas's graph was investigated, then it could be said that the location of the critical point was not too different. The critical point of the pure gas was seen as 1060 psi and 88 °F. The literature also checked (Voormeij, 2010) and it said that CO<sub>2</sub> gas critical point was 1050 psi and 31 °C (87.8 °F) as PVTsim results gave for pure CO<sub>2</sub>.

The gas's pressure should be over 1100 psi with a confidential interval within the framework of the knowledge up to this point to reach the supercritical point. The temperature was applied as 65 °C to express B. Raman field as much as it could be, so it has already above 31 °C.

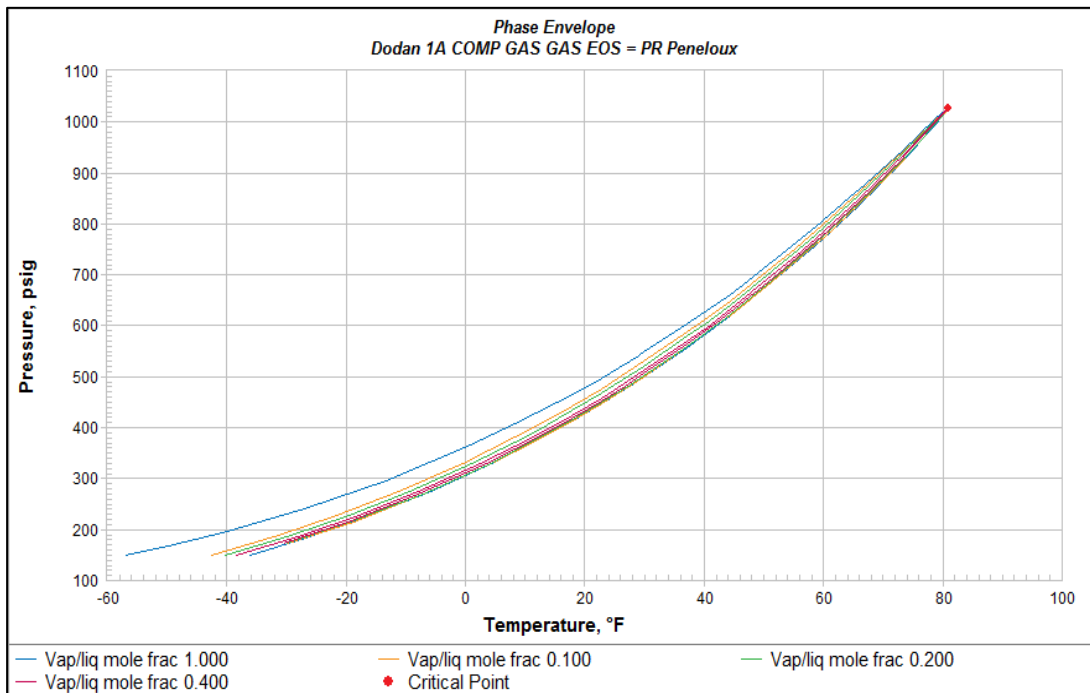


Figure 5.12. Phase diagram of the Dodan gas

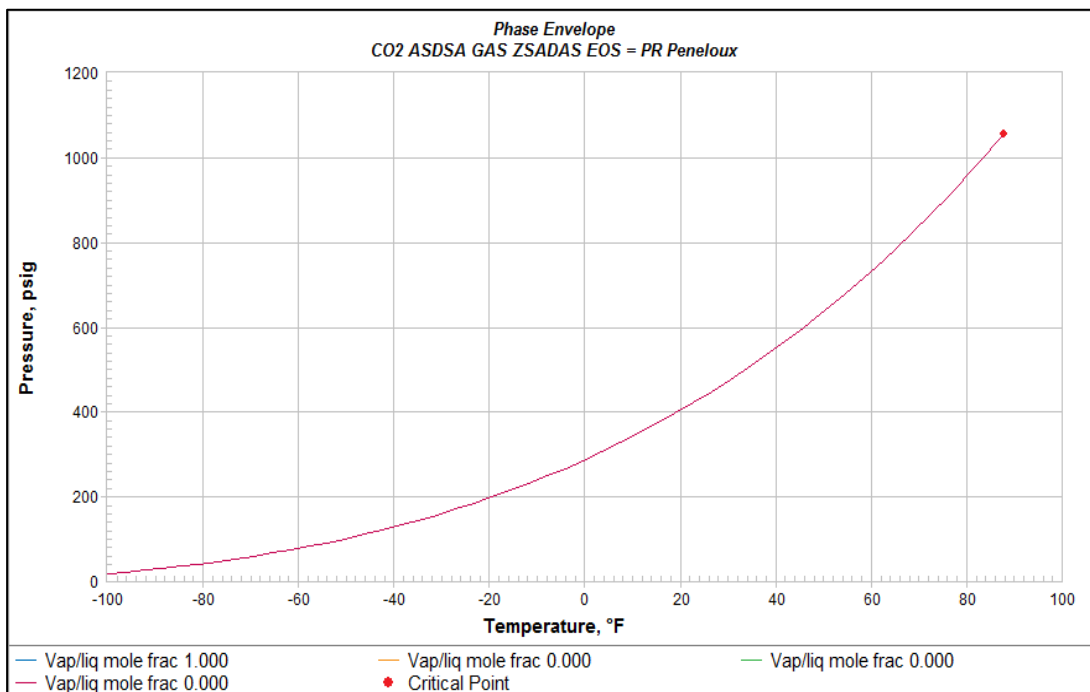


Figure 5.13. Phase diagram of the pure CO2

#### 5.4. FOAM GENERATION FLOOD TEST

Flooding test was run by using the Core Flooding System which was described before. The flow diagram was shown in Figure 5.14. The aim of the test was seeing the pressure differences during flooding test and visualized foam. These differences were going to be used as a proof of the foam generation. Because this denser foam form will increase the differences between upstream and downstream pressure. In addition, a sapphire observation cell was inserted to the system to see whether or not foam could be generated.

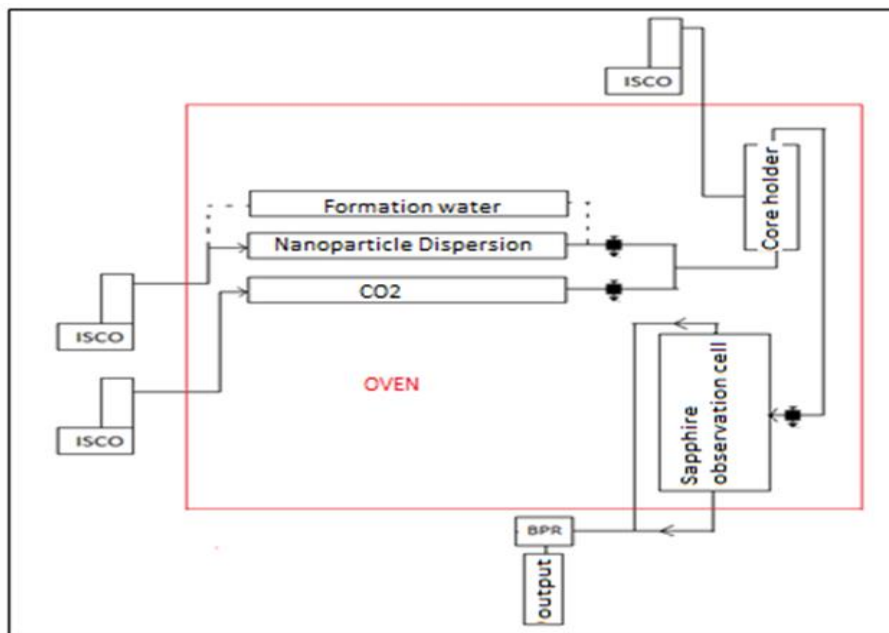


Figure 5.14. Flow diagram of the core flooding system for foam generation test

All information which was obtained from the tests and literature designated the foam generation test conditions. That means, %1Nano+%1NaCl concentrated dispersions were prepared and the test conducted at 65 °C temperature and both 650 and 1200 psi pressure. Different flow ratio and flow rate were applied to find optimum condition for foam formation as well. 0.1% and 0.5 % concentration was also evaluated but no foam was visualized.

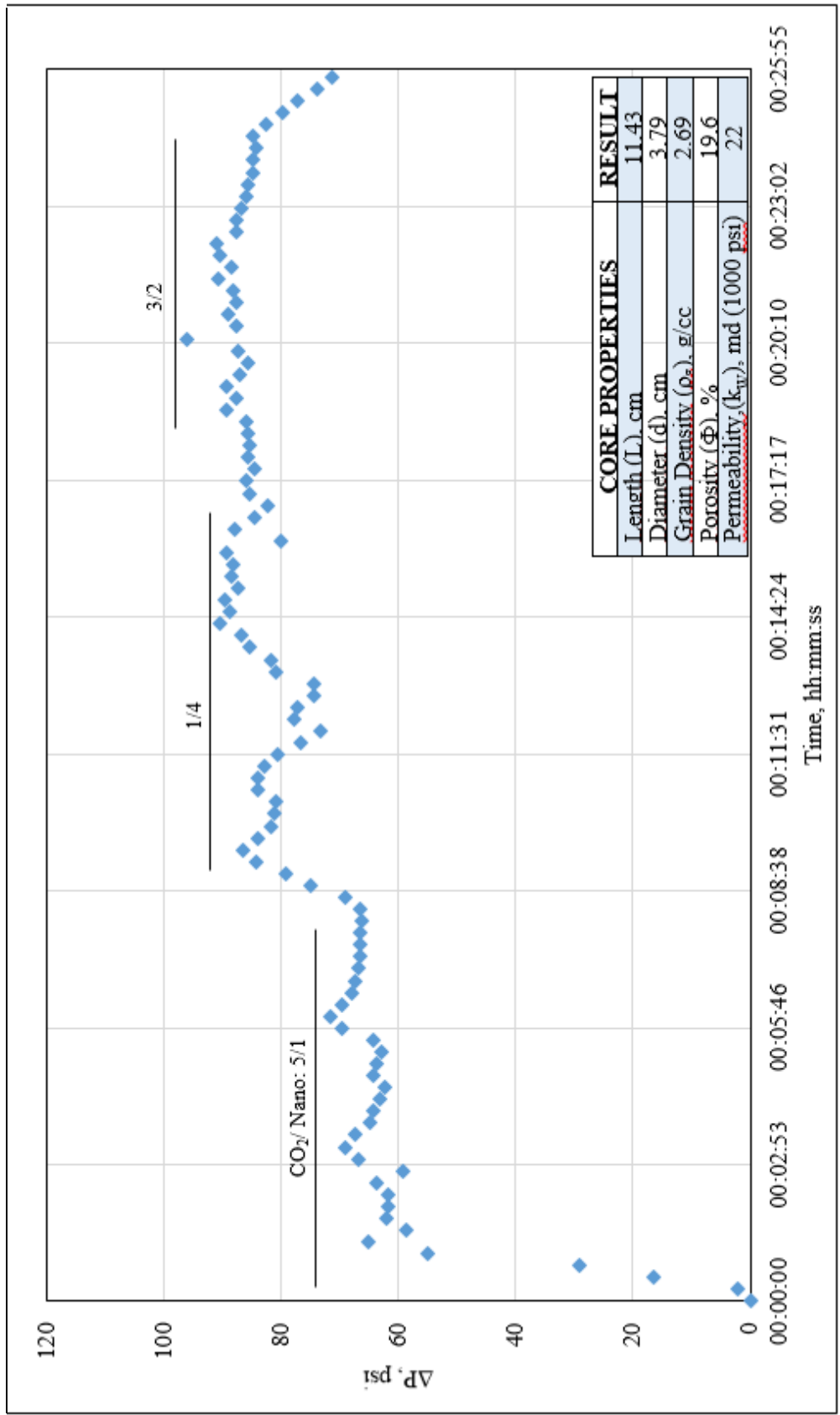


Figure 5.15. Pressure differences during simultaneous injection of the formation water and CO<sub>2</sub> at 650 psi 65 °C

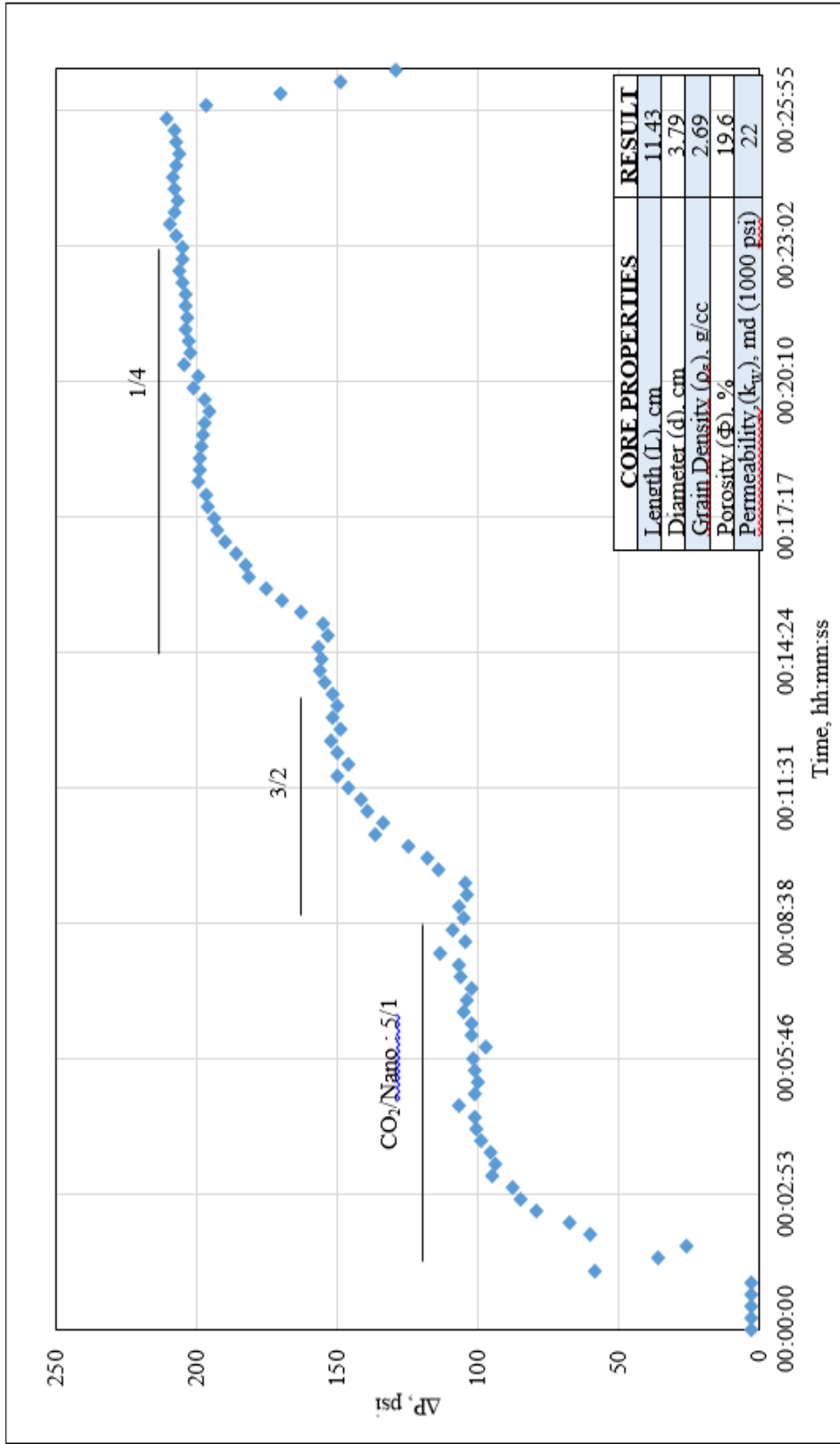


Figure 5.16. Pressure differences during simultaneous injection of the formation water and CO<sub>2</sub> at 1200 psi 65 °C

First of all, the core was saturated with B. Raman formation water at 1000 psi for 2 days. Then, CO<sub>2</sub> and formation water was flooded simultaneously through the core sample at both 650 and 1200 psi as the bases. The graphs were demonstrated in Figure 5.15 and *Figure 5.16*.

At 650 psi, CO<sub>2</sub> and water couldn't flow together as seen from the observation cell with the used core system. In other words, CO<sub>2</sub> and water got into the core sample slug by slug. Because the gas form of the CO<sub>2</sub> couldn't effort any pressure differences at the core entrance as much as water due to the compressibility of the gas phase. These sentences were proved by the fluctuation of the pressure differences in the graph of the flooding at 650 psi. However, when the pressure was increased to the 1200 psi, CO<sub>2</sub> acted as both liquid and gas phase, then flowed together.

*Figure 5.16* demonstrated this scenario. When pressure differences reached a steady state then flow rate and phase ratio was changed. All steps were reached the steady state in 3 seconds. This was stated because when the foam was generated, it was expected to see long term increase in pressure differences.

After this stage, the core sample was changed and saturated with formation water. Then, PEG and CO<sub>2</sub> were injected simultaneously. As told before, the properties of the core samples were given in their own graph. 650 psi was practiced first and the same result was attained again. The accumulation of the foam couldn't be displayed because it was not possible to see the top of the cell and also the shape of the sapphire cell (U shape) did not allow. Also, the graph of the pressure differences was pointed out in *Figure 5.17*. Now it was clear that it was not possible to inject gas and liquid form simultaneously with this system. Therefore, for CC301, 650 psi wouldn't be evaluated. Also, for recovery test step, it was decided to try a separate injection of the nanoparticle dispersion and CO<sub>2</sub> at 650 psi as a WAG. This subject going to be detailed later. Thereafter, the pressure was increased up to 1200 psi and differences between

downstream and upstream pressure were recorded. Different phase ratio (CO<sub>2</sub>/Nano dispersion) was executed and the higher increase of the pressure differences was tracked. The phase ratios were indicated on the graph which was named as Figure 5.18. The literature stated that when foam quality was 0.75, higher viscosity was reached means higher pressure differences (Di Carlo, 2015). On the other hand, they mostly used the phase ratio as 1. In this study, the viscosity of the foam didn't measure. The foam generation was detected with the increase in pressure differences as mentioned before. Foam quality describes as the fraction of the CO<sub>2</sub> to total CO<sub>2</sub>-nano dispersion mixture. In this study, the higher slope of pressure differences line was acquired when foam quality was 0.5 where the phase ratio was 1 and the total flow rate was 8 cc/min. Di Carlo et al. (2015) also couldn't see the foam at the lower total flow rate in their study as expected. Because the higher flow rate is going to create a higher shear rate and this shear will cause foam generation. Therefore higher value was selected this time, just to be on the safe side, because the main aim of this study was visualizing the foam. This much flow rate couldn't be used during recovery test due to high pressure generation anyway.

Afterward, the system was dismantled, the dispersion accumulator was cleaned and the core sample was changed. This time, CC301 dispersion was put into the accumulator and system was again heated to 65 °C. Then formation water was flooded through the core to saturate and later, CC301 and CO<sub>2</sub> were flooded together at 1200 psi. The graph was demonstrated in Figure 5.19. For this case, the total flow rate was also changed. The foam was visualized when passing through the sapphire observation cell. As expected, the foam was more visible with increased flow rate.

It was not planned to do this experiment with H30 due to the stability problem. But, as the literature stated, better foam formation was expected with this dispersion. Therefore, the plan was changed and 2% H30 dispersion was prepared with 1% NaCl. Then, this dispersion was filtered by using a 200 nm filter. It was pursued that after this filtration, nanoparticles did not plug the matrix. The reason why 2% concentrated dispersion was prepared was effluent after filtration might have enough silica content to generate foam. It was known that the graph of this run was not too meaningful because the pressure differences could be due to both plugging and foam formation. The graph (Figure 5.20) was given just for the information.

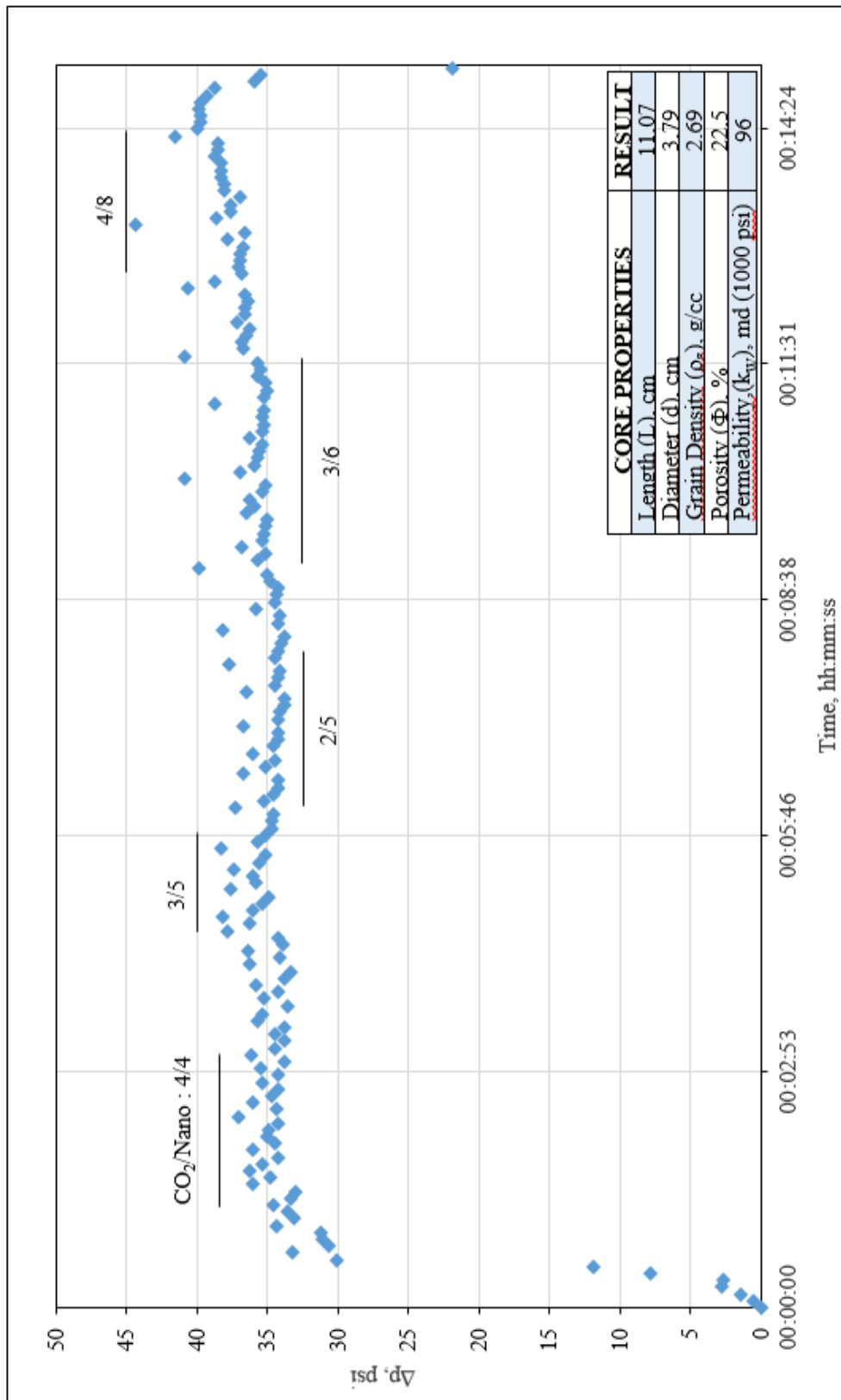


Figure 5.17. Pressure differences during simultaneous injection of the PEG and CO<sub>2</sub> at 650 psi 65 °C

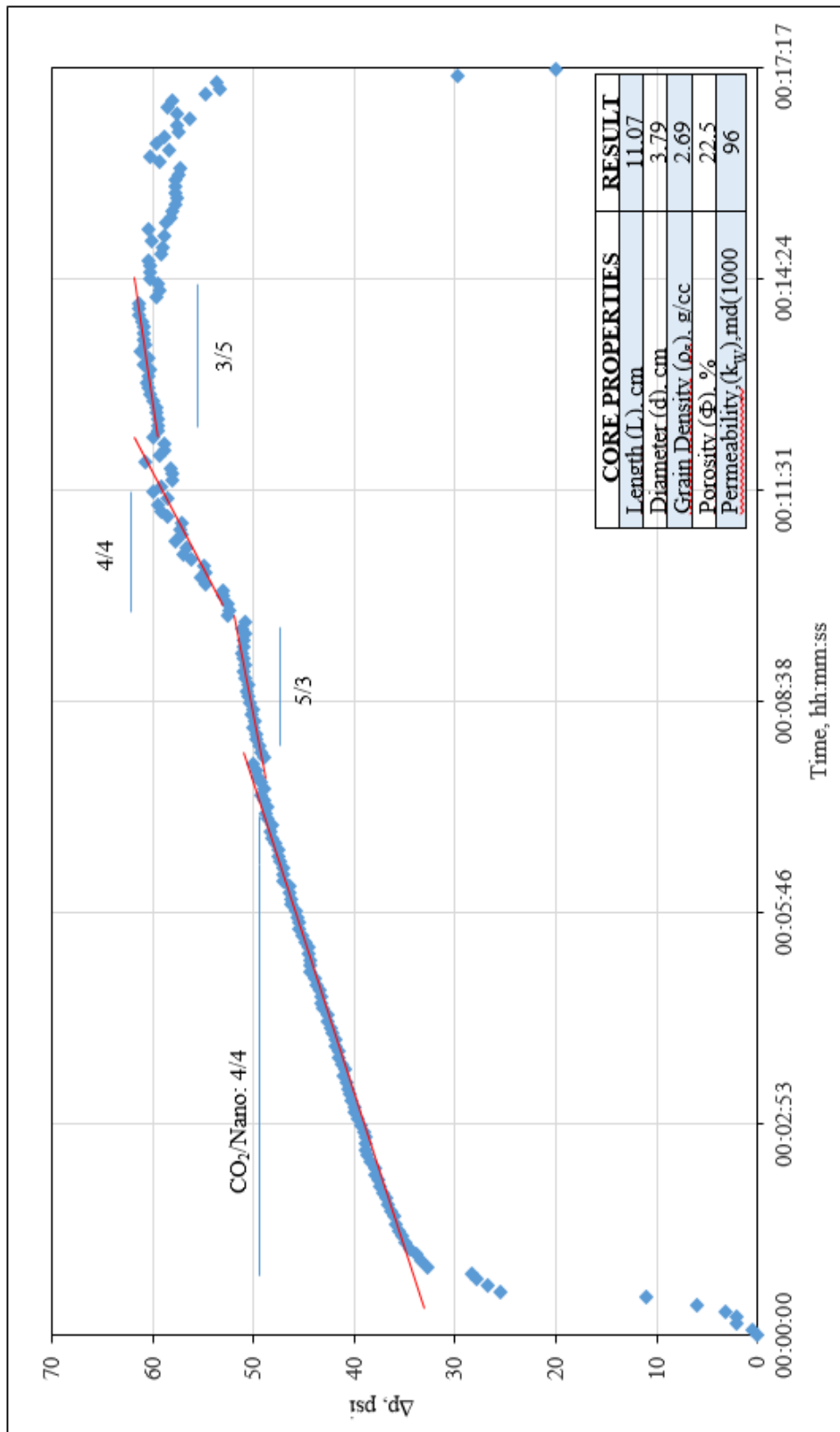


Figure 5.18. Pressure differences during simultaneous injection of the PEG and CO2 at 1200 psi 65 °C

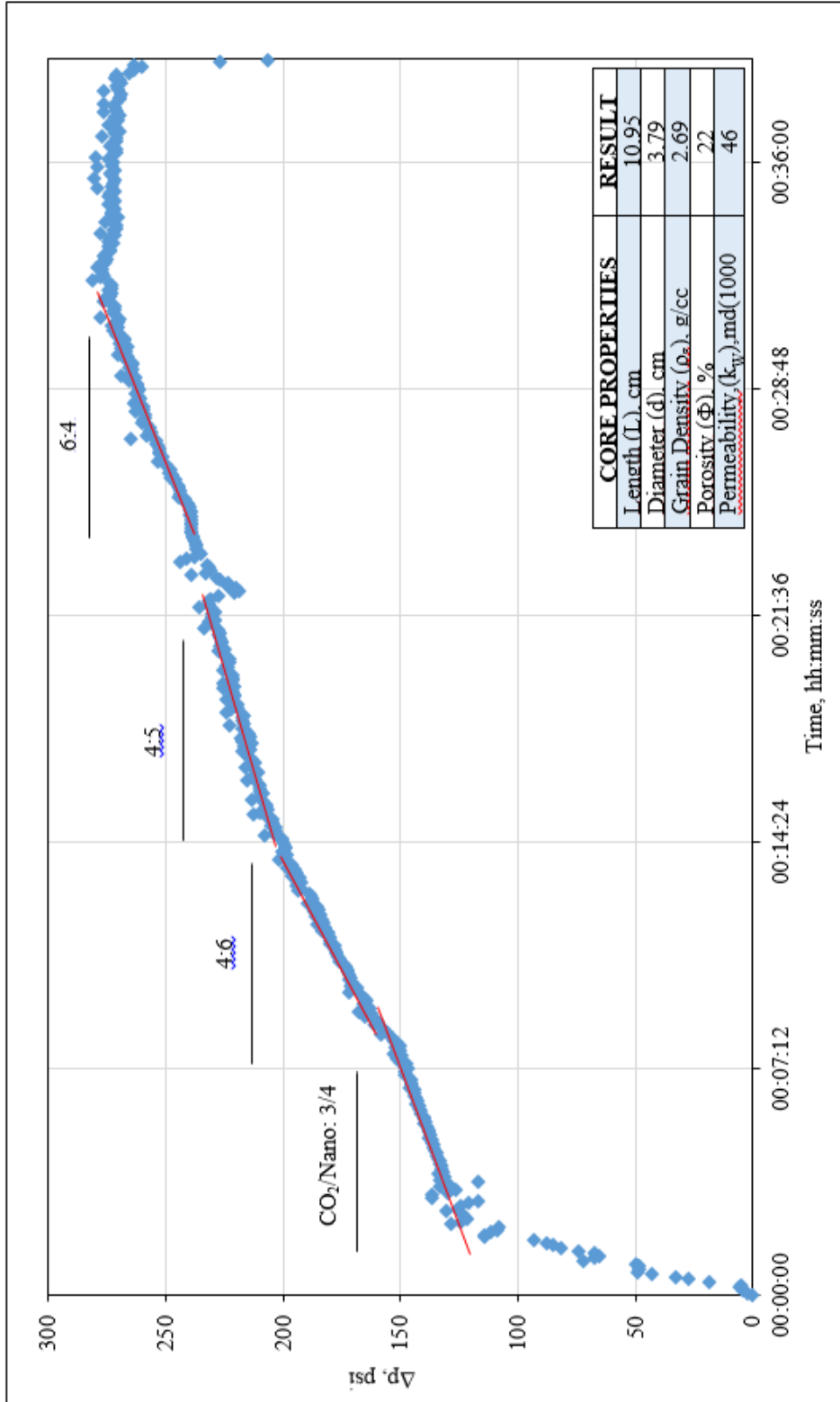


Figure 5.19. Pressure differences during simultaneous injection of the CC301 and CO2 at 1200 psi 65 °C

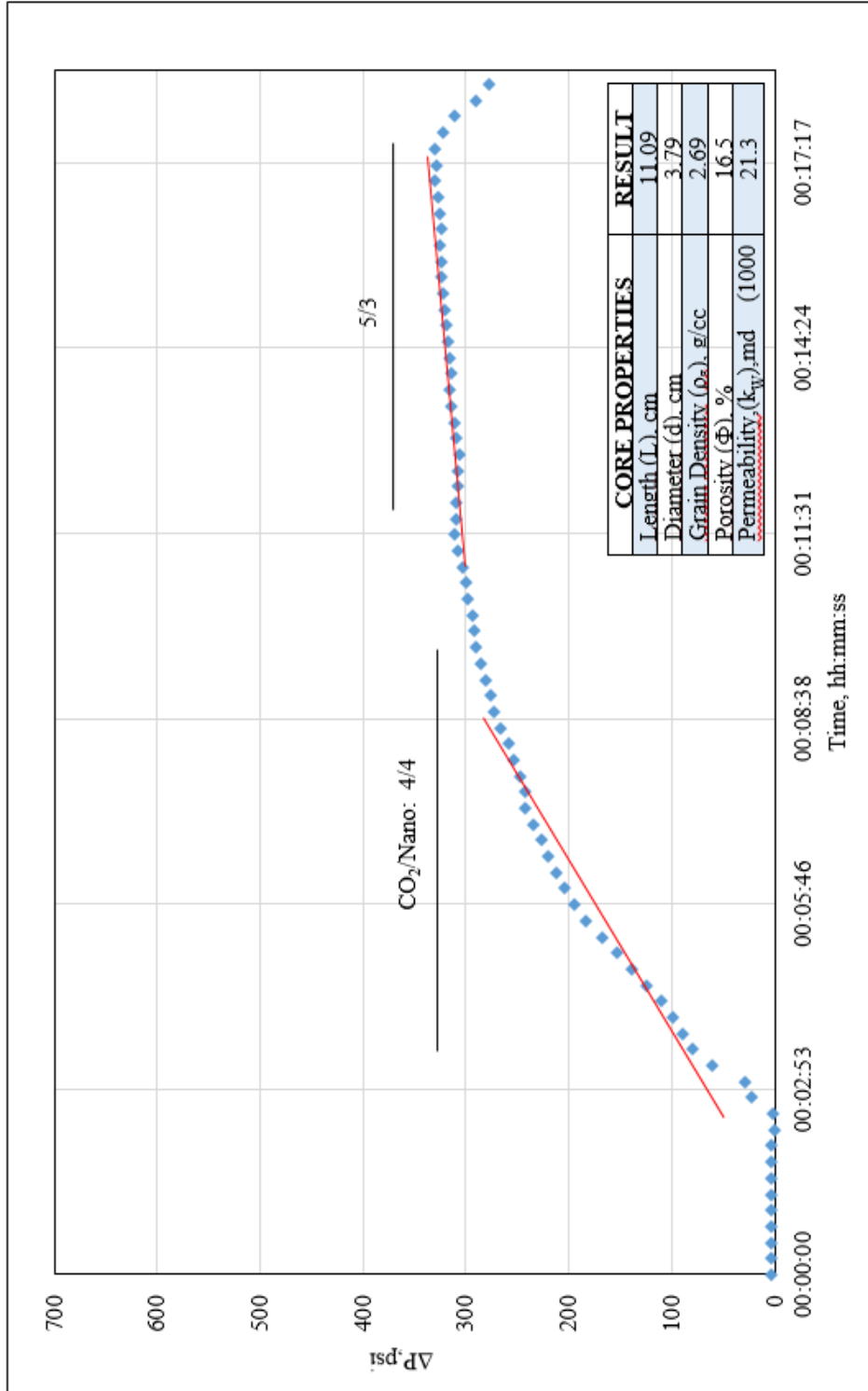


Figure 5.20. Pressure differences during simultaneous injection of the H3O and CO2 at 1200 psi 65 °C

Visualizing the foam in the observation cell was the purpose of H30 dispersion flooding. The foam with H30 was seen more visible than other flood experiments. The observation cell was filled with foam quickly. This study also had the same results; hydrophobicity effect to foamability positively. However, due to the stability problem, this nanoparticle is not going to be used for the recovery test. All input and the output of the flooding experiments were listed in *Table 5.7*. Moreover, *Figure 5.21* and *Figure 5.22* picturized the foam with CC301 and H30, respectively. The video of the foam during tests will be provided with a CD named as APPENDIX F.

*Table 5.7. Particle size distribution analysis results before and after pH adjustment*

Name	$k_w$ mD	$\Phi$ %	P psi	$C_{nano}$ %	$C_{NaCl}$ %	Phase Ratio (CO <sub>2</sub> :liquid)	$Q_{Total}$ cc/min	Foam Visual	Statement
Formation water	22	19.6	650	-	9	5:1	6	N	couldn't be coinjecte
						2:3	5	N	
						1:4	5	N	
			1200	-	9	5:1	6	N	
						3:2	5	N	
						1:4	5	N	
PEG	96	22.5	650	1	1	4:4	8	N	couldn't be coinjecte
						3:5	8	N	
						2:5	7	N	
			1200	1	1	3:6	9	N	
						4:8	12	N	
						4:4	8	Y	
CC301	46	22.0	1200	1	1	5:3	8	Y	Low quality
						3:5	8	Y	
						3:4	7	Y	
						4:5	9	Y	
						4:6	10	N	
						6:4	10	Y	
H30	21	16.5	1200	< 2	1	4:4	8	Y	
						5:3	8	Y	

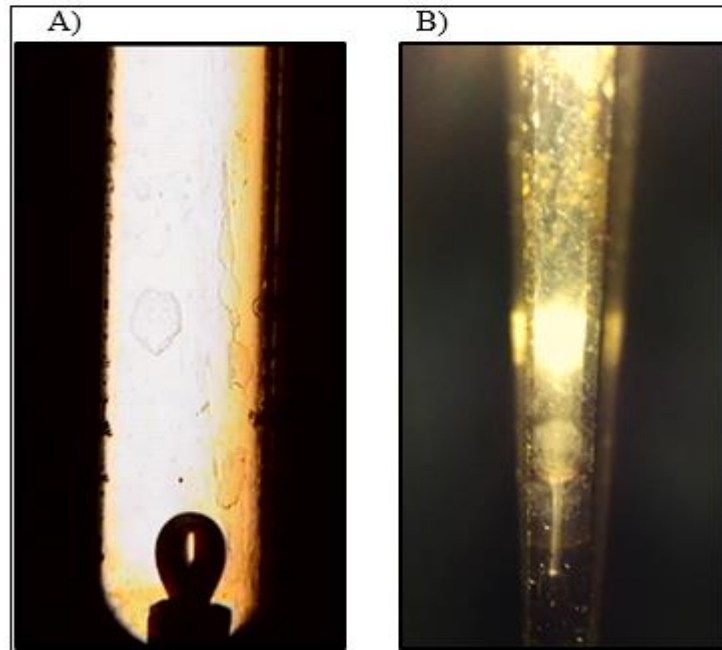


Figure 5.21. Sapphire observation cell image A) during the simultaneous injection of CO<sub>2</sub> and formation water B) during the simultaneous injection of CO<sub>2</sub> and CC301 dispersion

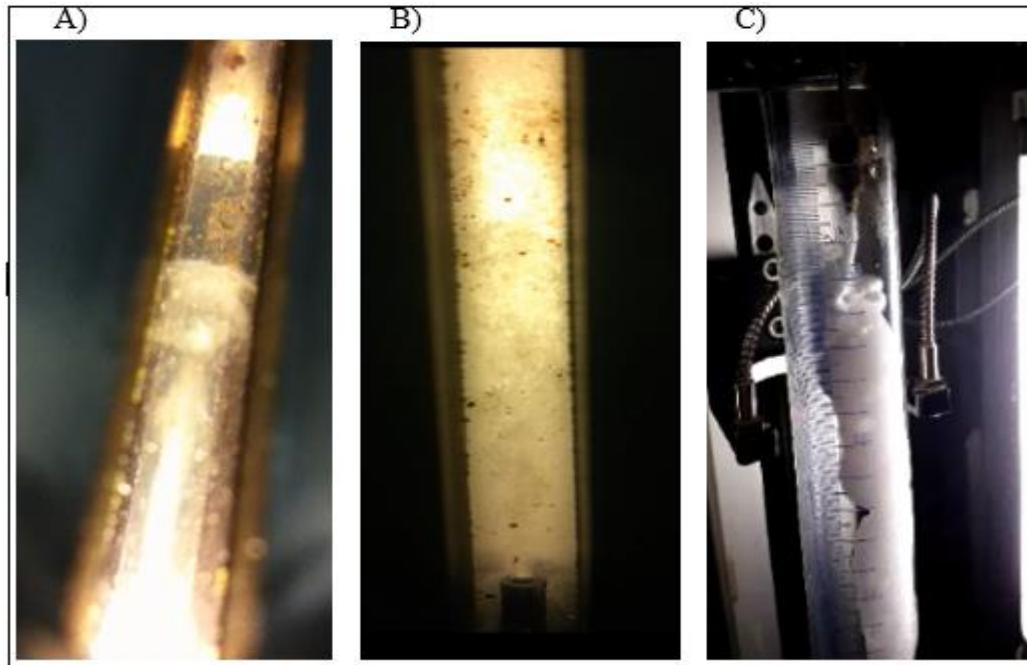


Figure 5.22. Foam image A) during the simultaneous injection of CO<sub>2</sub> and H<sub>3</sub>O B) when covered the observation cell C) when foam go out the system to the atmospheric condition

The foam in the core sample was visualized by using SEM/EDS system. The used silica nanoparticles are amorphous. The SEM system is not perfect for picturized these type of particles but at least give a rough picture. The image and EDS results were given in Figure 5.23. The reservoir of the B. Raman field has 100% carbonate rock. Thus, the display from the SEM and the silica peak from the EDS indicated the silica existing in the rock.

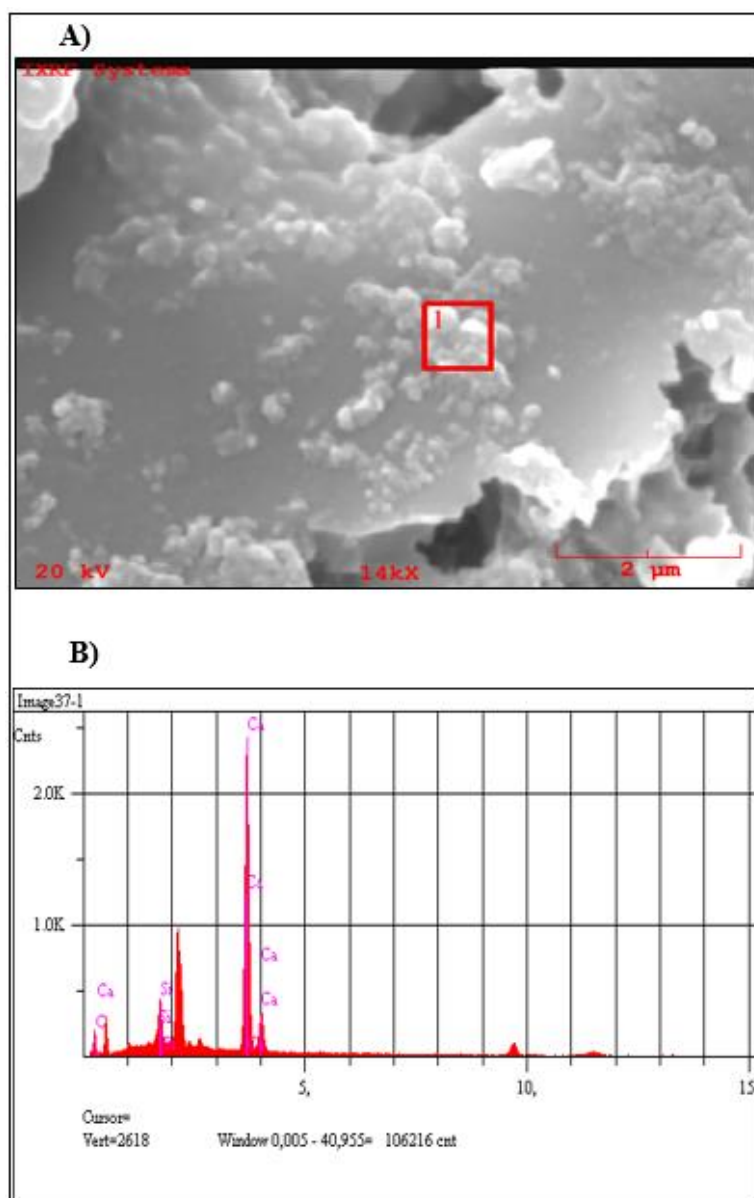


Figure 5.23. Results of the SEM/EDS A) picture of the silica particles B) chemical analysis

## 5.5. OIL RECOVERY

This study was performed to reveal extra oil production when the foam was applied. CO<sub>2</sub> injection and WAG application were run before foam to better representation of the B. Raman field case. Additionally, nanodispersions and CO<sub>2</sub> was also injected separately at 650 psi before foam application which was named as NWAG as declared before. 4.5 inch carbonate core and Dodan gas sample were used for oil recovery tests. The properties and the picture of the core sample were placed in the below table (Table 5.8). Dodan gas sample properties were also touched on CHAPTER 4.

Table 5.8. The properties and the picture of the core sample

PARAMETERS	RESULTS
Length (L), cm	14.02
Diameter (d), cm	8.75
Pore volume (V <sub>p</sub> ), cc	136.13
Grain density (ρ <sub>g</sub> ), g/cc	2.68
Porosity (Φ), %	16.1
Permeability (k <sub>w</sub> ), md	10.08



As mentioned early section, only PEG and CC301 was evaluated due to the instability of the H30 dispersion. Again, %1NaCl+%1 nanoparticle concentrated dispersion was used. System temperature was 65 °C and the phase ratio was 1. Flow diagram of the core flooding system was also demonstrated in Figure 5.24. The test will be detailed step by step for both PEG and CC301 dispersions.

### 5.5.1. Oil Recovery with CC301 Dispersion

1% NaCl + 1% CC301 dispersion was prepared first. All fluids (nanodispersion, Dodan gas and B. Raman oil) were placed into accumulators and core sample was inserted into core holder. After all, the system was heated up to 65 °C. Recovery test steps were listed below.

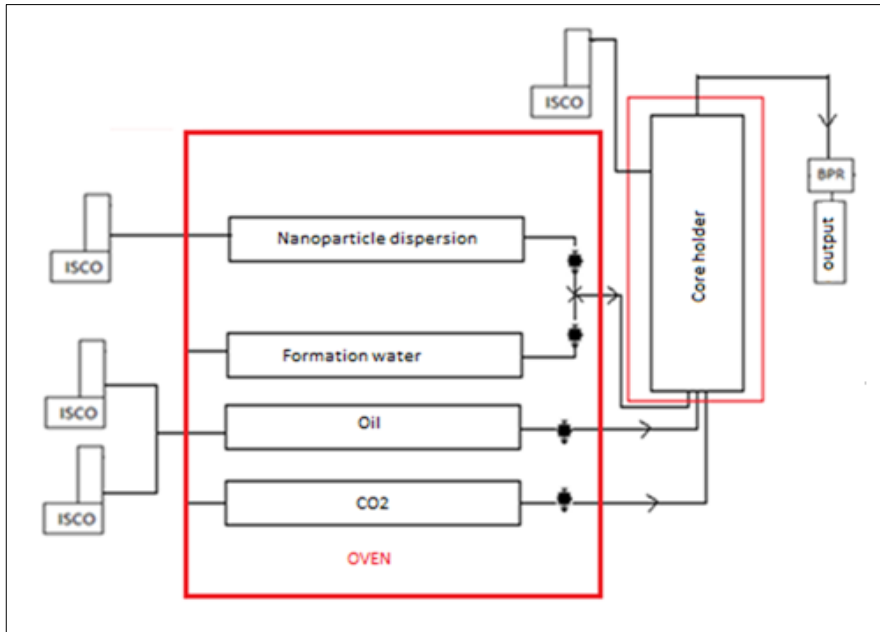


Figure 5.24. Flow diagram of the core flooding system for oil recovery test

- When the system reached the desired temperature, formation water was flooded through the core and saturated for two days at 1000 psi. Then, 2 PV B. Raman oil were injected till the residual water saturation and it was calculated as 10 %.
- After, CO<sub>2</sub> was flowed at 650 psi to reflect B. Raman field case. Because at this field, CO<sub>2</sub> injection has already been applied at this pressure. 28% of OOIP was produced at this step.
- At B. Raman field, CO<sub>2</sub> injection cuts and water injects to the system at regular intervals. Therefore, again to the better projection of the field, WAG was applied at 650 psi as another step. The flow was stopped when no more oil production was detected after 6 cycles of injection. Each cycle includes gas and water flow. The flooding was made at a flow rate of 0.25 cc/min and each was 0.2 PV. After this process, approximately 18% additional recovery was provided. It was also observed that the WAG system was more effective

than continuous CO<sub>2</sub> injection for a carbonate reservoir and provided extra recovery.

- After this step, the CO<sub>2</sub> and nanodispersion were injected sequentially (NWAG) at 650 psi as touched on before. Again, the flow was made at a flow rate of 0.25 cc/min and each of 0.2 PV. Although 3 cycles were applied, no significant production was observed. Even, foam formation was noticed barely in the sapphire observation cell, they were not of expected quality. Additional production in this step was below 1%.
- Finally, the system was pressurized to 1200 psi and the nanodispersion was coinjected with supercritical CO<sub>2</sub>. CO<sub>2</sub> / Nano phase ratio of 1: 1 was used. In this case, foam formation was observed in the production cell. The video of the oil that comes with the foam is added to the report with a CD named as APPENDIX F. The resulting oil was taken up in an emulsion form with foam as seen in Figure 5.25. The breaker was added to the emulsion and centrifuged. Then, the volume of the separated oil from emulsion was noted and calculated. An additional 25% recovery was obtained. After this result, it could be stated that CO<sub>2</sub> mobility was controlled with the formation of nanoparticle stabilized foam and this denser form penetrated to the matrix and swept the oil better than the gas form of the CO<sub>2</sub>.

After all these steps, total oil recovery was approximately 71 % of the OOIP. The graph of the experiment which includes all stages were shown in Figure 5.26.



*Figure 5.25.* The image of the production after centrifuge which was obtained when foam was applied

### **5.5.2. Oil Recovery with PEG Dispersion**

This time dispersion included 1% NaCl + 1% PEG. The system was again set up the same conditions.

- The same core sample was used for this experiment also. For this reason, formation water was injected first to clean core. Then, again, 2 pore volume reservoir oil was flooded through the core at 1000 psi. The pressure was decreased to 650 psi.
- First of all, CO<sub>2</sub> was injected to the core at 650 psi and 65 °C and 16% of the OOIP was produced. This amount is too smaller than the production with CC301. This may be due to aging or plugging during the oil recovery test using the dispersion of the CC301.

- Then, WAG was applied. After 6 cycles, each of them was 2PV, was introduced, 9% extra production was observed. Again, the flow rate of each application was 0.25 cc/min.
- The next was NWAG at 650 psi. After this application, extra oil production was noted as 4%. This time 5 cycle was enough. Again 0.2 PV and 0.25 cc/min fluids were flooded. This amount was higher than CC301 NWAG application.
- While working with the CC301, it was noticed that CO<sub>2</sub> injection at 1200 psi was not studied. However, some part of the extra oil recovery which was gained from the foam application could be achieved by only 1200 psi CO<sub>2</sub> injection. Another word, if CO<sub>2</sub> injection could produce to that much oil recovery which was obtained from foam application alone at that pressure. Therefore, at this step, only CO<sub>2</sub> at 1200 psi was flooded. Almost 8 PV of CO<sub>2</sub> was injected and only 1% of OOIP could be recovered.
- Lastly, PEG dispersion and CO<sub>2</sub> were flooded simultaneously at 1200 psi. This foam application was ended with an extra 7% oil recovery. Again the phase ratio was 1:1.

The graph of this experiment was demonstrated in Figure 5.27. When the amount of oil production in each step was evaluated, it could be stated that all steps of the PEG dispersion study were almost half of the CC301 dispersion case. As mentioned, these differences could be due to aging or plugging. Because the same core samples were used, so, a long time oil contamination has occurred before the PEG application. Also, CC301 could plug some tiny pores which led us to a low recovery. But, it can be declared that foam application is successful if the conditions are suitable. All results of each step for both CC301 and PEG studies were listed below table (*Table 5.9*). Also,

making more meaningful of these numerical values, the production of each step in total production was graphed and showed in *Figure 5.28*.

Table 5.9. *Oil recoveries of each step for all experiments*

<b>Oil Recovery, % OOIP</b>						
Dispersion	650 psi CO <sub>2</sub>	650 psi WAG	650 psi NWAG	1200 psi CO <sub>2</sub>	1200 psi Foam	Total
<b>CC301</b>	28	18	<1	-	25	71
<b>PEG</b>	16	9	4	1	7	37

The production data was provided as APPENDIX E and the live data of the recovery experiment was handed in a CD named as APPENDIX F.

Core saturation was calculated after the tests by using a Dean-Stark test system to verify the first condition and check the results of the tests. After, PEG experiment, the core was inserted to the Dean-Stark system and saturation was checked.

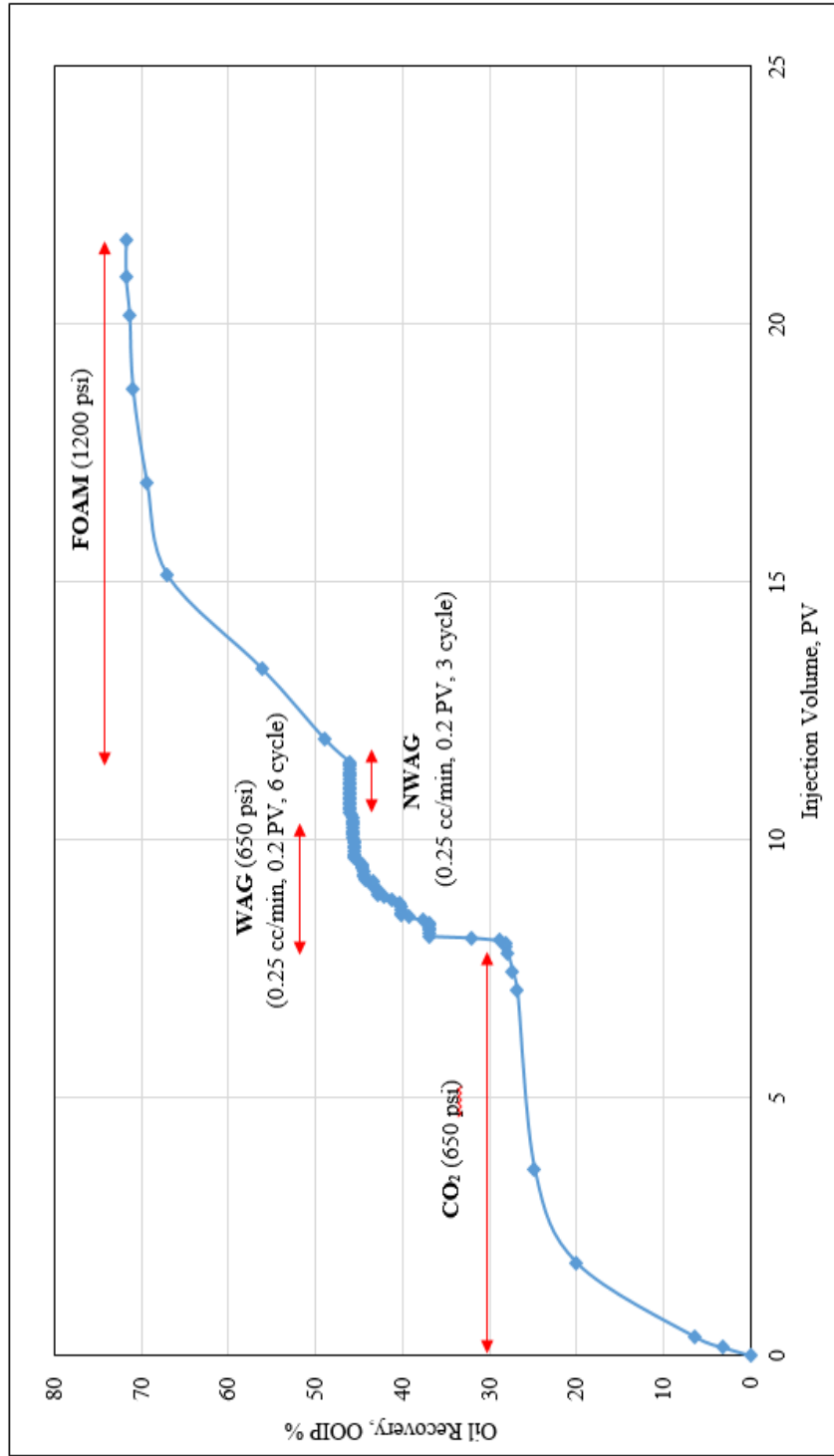


Figure 5.26. Oil recoveries in each step of the CC301 experiment

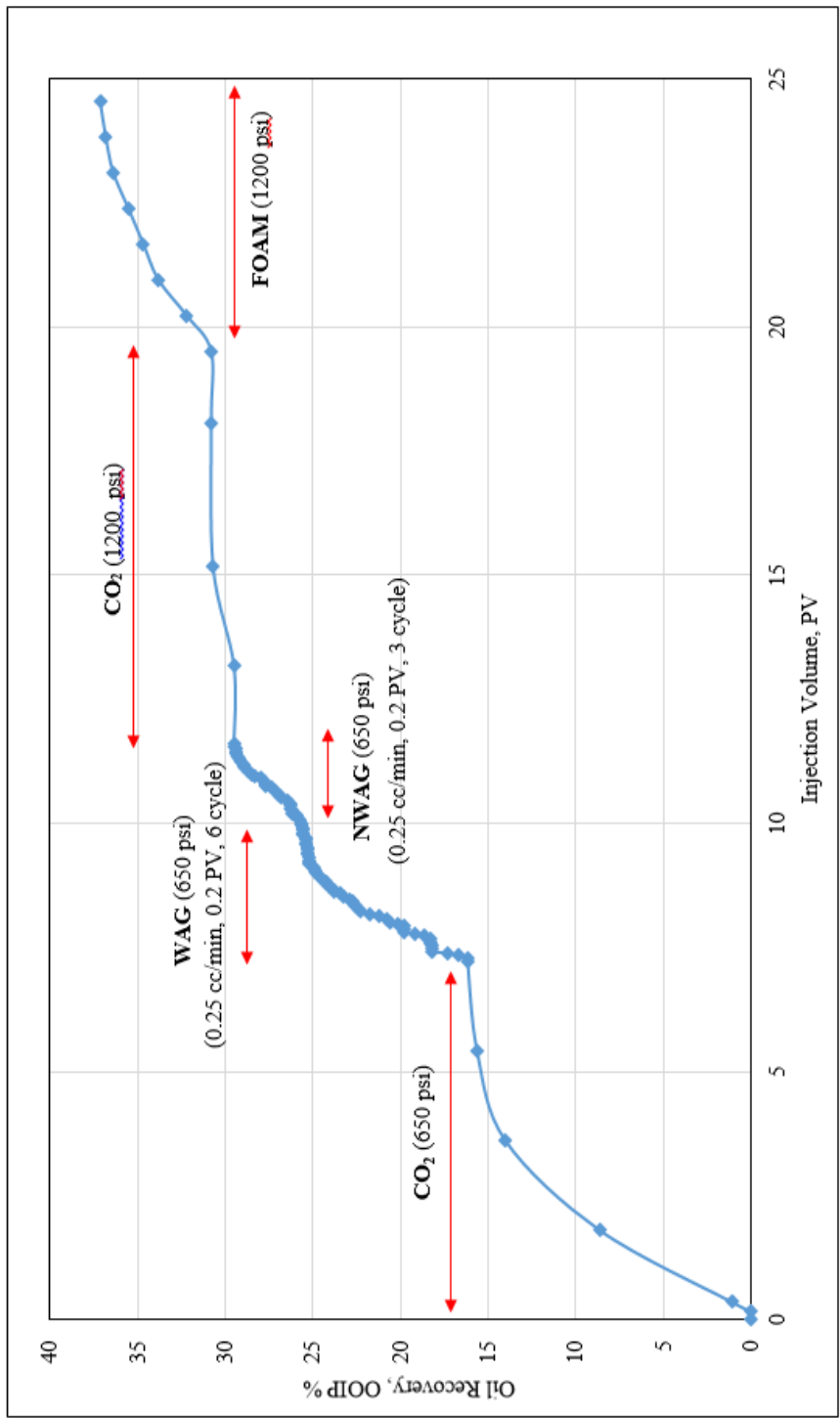


Figure 5.27. Oil recoveries in each step of the PEG experiment

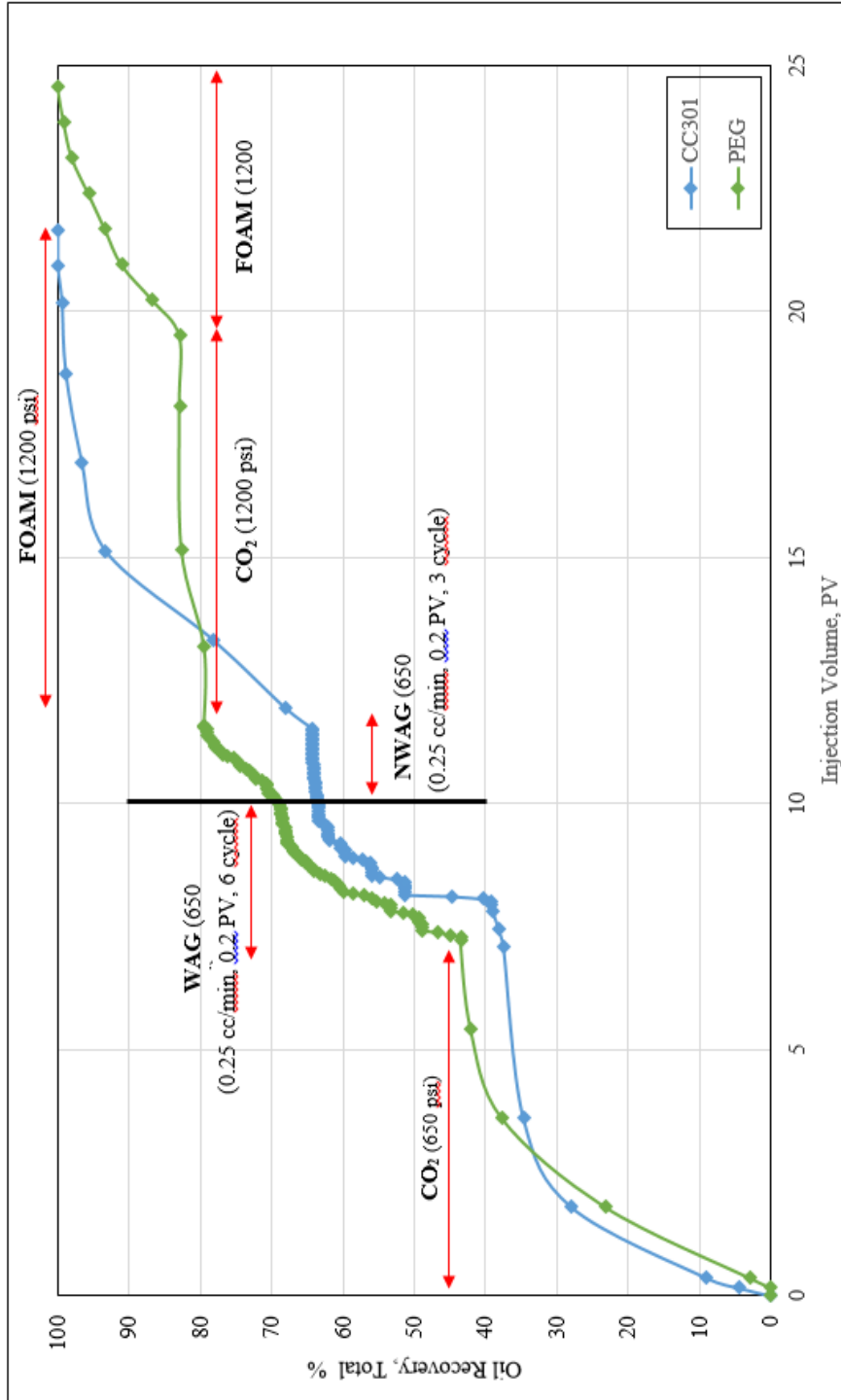


Figure 5.28. Oil recoveries in total recovery for both CC301 and PEG experiment

## 5.6. IFT MEASUREMENT

IFT between the nanodispersion - CO<sub>2</sub> and nanodispersion-oil were also evaluated to figure out if IFT was changing or not. As stated before, according to literature, the adsorption of the nanoparticle between the gas-liquid interfaces do not change the interfacial tension as a surfactant. It changes the contact angle (Sheng, 2013).

### 5.6.1. IFT between Nanodispersion-CO<sub>2</sub>

The cell was loaded with the nanodispersion and the CO<sub>2</sub> was sent to the cell. The system was heated and pressurized. The IFT700 system was used to analyze the IFT between these liquids by using the pendant drop method. CC301 dispersion was used for this experiment. The IFT of the NaCl solution was also measured to make a comparison if IFT was changing when nanodispersion was used. Moreover, the pressure effect of the temperature was evaluated. The before experiments show that the pressure does not change the IFT too much. Therefore, the pressure was kept in 600 psi. All results were given in *Table 5.10*. As seen from the table, not a significant change of IFT was obtained with the presence of nanoparticles as expected. Also, IFT was decreasing with the increase of the temperature. In order to see the temperature and nanoparticle effects on the IFT, Figure 5.29 and Figure 5.30 were plotted, respectively.

Table 5.10. *IFT between gas-liquid*

Cell Fluid	T (°C)	IFT (mN/m)
1 % NaCl solution	25	37
	65	30
1 % NaCl + 1 % CC301 dispersion	25	30
	65	24

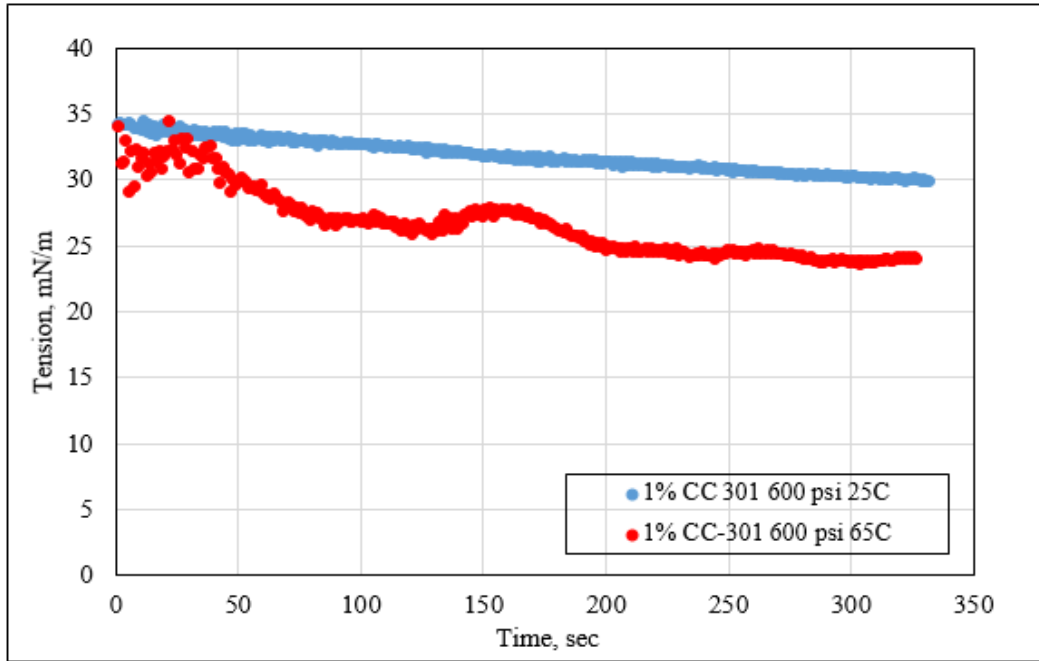


Figure 5.29. Temperature effect on the IFT

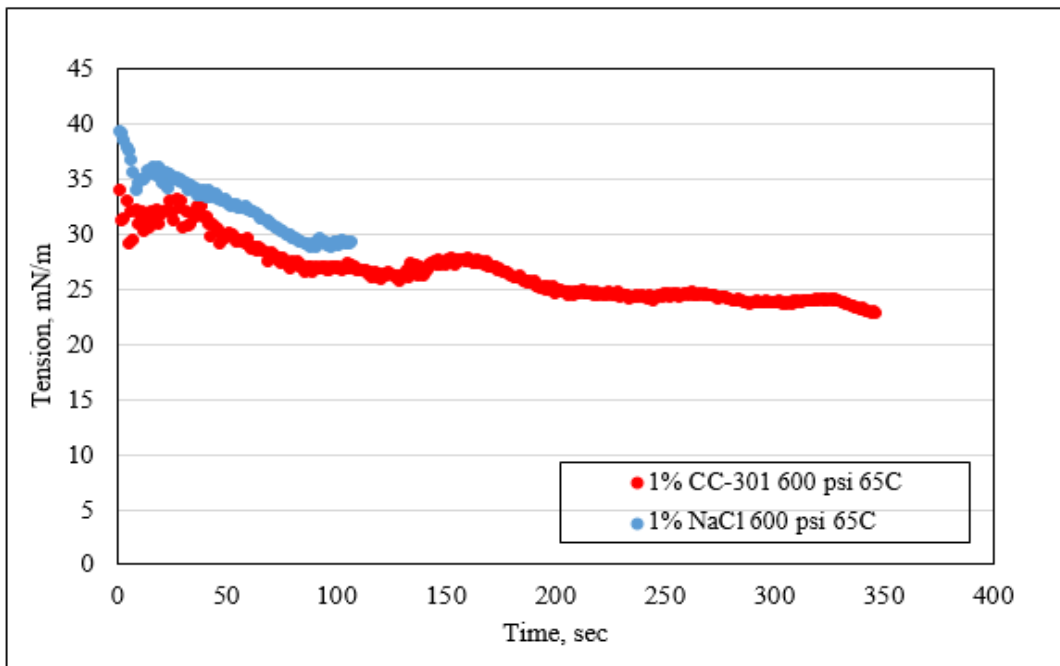


Figure 5.30. Nanosilica effect on IFT

### 5.6.2. IFT between Nanodispersion-Oil

The interfacial tension between nanodispersions and B. Raman oil was also conducted. Because if the foam decomposes in the reservoir, then nanodispersion will be release and contact with the reservoir fluids. This experiment will be an answer for this case.

The cell was again loaded with nanodispersion and oil drop was injected into the cell. Rising drop method was used this time and the shape of the drop was analyzed to measure IFT. Pressure again kept at 600 psi and the analysis temperature was 65 °C. The results indicated that IFT was decreasing significantly when nanosilica was used as shown in *Table 5.11*. Sedaghat et al. (2018) also stated the same result. Therefore, it was deduced that nanosilica can act as a surfactant in the reservoir, gladly.

Table 5.11. *IFT between liquid-oil*

Cell Fluid	T (°C)	IFT (mN/m)
B.Raman formation water		30-35
1 % CC301 dispersion	65	4.5
1% PEG dispersion		1.4

## CHAPTER 6

### CONCLUSION AND RECOMMENDATION

The whole of the studies was performed to increase the productivity of the already existing CO<sub>2</sub> injection system at B. Raman field. Nanoparticles were used to create foam to control CO<sub>2</sub> mobility in the reservoir. Therefore, the first different type of nanoparticles' dispersion stabilization and their foamability were evaluated. After this step two of them was eliminated due to lack of ability of foam generation. Also, H30 was found as better foamability dispersion. Then the dispersions were sent for particle size distribution analyses. H30 was at the nanoscale as results showed. The effect of the salinity, concentration, temperature and pH was studied on the foamability and stabilization. It was found that NaCl content has improved foam generation however higher concentration caused instability. The concentration of the nanoparticle was also important for stabilization and foamability. The higher the nanoparticle concentration, the higher the ability of foam formation. But, in that case, the cost of the application should be thought. Thus, 1% of concentrated nanoparticle dispersion was applied as the optimum value. Also, it wondered if the dispersion were stable at 65 °C which was B. Raman reservoir temperature. The results indicated that PEG and CC301 dispersions were stable but H30 dispersion was not. The pH adjustment was also conducted to stabilize H30 dispersion. For this purpose, the zeta potential was measured for every pH change. Form this experiment, it was figured out that above 9 H30 dispersions should be stable. Then, the pH of the dispersion was adjusted to 10 and the particle size was analyzed again. In that case, particle size was found below 200 nm which was appropriate for B. Raman reservoir.

Even it seemed all dispersion were stabilized, the dispersions were flooded through the B. Raman core samples for ensuring if plugging occurred or not. Then, plugging

existed during H30 dispersion flooding. Therefore, it was planned that H30 was not going to be used for later tests. Before starting foam generation tests, PVTsim program was run for graphing the phase diagram of the Dodan gas which was the source of B. Raman CO<sub>2</sub> injection system and pure CO<sub>2</sub>. The supercritical point was found as approximately above 1100 psi and 30 °C for both.

Then the test system was designed for foam generation flooding. The effect of the pressure, phase ratio and flow rate on the foam formation were also studied. Better foams were obtained when pressure differences were evaluated at CO<sub>2</sub>: nanodispersion phase ratio was 1. Also, it was found that the pressure should be above 1100 psi where CO<sub>2</sub> was in the supercritical phase to create foam with current core flooding system. Silica particle in the core was picturized with SEM/EDS system.

After, PEG and CC301 dispersion were used for oil recovery test. First, CO<sub>2</sub> injection and then WAG were studied to express B. Raman field case and it was found that WAG gave an extra oil production after the production with CO<sub>2</sub> injection stopped. NWAG at 650 psi and foam at 1200 psi was tested, later. It could be stated that the foam application was successful if appropriate conditions existed. On the other hand, not a significant production was obtained with NWAG application at 650 psi. Almost 35% of the total recovery was recovered with nanoparticles.

Interfacial measurements were also studied to evaluate the working principle of the nanoparticles. Nanoparticles were not changing IFT markedly even if they were located at the interface of the water and CO<sub>2</sub> as the surfactant. However, a significant decrease in the IFT was obtained between water and oil in the presence of nanoparticles.

After these whole results, it can be said that the injection of the nanoparticle stabilized CO<sub>2</sub> foam to B. Raman reservoirs where the pressure is above 1100 psi can be ended with a higher production.

As mentioned before, oil recovery test results were different for PEG and CC301 dispersion application. Tests were conducted with the same core but the PEG was applied after CC301 which means core samples was exposed to the oil longer. The differences were not only at the foam application but also the CO<sub>2</sub> injection. Therefore, these differences could be due to aging or plugging after CC301 dispersion was used. This test may study again by using different but same structure core samples. At the same time, the repeatability should also be made.

Additionally, the literature and the results of this study indicated that the dispersion of H30 had the best ability to form foam. On the other hand, the stability problem was observed about this dispersion and couldn't be solved during the study. It is recommended that this stability problem should be studied more and oil production with H30 dispersion should be seen.

Lastly, the viscosity measurement of the foam by adding a capillary tube to the system can be done as future work for better understanding. Any increase in the viscosity can be proof of foam generation. Also, it can be figured out which foam has better quality with this examination.

The importance of the field studies which reflects the reality is obvious in the oil and gas industry. Thus, the results of the application of this method should be seen in the field after all the question marks are answered.



## REFERENCES

Abedini, A., & Torabi F. (2014). On the CO<sub>2</sub> Storage Potential of Cyclic CO<sub>2</sub> Injection Process for Enhanced Oil Recovery. *Fuel*, 124: 14-27.

Adkins, S.S., Chen, X., Chan, I., Torino, E., Nguyen, Q.P., Sanders, A.W., & Johnston, K.P. (2009) Morphology and Stability of CO<sub>2</sub>-in-Water Foams with Nonionic Hydrocarbon Surfactants. *Langmuir*. 26(8): 5335–5348.

Alargova, R.G., Warhadpande, D.S., Paunov V.N., & Velev, O.D. (2004). Foam Superstabilization by Polymer Microrods. *Langmuir*. 20: 10371-10374.

AlYousef, A., Almobarky, M., & Schechter, D. (2017). Enhancing the Stability of Foam by the Use of Nanoparticles. *Energy Fuels*. 31: 10620-10627.

Aminzadeh-Goharrizi, B., DiCarlo, D. A., Chung, D. H., Kianinejad, A., Bryant, S. L., & Huh, C. (2012). Effect of Nanoparticles on Flow Alteration during CO<sub>2</sub> Injection. *Society of Petroleum Engineers*. doi:10.2118/160052-MS.

Andrianov, A., Farajzadeh, R., Nick, M. M., Talanana, M., & Zitha, P. L. J. (2011). Immiscible Foam for Enhancing Oil Recovery: Bulk and Porous Media Experiments. *Society of Petroleum Engineers*. doi:10.2118/143578-MS.

Aroonsri, A., Worthen, A. J., Hariz, T., Johnston, K. P., Huh, C., & Bryant, S. L. (2013). Conditions for Generating Nanoparticle-Stabilized CO<sub>2</sub> Foams in Fracture and Matrix Flow. *Society of Petroleum Engineers*. doi:10.2118/166319-MS.

Azadgoleh, J.E, Kharrat, R., Barati, N., & Sobhani, A. (2014). Stability of Silica Nanoparticle Dispersion in Brine Solution: an Experimental Study. *Iranian Journal of Oil & Gas Science and Technology*, 3(4): 26-40

Bashir, A., Sharifi Haddad, A., & Rafati, R. (2018). Experimental Investigation of Nanoparticles/Polymer Enhanced CO<sub>2</sub>- Foam in the Presence of Hydrocarbon at High-Temperature Conditions. Society of Petroleum Engineers. doi:10.2118/193802-MS.

Bhattacharjee, S. (2016). DLS and Zeta Potential – What They Are and What They Are Not. *Journal of Controlled Release*. 235: 337-351.

Bikerman, J.J. (1973). *Foams*. Springer-Verlag. ISBN: 0387061088.

Binks, B.P., & Lumsdon, S.O. (2000). Influence of Particle Wettability on the Type and Stability of Surfactant-Free Emulsions. *Langmuir*. 16(23): 8622-8631.

Binks, B.P. (2002). Particles as Surfactants—Similarities and Differences. *Current Opinion in Colloid & Interface Science*. 7(1): 21–41.

Binks, B.P., & Horozov, T.S. (2005). Aqueous Foams Stabilized Solely by Silica Nanoparticles. *Angewandte Chemie*. 117(24): 3788–3791.

Caudle, B. H., & Dyes, A. B. (1958). Improving Miscible Displacement by Gas-Water Injection. Society of Petroleum Engineers.

Chou, S. I., Vasicek, S. L., Pisio, D. L., Jasek, D. E., & Goodgame, J. A. (1992). CO<sub>2</sub> Foam Field Trial at North Ward-Estes. Society of Petroleum Engineers. doi:10.2118/24643-MS.

Christensen, J. R., Stenby, E. H., & Skauge, A. (1998). Review of WAG Field Experience. Society of Petroleum Engineers. doi:10.2118/39883-MS.

DiCarlo, D.A., Huh, C., & Johnston, K.P. (2015). Use of Engineered Nanoparticle-Stabilized CO<sub>2</sub> Foams to Improve Volumetric Sweep Efficiency of CO<sub>2</sub>-EOR Processes. U.S. Department of Energy-NETL. DE-FE0005917.

Dickson, J.L., Binks, B.P., Johnston, K.P. (2004). Stabilization of Carbon Dioxide-in-Water Emulsions with Silica Nanoparticles. *Langmuir*. 20 (19): 7976–7983.

Dong, L., & Johnson D. (2003). Surface Tension of Charge-Stabilized Colloidal Suspensions at the Water-Air Interface. *Langmuir*. 19: 10205-10209.

Dong, M., Forai, J., Huang, S., & Chatzis, I. (2005). Analysis of Immiscible Water-Alternating-Gas (WAG) Injection Using Micromodel Tests. Petroleum Society of Canada. doi:10.2118/05-02-01.

Eftekhari, A. A., Krastev, R., & Farajzadeh, R. (2015). Foam Stabilized by Fly-Ash Nanoparticles for Enhancing Oil Recovery. Society of Petroleum Engineers. doi:10.2118/175382-MS.

Eide, Ø., Føyen, T., Skjelsvik, E., Rognmo, A., & Fernø, M. (2018). Nanoparticle Stabilized Foam in Harsh Conditions for CO<sub>2</sub> EOR. Society of Petroleum Engineers. doi:10.2118/193212-MS.

Elwy, M., Zekri, A. Y., Almehaideb, R. A., & Al-Attar, H. H. (2012). Optimization of CO<sub>2</sub> WAG Processes in Carbonate Reservoirs-An Experimental Approach. Society of Petroleum Engineers. doi:10.2118/161782-MS.

Emrani, A. S., & Nasr-El-Din, H. A. (2015). Stabilizing CO<sub>2</sub>-Foam using Nanoparticles. Society of Petroleum Engineers. doi:10.2118/174254-MS.

Emrani, A.S., & Nasr-El-Din H.A. (2017a). An Experimental Study of Nanoparticle-Polymer-Stabilized CO<sub>2</sub> Foam. *Colloids and Surfaces A*. 524: 17-37.

Emrani, A. S., Ibrahim, A. F., & Nasr-El-Din, H. A. (2017b). Mobility Control using Nanoparticle-Stabilized CO<sub>2</sub> Foam as a Hydraulic Fracturing Fluid. Society of Petroleum Engineers. doi:10.2118/185863-MS.

Espinoza, D. A., Caldelas, F. M., Johnston, K. P., Bryant, S. L., & Huh, C. (2010). Nanoparticle-Stabilized Supercritical CO<sub>2</sub> Foams for Potential Mobility Control Applications. Society of Petroleum Engineers. doi:10.2118/129925-MS.

Farhadi, H., Riahi, S., Ayatollahi, S., & Ahmadi, H. (2016). Experimental Study of nanoparticle-Surfactant-Stabilized CO<sub>2</sub> Foam: Stability and Mobility Control. Chemical Engineering Research and Design 111: 449–460.

Feng H, Haidong H., Yanqing W., Jianfeng R., Liang Z., Bo R., Butt H., Shaoran R., & Guoli C. (2016). Assessment of Miscibility Effect for CO<sub>2</sub> Flooding EOR in a Low Permeability Reservoir. Journal of Petroleum Science and Engineering. 145: 328-335.

Fu, C., Yu J., & Liu, N. (2018). Nanoparticle-Stabilized CO<sub>2</sub> Foam for Waterflooded Residual Oil Recovery. Fuel. 234: 809-813.

Fujii, S., Ryan, A.J., & Armes, S.P. (2006). Long-Range Structural Order, Moiré' Patterns, and Iridescence in Latex-Stabilized Foams. Journal of the American Chemical Society . 128(24): 7882-7886.

General Directorate of the Mining and Oil Works (MAPEG). (2018). 2017 Yıl Sonu İtibari ile Türkiye Ham Petrol Rezervleri. Retrieved from [http://www.mapeg.gov.tr/petrol\\_istatistik.aspx](http://www.mapeg.gov.tr/petrol_istatistik.aspx).

Golomb, D., Barry, E., Ryan, D., Swett P., & Duan, H. (2006). Macroemulsions of Liquid and Supercritical CO<sub>2</sub>-in-Water and Waterin-Liquid CO<sub>2</sub> Stabilized by Fine Particles. Industrial & Engineering Chemistry Research. 45(8): 2728-2733.

Gozalpour, F., Ren, S.R., & Tohidi, B. (2005). CO<sub>2</sub>-EOR and Storage in Oil Reservoirs. Oil & Gas Science and Technology. Rev.IFP, 60(3): 537-546.

Guo, F., & Aryana, S. (2016). An Experimental Investigation of Nanoparticle-Stabilized CO<sub>2</sub> Foam Used in Enhanced Oil Recovery. Fuel. 186: 430-442

Hadlow, R. E. (1992). Update of Industry Experience With CO<sub>2</sub> Injection. Society of Petroleum Engineers. doi:10.2118/24928-MS.

Harpole, K. J., Siemers, W. T., & Gerard, M. G. (1994). CO<sub>2</sub> Foam Field Verification Pilot Test at EVGSAU: Phase IIIC--Reservoir Characterization and Response to Foam Injection. Society of Petroleum Engineers. doi:10.2118/27798-MS.

Haynes, S., & Alston, R. B. (1990). Study of the Mechanisms of Carbon Dioxide Flooding and Applications to More Efficient EOR Projects. Society of Petroleum Engineers. doi:10.2118/20190-MS.

Heerschap, S., Marafino, J.N., Mckenna, K., Caran, K.L., & Fetosa, K. (2015). Foams Stabilized by Tricationic Amphiphilic Surfactants. *Colloids and Surfaces A: Physicochemical Engineering Aspects*. 487:190–197.

Heidari, P., Kharrat, R., Alizadeh, N., & Ghanzanfari, M.H. (2013). A Comparison of WAG and SWAG Processes: Laboratory and Simulation Studies. *Energy Sources, Part A: Recovery, Utilization and Environmental Effects*. 35(23): 2225-2232.

Holm, L. W., & Josendal, V. A. (1974). Mechanisms of Oil Displacement by Carbon Dioxide. Society of Petroleum Engineers. doi:10.2118/4736-PA.

Hunter, T.N., Pugh, R.J., Franks, G.V., & Jameson, G.J. (2008). The Role of Particles in Stabilizing Foams and Emulsions. *Advances in Colloid and Interface Science*. 137: 57–81.

Ibrahim, F. A., & Nasr-El-Din, H. (2018). Stability Improvement of CO<sub>2</sub> Foam for Enhanced Oil Recovery Applications Using Nanoparticles and Viscoelastic Surfactants. Society of Petroleum Engineers. doi:10.2118/191251-MS.

Issever, K., Pamir, A. N., & Tirek, A. (1993). Performance of a Heavy-Oil Field Under CO<sub>2</sub> Injection, Bati Raman, Turkey. Society of Petroleum Engineers. doi:10.2118/20883-PA

Jarrell, P.M., Fox, C.E., Stein, M.H., & Webb, S.L. (2002). Practical Aspects of CO<sub>2</sub> Flooding. Society of Petroleum Engineers. ISBN: 978-1-55563-096-6.

Jiang, H., Nuryaningsih, L., & Adidharma, H. (2012). The Influence of O<sub>2</sub> Contamination on MMP and Core Flood Performance in Miscible and Immiscible CO<sub>2</sub> WAG. Society of Petroleum Engineers. doi:10.2118/154252-MS.

Kalyanaraman, N., Arnold, C., Gupta, A., Tsau, J. S., & Barati, R. (2015). Stability Improvement of CO<sub>2</sub> Foam for Enhanced Oil Recovery Applications Using Polyelectrolytes and Polyelectrolyte Complex Nanoparticles. Society of Petroleum Engineers. doi:10.2118/174650-MS.

Karabakal, U. (2008). B. Raman Sahasi Karot Analizi Verilerinin Rezervuar Simulasyonuna Yönelik Olarak Değerlendirilmesi. TPAO Ar-Ge Merkezi Arşivi. Rapor No: 3341

Karakashev, S. I., & Grozdanova, M.V. (2012). Foams and Antifoams. *Advances in Colloid and Interface Science*. 176–177: 1–17.

Karaoguz, O. K., Topguder, N. N. S., Lane, R. H., Kalfa, U., & Celebioglu, D. (2007). Improved Sweep in Bati Raman Heavy-Oil CO<sub>2</sub> Flood: Bullhead Flowing Gel Treatments Plug Natural Fractures. Society of Petroleum Engineers. doi:10.2118/89400-PA

Kanokkarna, P., Shiina T., Santikunaporn M., & Chavadeja, S. (2017). Equilibrium and Dynamic Surface Tension in Relation to Diffusivity And Foaming Properties: Effects of Surfactant Type and Structure. *Colloids and Surfaces A*. 524: 135–142.

Kantar, K., Karaoguz, D., Issever, K., & Varana, L. (1985). Design Concepts of a Heavy-Oil Recovery Process by an Immiscible CO<sub>2</sub> Application. Society of Petroleum Engineers. doi:10.2118/11475-PA

Koottungal, L. (2012). General interest: 2012 Worldwide EOR Survey. *Oil and Gas Journal*. 110. 57-69.

Kruglyakov, P.M., Elaneva, S.I., & Vilkova, N.G. (2011). About Mechanism of Foam Stabilization by Solid Particles. *Advances in Colloid and Interface Science*. 165: 108-116.

Langston, M. V., Hoadley, S. F., & Young, D. N. (1988). Definitive CO<sub>2</sub> Flooding Response in the SACROC Unit. Society of Petroleum Engineers. doi:10.2118/17321-MS.

Lee, D., Cho, H., Lee, J., Huh, C., & Mohanty, K. (2015). Fly Ash Nanoparticles as a CO<sub>2</sub> Foam Stabilizer. *Powder Technology*. 283: 77-84.

Li, S., Li, Z., & Wang, P. (2016). Experimental Study of the Stabilization of CO<sub>2</sub> Foam by Sodium Dodecyl Sulfate and Hydrophobic Nanoparticles. *Industrial & Engineering Chemistry Research*. 55(5): 1243–1253.

Liu, Y., Grigg, R. B., & Bai, B. (2005). Salinity, pH, and Surfactant Concentration Effects on CO<sub>2</sub>-Foam. Society of Petroleum Engineers. doi:10.2118/93095-MS.

Martin, D. F., & Taber, J. J. (1992). Carbon Dioxide Flooding. Society of Petroleum Engineers. doi:10.2118/23564-PA.

Martinez, A.C., Rio, E., Delon, G., Saint-Jalmes, A., Langevin, D., Binks, B.P. (2008). On the origin of the remarkable stability of aqueous foams stabilised by nanoparticles: link with microscopic surface properties. *Soft Matter*. 4 (7): 1531–1535.

Metin, C., Lake, L., Miranda, C., & Nguyen, Q. (2011). Stability of Aqueous Silica Nanoparticle Dispersions. *Journal of Nanoparticle Research*. 13: 839-850

Mo, D., Yu, J., Liu, N., & Lee, R. L. (2012). Study of the Effect of Different Factors on Nanoparticle-Stabilized CO<sub>2</sub> Foam for Mobility Control. Society of Petroleum Engineers. doi:10.2118/159282-MS.

Mo, D., Jia, B., Yu, J., Liu, N., & Lee, R. (2014). Study Nanoparticle-stabilized CO<sub>2</sub> Foam For Oil Recovery At Different Pressure, Temperature, And Rock Samples. Society of Petroleum Engineers. doi:10.2118/169110-MS.

Mohamed, I. M., He, J., & Nasr-El-Din, H. A. (2011). Permeability Change during CO<sub>2</sub> injection in Carbonate Rock: A Coreflood Study. Society of Petroleum Engineers. doi:10.2118/140943-MS.

Mohd, T.A.T., Muhayyidi, A.H.M., Ghazali, N.A., Shahrudin, M.Z., Alias, N., Arina, S., Ismail, S.N., & Ramlee N.A. (2014). Carbon Dioxide (CO<sub>2</sub>) Foam Stability Dependence on Nanoparticle Concentration for Enhanced Oil Recovery (EOR). Applied Mechanics and Materials. 548-549: 1876-1880.

Nasir, F.M., & Chong, Y.Y. (2009). The Effect of Different Carbon Dioxide Injection Modes on Oil Recovery. International Journal of Engineering & Technology IJET-IJENS. 9(10): 54-60.

Nazari, N., Tsau, J.-S., & Barati, R. (2018). Improving CO<sub>2</sub> Foam for EOR Applications Using Polyelectrolyte Complex Nanoparticles Tolerant of High Salinity Produced Water. Society of Petroleum Engineers. doi:10.2118/190179-MS.

Nguyen, P., Fadaei, H., & Sinton, D. (2014). Nanoparticle Stabilized CO<sub>2</sub> in Water Foam for Mobility Control in Enhanced Oil Recovery via Microfluidic Method. Society of Petroleum Engineers. doi:10.2118/170167-MS

Picha, M. S. (2007). Enhanced Oil Recovery by Hot CO<sub>2</sub> Flooding. Society of Petroleum Engineers. doi:10.2118/105425-MS.

Pugh R.J. (1996). Foaming, Foam Films, Antifoaming and Defoaming. Advances in Colloid and Interface Science. 64: 67-142 .

Rahmani, O. (2018). Mobility Control in Carbon Dioxide-Enhanced Oil Recovery Process Using Nanoparticle-Stabilized Foam for Carbonate Reservoirs. Colloids and Surface A. 550: 245-255

Rognmo, A.U., Heldal, S., & Ferno, M.A. (2018). Silica Nanoparticles to Stabilize CO<sub>2</sub>-Foam for Improved CO<sub>2</sub> Utilization: Enhanced CO<sub>2</sub> Storage and Oil Recovery from Mature Oil Reservoirs. *Fuel*. 216: 621-626.

Sahin, S., Kalfa, U., & Celebioglu, D. (2007). Bate Raman Field Immiscible CO<sub>2</sub> Application: Status Quo and Future Plans. Society of Petroleum Engineers. doi:10.2118/106575-MS

Sahin, S., Kalfa, U., & Celebioglu, D. (2010). Unique CO<sub>2</sub> -Injection Experience in the Bati Raman Field May Lead to a Proposal of EOR/Sequestration CO<sub>2</sub> Network in the Middle East. Society of Petroleum Engineers. doi:10.2118/139616-MS

Sahin, S., Kalfa, U., Celebioglu, D., Duygu, E., & Lahna, H. (2012). A Quarter Century of Progress in the Application of CO<sub>2</sub> immiscible EOR Project in Bati Raman Heavy Oil Field in Turkey. Society of Petroleum Engineers. doi:10.2118/157865-MS

San, J., Wang, S., Yu, J., Lee, R., & Liu, N. (2016). Nanoparticle Stabilized CO<sub>2</sub> Foam: Effect of Different Ions. Society of Petroleum Engineers. doi:10.2118/179628-MS.

Schramm L.L. (2000). *Surfactants: Fundamentals and Applications in the Petroleum Industry*. Cambridge University Press. ISBN: 0521640679.

Schramm L.L. (2005). *Emulsions, Foams and Suspensions: Fundamentals and Applications*. Wiley. ISBN: 9783527307432.

Schramm L.L., & Wassmuth F. (1994) *Foams: Fundamentals and Applications in the Petroleum Industry, Advances in Chemistry*; American Chemical Society. Chapter 1 Foams: Basic Principles. 242: 3-45. ISBN: 9780841227194.

Sedaghat, M., Azdarpour, A., Sadr Nafisi, M. & Esfandiarian, A. (2018). Experimental Investigation of Using SDBS and SiO<sub>2</sub> Nanoparticle as a Novel Chemical EOR Process in a Micromodel System. Presented at the EAGE Conference and Exhibition, Denmark

Sheng J.J. (2013). Enhanced Oil Recovery Field Case Studies. Elsevier. ISBN: 9780123865458.

Singh, R., & Mohanty, K. K. (2017). Nanoparticle-Stabilized Foams for High-Temperature, High-Salinity Oil Reservoirs. Society of Petroleum Engineers. doi:10.2118/187165-MS.

Skauge, A., & Stensen, J.A. (2003). Review of the WAG Field Experience. Presented at 1<sup>st</sup> International Conference and Exhibition Modern Challenges in Oil Recovery, Russia.

Stevenson, P. (2012). Foam Engineering: Fundamentals and Applications. Wiley. ISBN: 0470660805.

Stocco, A., Rio, E., Binks B.P., & Langevin D. (2013). Aqueous Foams Stabilized Solely by Particles. *Soft Matter*, Royal Society of Chemistry. 7(4): 1260-1267.

Sun, Q., Li, Z., Li, S., Jiang, L., Wang, J., & Wang, P. (2014). Utilization of Surfactant Stabilized Foam for Enhanced Oil Recovery by Adding Nanoparticles. *Energy Fuel*. 28: 2384–2394.

Taber, J. J., Martin, F. D., & Seright, R. S. (1997). EOR Screening Criteria Revisited—Part 2: Applications and Impact of Oil Prices. Society of Petroleum Engineers. doi:10.2118/39234-PA.

Talebian, S.H., Masoudi, R., Tan, I.M., & Zitha, P.L.J. (2014). Foam Assisted CO<sub>2</sub> - EOR: A Review of Concept, Challenges, and Future Prospects. *Journal of Petroleum Science and Engineering*. 120: 202-215.

Thomas, J., Berzins, T. V., Monger, T. G., & Bassiouni, Z. A. (1990). Light Oil Recovery From Cyclic CO<sub>2</sub> Injection: Influence of Gravity Segregation and Remaining Oil. Society of Petroleum Engineers. doi:10.2118/20531-MS.

Thomas, S. (2007). Enhanced Oil Recovery - An Overview. *Oil & Gas Science and Technology - Rev.IFP*. 63(1): 9-19.

Tunio, S. Q., Tunio, A. H., Ghirano, N. A., & El Adawy, Z. M. (2011). Comparison of Different Enhanced Oil Recovery Techniques for Better Oil Productivity. *International Journal of Applied Science and Technology*. 1(5): 143–153.

Verma, M.K. (2015). Fundamentals of Carbon Dioxide-Enhanced Oil Recovery (CO<sub>2</sub>-EOR)—A Supporting Document of the Assessment Methodology for Hydrocarbon Recovery Using CO<sub>2</sub>-EOR Associated with Carbon Sequestration. U.S. Geological Survey Open-File Report 2015–1071.

Voormeij, D. A., & Simandl, G.J. (2004) Geological, Ocean and Mineral CO<sub>2</sub> Sequestration Options: A Technical Review. *Geoscience Canada*. 31(1): 11-22

Wang, Y., Zhang, Y., Liu, Y, Liang, Z. Ren, S., Lu, J., Wang, X., Fan, N. (2017). The Stability Study of CO<sub>2</sub> Foams at High Pressure and High Temperature. *Journal of Petroleum Science and Engineering*. 154: 234-243.

Wang, Z., Ren, G., Yang, J., Xu, Z., & Sun D. (2019). CO<sub>2</sub> -Responsive Aqueous Foams Stabilized by Pseudogemini Surfactants. *Journal of Colloid and Interface Science*. 536: 381-388.

Weaire, D., & Hutzler, S. (1999). *The Physics of Foams*. Oxford University Press, ISBN: 0198510977.

Whorton L.P., Brownscombe E.R., & Dyes A.B. (1952). Method for Producing Oil by Means of Carbon Dioxide. U.S, Patent 2,623,596.

Wolcott, J., Schenewerk, P., Berzins, T., & F. Brim (1995). A Parametric Investigation of the Cyclic CO<sub>2</sub> Injection Process. *Journal of Petrol Science and Engineering*, 14: 35-44.

Worthen, A., Bagaria, H., Chen, Y., Bryant, S. L., Huh, C., & Johnston, K. P. (2012a). Nanoparticle Stabilized Carbon Dioxide in Water Foams for Enhanced Oil Recovery. Society of Petroleum Engineers. doi:10.2118/154285-MS.

Worthen A.J., Bagaria H.G., Chen Y., Bryant S.L., Huh C., & Johnston K.P. (2012b). Nanoparticle-Stabilized Carbon Dioxide-in-Water Foams with Fine Texture. *Journal of Colloid and Interface Science*. 391: 142-151.

Xue, Z., Worthen, A., Qajar, A., Robert, I., Bryant, S.L., Huh C., Prodanovic', M., & Johnston, K.P. (2016). Viscosity and Stability of Ultra-High Internal Phase CO<sub>2</sub>-in-Water Foams Stabilized with Surfactants and Nanoparticles with or without Polyelectrolytes. *Journal of Colloid and Interface Science*. 461: 383-395.

Yekeen, N., Manan, M.A., Idris, A.K., Padmanabhan, E., Junin, R., Samin, A. M., Gbadamosi, A.O., & Oguamah, I. (2018). A Comprehensive Review of Experimental Studies of Nanoparticles-Stabilized Foam for Enhanced Oil Recovery. *Journal of Petroleum Science and Engineering*. 164: 43-74.

Yu, J., Liu, N., Li, L., & Lee, R. L. (2012a). Generation of Nanoparticle-Stabilized Supercritical CO<sub>2</sub> Foams. Carbon Management Technology Conference. doi:10.7122/150849-MS.

Yu, J., An, C., Mo, D., Liu, N., & Lee, R. L. (2012b). Foam Mobility Control for Nanoparticle-Stabilized Supercritical CO<sub>2</sub> Foam. Society of Petroleum Engineers. doi:10.2118/153336-MS.

Yu, J., Mo, D., Liu, N., & Lee, R. (2013). The Application of Nanoparticle-Stabilized CO<sub>2</sub> Foam for Oil Recovery. Society of Petroleum Engineers. doi:10.2118/164074-MS.

Yu, J., Wang, S., Liu, N., & Lee, R. (2014). Study of Particle Structure and Hydrophobicity Effects on the Flow Behavior of Nanoparticle-Stabilized CO<sub>2</sub> Foam in Porous Media. Society of Petroleum Engineers. doi:10.2118/169047-MS.

Yusuf, S., Manan, M., & Jaafar, M.Z. (2013). Aqueous Foams Stabilized by Hydrophilic Silica Nanoparticles via In-Situ Physisorption of Nonionic TX100 Surfactant. *Iranica Journal of Energy & Environment* 4 (1) Special Issue on Nanotechnology: ISSN 2079-2115.

Zang, D.Y., Rio, E., Delon, G., Langevin, D., Wei B., & Binks B.P. (2010). Influence of the Contact Angle of Silica Nanoparticles at the Air-Water Interface on the Mechanical Properties of the Layers Composed of These Particles. *Molecular Physics*, 109(7-10); 1057-1066.

Zhang, C., Li, Z., Sun, Q., Wang, P., Wang, S., & Liu, W. (2015). CO<sub>2</sub> Foam Properties and the Stabilizing Mechanism of Sodium Bis(2-Ethylhexyl) Sulfosuccinate and Hydrophobic Nanoparticle Mixtures. *Soft Matter*. DOI: 10.1039/C5SM01408E.

Zhang, T., Murphy, M. J., Yu, H., Bagaria, H. G., Yoon, K. Y., Nielson, B. M., & Bryant, S. L. (2015). Investigation of Nanoparticle Adsorption during Transport in Porous Media. *Society of Petroleum Engineers*. doi:10.2118/166346-PA.

Zhu, Y., Tian, J., Hou, Q., Luo, Y., & Fan, J. (2017). Studies on Nanoparticle-Stabilized Foam Flooding EOR for a High Temperature and High Salinity Reservoir. *Society of Petroleum Engineers*. doi:10.2118/188964-MS.

Zeng, Y., Farajzadeh, R., Biswala, S.L., & Hirasakia, G.J. (2019). A 2-D Simulation Study on CO<sub>2</sub> Soluble Surfactant for Foam Enhanced Oil Recovery. *Journal of Industrial and Engineering Chemistry*. 72: 133-143.

Zuta, J., Fjelde, I., & Berenblyum R. (2009). Oil Recovery during CO<sub>2</sub>-Foam Injection in Fractured Chalk Rock at Reservoir Conditions. Presented at the International Symposium of the Society of Core Analysts, The Netherlands



## APPENDICES

### A. Nanoparticle Data Sheet

Eka Chemicals Industrial Specialties	<b>Product Data Sheet</b>	Updated: May 19, 2009	
			<b>AkzoNobel</b> Tomorrow's Answers Today
<b>Bindzil® CC301</b>			
Bindzil® CC 301 is a neutral, aqueous dispersion of colloidal silica at a 30 % concentration. The amorphous silica particles are discrete, spherical and mono-dispersed. The particles have been surface modified by silane and have a slightly negative surface charge. Bindzil® CC 301 is a clear liquid, slightly more viscous than water.			
<b>Typical Properties</b>			
Silica, wt%:			29
Average particle size, nm:			7
pH:			8
Viscosity, mPas (20°C)			5
Density g/cm <sup>3</sup> :			1.2
Reactive hydroxyl groups			0.45 mole per kg product
<b>End Uses</b>			
Bindzil® CC 301 is specially developed and designed for the use in waterborne coatings. Bindzil® CC 301 offers superior stability and binding properties in most latex coating compositions and enhances properties like abrasion and scratch resistance, reduced tackiness and drying time. Because colloidal silica can be applied to several different uses, please refer to our web site or contact us below for specific application / product recommendations.			
<b>Chemical Storage</b>			
Bindzil® CC 301 is freeze sensitive and has a recommended storage temperature of 5-35°C (40-95°F). Bindzil® CC301 is best stored in a dark closed tank made of non-rusting materials such as plastic, fiberglass reinforced plastic, or stainless steel. Aluminum, copper or non-stainless steel should be avoided. Bindzil® CC 301 stored under recommended conditions has a shelf life of at least twelve months.			
<b>Packaging</b>			
Bindzil® CC 301 is available in bulk tankers or IBCs / poly drum packages. Exact packaging types, sizes, net weights, etc., will vary by region.			
<b>Health, Safety, and Environment</b>			
Before handling this material, read the corresponding Material Safety Data Sheet. If you have misplaced your copy, please contact Eka Chemicals for a replacement via information below.			
Website: <a href="http://www.colloidal silica.com">http://www.colloidal silica.com</a>		Email: <a href="mailto:colloidal.silica@akzonobel.com">colloidal.silica@akzonobel.com</a>	
Information herein is accurate to the best of our knowledge. Suggestions are made without warranty or guarantee of results. Before using, user should determine the suitability of the product for his intended use and user assumes the risk and liability in connection therewith. We do not suggest violation of any existing patents or give permission to practice any patented invention without a license.			
<b>Head Office:</b>	Eka Chemicals AB; Bohus Sweden; Phone: +46 31 58 70 00		
<b>Asia:</b>	Eka Chemicals Taiwan Co Ltd.; Taichung, Taiwan, Phone:+886 4 2327 0520		
<b>Brazil:</b>	Eka Chemicals Do Brazil S.A.; Jundiai Brazil; Phone:+55 11 4589 4800		
<b>China:</b>	Eka Chemicals (Suzhou) Co., Ltd.; Suzhou City China; Phone: +86 512 6258 2276		
<b>Europe/Africa:</b>	AkzoNobel Chemicals GmbH; Düren Germany; Phone: +49 2421 595 01		
<b>Latin America:</b>	Eka Chemicals AB; Bohus Sweden; Phone: +46 31 58 70 00		
<b>North America:</b>	Eka Chemicals Inc.; Marietta, Georgia USA; Phone: +1 770 578 0858		
			

## HDK® N20

PYROGENIC SILICA

### Product description

Synthetic, hydrophilic, amorphous silica, produced via flame hydrolysis. Standard product for industrial applications.

### Special features

White colloidal powder of high purity.

### Application

HDK® N20 is applied as a thickening and thixotropic agent in many organic systems, e.g. in unsaturated polyesters, coatings, printing inks, adhesives, cosmetics and others. HDK® N20 is used as a reinforcing filler in elastomers, mainly silicone-elastomers. HDK® N20 acts as a free flow additive in the production of technical powders.

HDK® N20 is not suitable for pharmaceuticals, food and feed.

### Processing

A good dispersion of HDK® N20 is a must to assure optimum performance.

More detailed information about the application and processing of HDK® N20 is available in our HDK-brochures and on the WACKER web site (<http://www.wacker.com/hdk>).

### Storage

The 'Best use before end' date of each batch is shown on the shipping label and the certificate of analysis.

HDK® N20 should be stored in the original packaging in dry storage areas.

Storage beyond the date specified on the label does not necessarily mean that the product is no longer usable. In this case however, the properties required for the intended use must be checked for quality assurance reasons.

Due to the high surface area HDK® adsorbs volatiles and should be protected from humidity and volatiles. If single bags are taken away from an original pallet, the remaining bags of this pallet must again be protected against humidity and volatiles.

### Packaging

HDK® N20 is offered in following packaging:

- pallet with paper bags:  
10 kg bags
- Big bags:  
150 kg (big bags on pallets)
- Silotruck:  
depending on size of truck, approx. 3.5 to 5 tons

Details about packaging and handling:  
(<http://www.wacker.com/hdk>).

### Safety notes

Comprehensive instructions are given in the corresponding Material Safety Data Sheets. They are available on request from WACKER subsidiaries or may be printed via the WACKER web site (<http://www.wacker.com/hdk>).

During transportation and processing HDK® N20 may cause electrostatic charges. Like other amorphous silicas HDK® N20 does not show either carcinogenic (IARC classification, Volume 68, 1997) or mutagenic properties.

Product data		
Typical general characteristics	Inspection Method	Value
SiO <sub>2</sub> content (based on the substance heated at 1000 °C for 2 h)	DIN EN ISO 3262-19	> 99,8 %
Loss of weight at 1000 °C / 2h (based on the substance dried at 105 °C for 2 h)	DIN EN ISO 3262-19	< 2 %
Density at 20 °C (SiO <sub>2</sub> )	DIN 51757	approx. 2,2 g/cm <sup>3</sup>
Refraction index at 20 °C		1,46
Silanol group density		2 SiOH/nm <sup>2</sup>
INCI name		Silica
Physical-chemical properties		
BET surface	DIN ISO 9277 DIN 66132	175 - 225 m <sup>2</sup> /g
pH-Value	DIN EN ISO 787-9	3,8 - 4,3
Tamped density	DIN EN ISO 787-11	approx. 40 g/l
Loss on drying , ex works (2 h at 105 °C)	DIN EN ISO 787-2	< 1,5 %
Sieve residue , acc. to Mocker > 40 µm	DIN EN ISO 787-18	< 0,03 %

These figures are only intended as a guide and should not be used in preparing specifications.

The data presented in this medium are in accordance with the present state of our knowledge but do not absolve the user from carefully checking all supplies immediately on receipt. We reserve the right to alter product constants within the scope of technical progress or new developments. The recommendations made in this medium should be checked by preliminary trials because of conditions during processing over which we have no control, especially where other companies' raw materials are also being used. The information provided by us does not absolve the user from the obligation of investigating the possibility of infringement of third parties' rights and, if necessary, clarifying the position. Recommendations for use do not constitute a warranty, either express or implied, of the fitness or suitability of the product for a particular purpose.

The management system has been certified according to DIN EN ISO 9001 and DIN EN ISO 14001

WACKER® is a trademark of Wacker Chemie AG. HDK® is a trademark of Wacker Chemie AG.

For technical, quality, or product safety questions, please contact:

Wacker Chemie AG  
Hanns-Seidel-Platz 4  
81737 München, Germany  
hdk@wacker.com

www.wacker.com/hdk

## HDK® H30

PYROGENIC SILICA

### Product description

Synthetic, hydrophobic, amorphous silica, produced via flame hydrolysis.

### Special features

White colloidal powder of high purity.

### Application

HDK® H30 is applied as a thickening and thixotropic agent in coatings, printing inks, adhesives, cosmetics and others. HDK® H30 is used as a reinforcing filler in elastomers, mainly silicone-elastomers. HDK® H30 acts as a free flow additive in the production of powder coatings.

HDK® H30 is not suitable for pharmaceuticals, food and feed.

### Processing

A good dispersion of HDK® H30 is a must to assure optimum performance.

More detailed information about the application and processing of HDK® H30 is available in our HDK-brochures and on the WACKER web site (<http://www.wacker.com/hdk>).

### Storage

The 'Best use before end' date of each batch is shown on the shipping label and the certificate of analysis.

HDK® H30 should be stored in the original packaging in dry storage areas.

Storage beyond the date specified on the label does not necessarily mean that the product is no longer usable. In this case however, the properties required for the intended use must be checked for quality assurance reasons.

### Packaging

HDK® H30 is offered in following packaging:

- pallet with paper bags:  
10 kg bags

Details about packaging and handling:  
(<http://www.wacker.com/hdk>).

### Safety notes

Comprehensive instructions are given in the corresponding Material Safety Data Sheets. They are available on request from WACKER subsidiaries or may be printed via the WACKER web site (<http://www.wacker.com/hdk>).

During transportation and processing HDK® H30 may cause electrostatic charges.

Like other amorphous silicas HDK® H30 does not show either carcinogenic (IARC classification, Volume 68, 1997) or mutagenic properties.

**Product data**

Typical general characteristics	Inspection Method	Value
SiO <sub>2</sub> content (based on the substance heated at 1000 °C for 2 h)	DIN EN ISO 3262-19	> 99,8 %
Density at 20 °C (SiO <sub>2</sub> )	DIN 51757	approx. 2,2 g/cm <sup>3</sup>
Residual silanol content (relative silanol content in relation to the hydrophilic silica, which shows approx. 2 SiOH/nm <sup>2</sup> )		50 %
BET surface of the hydrophobic silica	DIN ISO 9277 DIN 66132	approx. 250 m <sup>2</sup> /g
INCI name		Silica Dimethyl Silylate

**Physical-chemical properties**

BET surface of the hydrophilic silica	DIN ISO 9277 DIN 66132	270 - 330 m <sup>2</sup> /g
Carbon content	DIN ISO 10694	1,4 - 2,6 %
pH-Value in 4 % dispersion (1 : 1 mixture of water-methanol)	DIN EN ISO 787-9	3,8 - 4,5
Tamped density	DIN EN ISO 787-11	approx. 40 g/l
Loss on drying , ex works (2 h at 105 °C)	DIN EN ISO 787-2	< 0,6 %
Sieve residue , acc. to Mocker > 40 µm	DIN EN ISO 787-18	< 0,05 %
Surface modification	Dimethylsiloxy	

These figures are only intended as a guide and should not be used in preparing specifications.

The data presented in this medium are in accordance with the present state of our knowledge but do not absolve the user from carefully checking all supplies immediately on receipt. We reserve the right to alter product constants within the scope of technical progress or new developments. The recommendations made in this medium should be checked by preliminary trials because of conditions during processing over which we have no control, especially where other companies' raw materials are also being used. The information provided by us does not absolve the user from the obligation of investigating the possibility of infringement of third parties' rights and, if necessary, clarifying the position. Recommendations for use do not constitute a warranty, either express or implied, of the fitness or suitability of the product for a particular purpose.

The management system has been certified according to DIN EN ISO 9001 and DIN EN ISO 14001

WACKER® is a trademark of Wacker Chemie AG. HDK® is a trademark of Wacker Chemie AG.

For technical, quality, or product safety questions, please contact:

Wacker Chemie AG  
Hanns-Seidel-Platz 4  
81737 München, Germany  
hdik@wacker.com

www.wacker.com/hdk

Product information

## AERODISP® WR 8520

### Aqueous dispersion of hydrophobic fumed silica

#### Characteristic physico-chemical data

Properties and test methods	Unit	Value
pH value		10 - 11
Density 20 °C	g/cm <sup>3</sup>	1.13
Stabilizing agent		DMEA
Solids content based on the ignition residue of the dispersion	%	19 - 21
Mean aggregate size d-50 value	µm	
Viscosity measured at a shear rate of 100 s <sup>-1</sup> , 23 °C	mPas	

The data represents typical values (no product specification).

#### Registrations (substance or product components)

AERODISP® WR 8520

CAS-No.	68611-44-9
EINECS (Europe), TSCA (USA), DSL (Canada), AICS (Australia), ENCS (Japan), IECSC (China), KECI (Korea)	All components of this dispersion are registered in the mentioned inventories.

AERODISP® WR 8520 is a special, structured, highly filled dispersion of hydrophobic AEROSIL®.

#### Applications and properties

##### Applications

In waterbased pigmented coatings or in waterbased clear coatings:

- Rheology control
- Anti-settling
- Pigment stabilization
- Improvement of mechanical properties

##### Recommendations for waterbased coatings

Addition: 5-10% dispersion (respect. 1-2% AEROSIL®) calculated on total coating formulation. The dispersion should be added into the coating while stirring under low or medium shear forces (e.g. dissolver)

#### Safety and handling

A safety data sheet will be provided with your first delivery and with subsequent revisions. Additionally, the Product Safety Department of Evonik Resource Efficiency GmbH can be contacted via mail at [sds-hu@evonik.com](mailto:sds-hu@evonik.com) for specific questions. We recommend to reach the safety data sheet carefully prior to use of the product.

#### Packaging and storage

Depending on the region, AERODISP® WR 8520 is available in 60 kg containers, 220 kg drums, 1000 kg intermediate bulk containers (IBC's). All dispersions must be protected from extreme heat and frost. The product should be used within twelve months from the date of production.

## B. Test Report of the B.Raman Formation Water and Dodan Gas

	<b>TP AR-GE MERKEZİ</b> <b>ÜRETİM TEKNOLOJİSİ MÜDÜRLÜĞÜ</b> <b>ANALİZ RAPORU</b>	
		06.16

<b>Numune Kodu</b>	: 16.02.055-2
<b>Numunenin Üniteye Geliş Tarihi</b>	: 27.06.2016
<b>Yapılan Analiz(ler)</b>	: Su analizleri
<b>Analizin Yapıldığı Tarih</b>	: 27-30.06.2016

### B.RAMAN 3TP2 ATIK SU

#### ANALİZ SONUÇLARI

##### ÇÖZÜNMÜŞ KATILAR

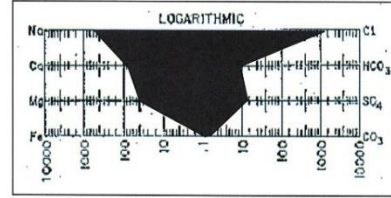
KATYONLAR	mg/l	ppm	epm	epm(%)
Sodyum	26.270,00	24.551,63	1.068,00	36,10
Potasyum	689,40	644,31	16,49	0,56
Kalsiyum	4.647,00	4.343,03	216,72	7,33
Magnezyum	1.141,00	1.066,37	87,76	2,97
Demir (Toplam)	37,75	35,28	1,89	0,06
Stronsiyum	246,90	230,75	5,26	0,18
Baryum	0,24	0,23	0,00	0,00

##### ANYONLAR

Klorür	58.610,00	54.776,21	1.544,69	52,21
Sulfat	525,00	490,66	10,21	0,34
Karbonat	0,00	0,00	0,00	0,00
Bikarbonat	480,00	448,60	7,36	0,25

##### DİĞER PARAMETRELER

pH	6,51	/25,7°C
Sp.Gravite	1,070	/15,6°C
Resistivite (25,4°C)	0,08	ohm-m
Top. Çözünen Katı Madde	92.647	mg/l
Toplam Tuzluluk (NaCl)	96.583	mg/l
Kondaktivite (25,4°C)	127800	µS/cm



ANALİZİN YAPILDIĞI ÜNİTE	YAZAN	ONAYLAYAN
ÜRETİM TEKNOLOJİSİ MÜDÜRLÜĞÜ	 Beril ARAÇ Kıd. Uzman Mühendis	 Selçuk SALDI Ünite Müdürü



TP AR-GE MERKEZİ  
ÜRETİM TEKNOLOJİSİ MÜDÜRLÜĞÜ  
ANALİZ RAPORU

06-16

**Numune Kodu** : 16.02.055-3  
**Numunenin Üniteye Geliş Tarihi** : 27.06.2016  
**Yapılan Analiz(ler)** : Gaz numunesinde hidrokarbon bileşen analizi, kükürt bileşen analizi ve alt üst ısı değer hesaplanması.  
**Analizin Yapıldığı Tarih** : 29-30.06.2016

GAZ ANALİZ SONUCU

<b>Örneklem Yeri:</b> DODAN	<b>Analiz Tarihi:</b> 29-30.06.2016
<b>Sıcaklık (°C):</b> -	<b>Örneklem Tarihi:</b>
<b>Basınç (psi):</b> -	<b>Derinlik/Aralık (m):</b>
<b>Ünite Numune Numarası:</b> 16.2.055	

<b>Bileşenler</b>	<b>Mol, %</b>	<b>Ölçüm Belirsizliği (±)</b>	<b>Yöntem</b>
H <sub>2</sub> Hidrojen	0,000		ASTM D-1945
Ar/O <sub>2</sub> Argon/Oksijen	0,000		
N <sub>2</sub> Azot	3,562		
CO <sub>2</sub> Karbondioksit	86,878		
C <sub>1</sub> Metan	7,315		
C <sub>2</sub> Etan	0,469		
C <sub>3</sub> Propan	0,518		
iC <sub>4</sub> iso-Butan	0,204		
nC <sub>4</sub> n-Butan	0,590		
iC <sub>5</sub> iso-Pentan	0,173		
nC <sub>5</sub> n-Pentan	0,133		
nC <sub>6</sub> n-Hekzan	0,157		
<b>Toplam</b>	<b>100,000</b>		

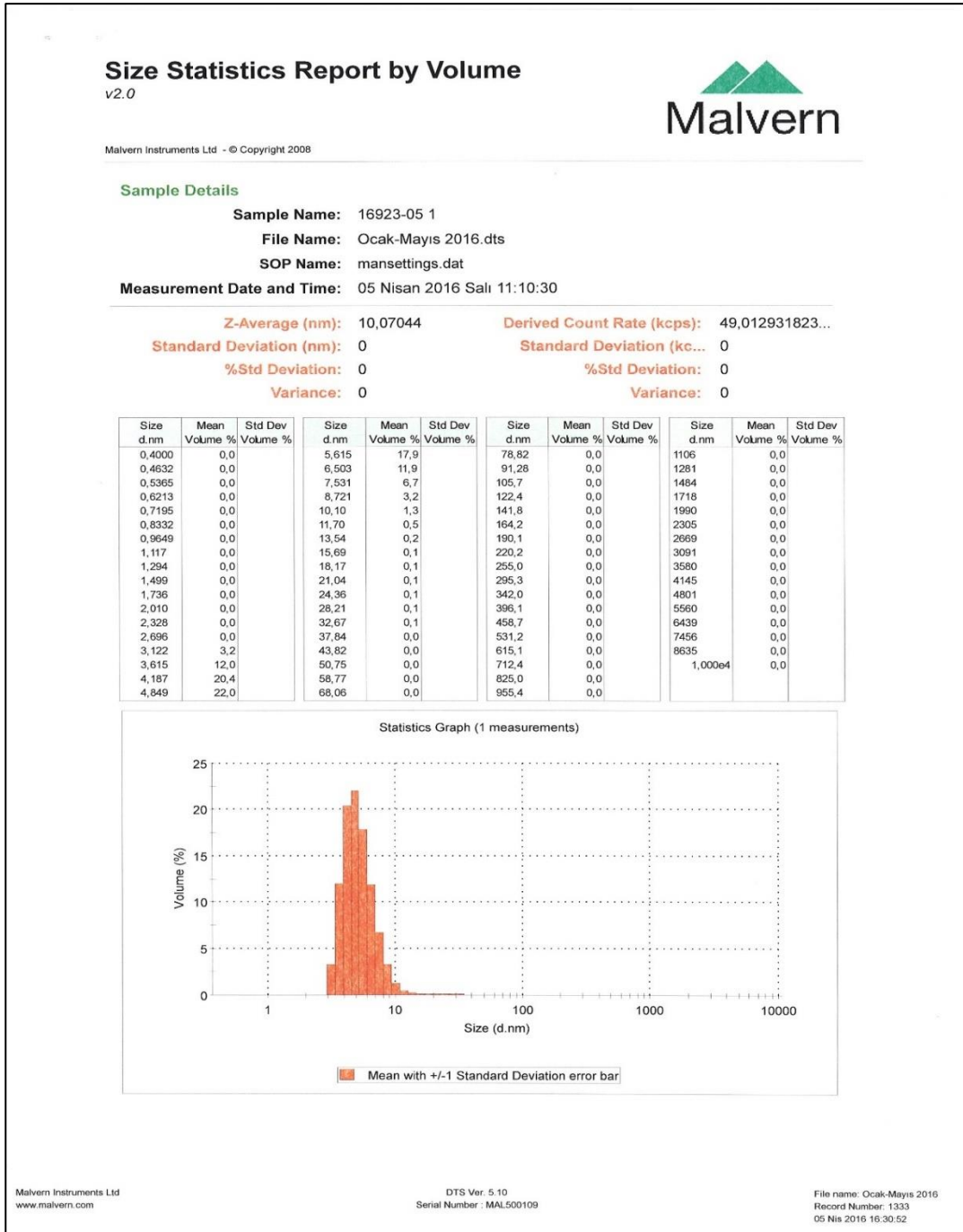
<b>Diğer Sülfür Bileşikleri</b>	<b>ppm</b>	<b>Yöntem</b>
H <sub>2</sub> S Hidrojen Sülfür	483,1	ASTM D-5504
COS Karbonil Sülfür	8,1	
CH <sub>3</sub> SH Metil Merkaptan	0,2	
C <sub>2</sub> H <sub>5</sub> SH Etil Merkaptan	0,9	

<b>Bazı Gaz Özellikleri:</b>		<b>Yöntem</b>
Pseudo Kritik Basınç, psia	1010,0	ISO 6976
Pseudo Kritik Sıcaklık, °R	524,9	
Mol Ağırlık, g/mol	41,594	
Özgül Ağırlık (25 °C-1 atm)	1,443	
Üst Isı Değeri, kcal/sm <sup>3</sup>	1262,99	
Alt Isı Değeri, kcal/sm <sup>3</sup>	1150,08	
Wobbe Sayısı, kcal/sm <sup>3</sup>	1051	
Sıkıştırma Faktörü	0,9947	

ANALİZİN YAPILDIĞI ÜNİTE	YAZAN	ONAYLAYAN
ÜRETİM TEKNOLOJİSİ MÜDÜRLÜĞÜ	 Sema ÇETİN Mühendis	 Selçuk SALDI Ünite Müdürü

### C. Test Report of Nanoparticle Size Distribution

- 1% PEG + 1 % NaCl



# Size Distribution Report by Volume

v2.0



Malvern Instruments Ltd - © Copyright 2008

## Sample Details

Sample Name: 16923-05 1 PEG

SOP Name: mansettings.dat

General Notes: evaporation method

File Name: Ocak-Mayis 2016.dts	Dispersant Name: Water
Record Number: 1333	Dispersant RI: 1,330
Material RI: 1,49	Viscosity (cP): 0,8864
Material Absorbtion: 0,00	Measurement Date and Time: 05 Nisan 2016 Salı 11:10:...

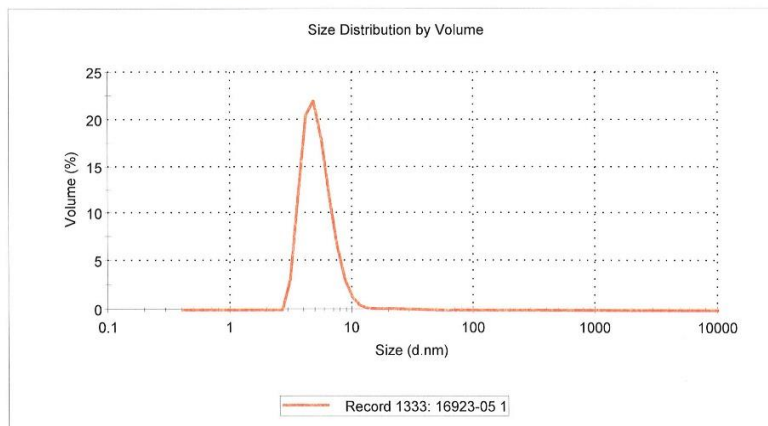
## System

Temperature (°C): 24,9	Duration Used (s): 150
Count Rate (kcps): 49,0	Measurement Position (mm): 4,65
Cell Description: Disposable sizing cuvette	Attenuator: 11

## Results

	Diam. (nm)	% Volume	Width (nm)
Z-Average (d.nm): 10,07	Peak 1: 5,282	99,3	1,568
Pdl: 0,413	Peak 2: 24,07	0,7	8,122
Intercept: 0,953	Peak 3: 0,000	0,0	0,000

Result quality **Good**



• 1% CC301 + 1 % NaCl

## Size Statistics Report by Volume

v2.0



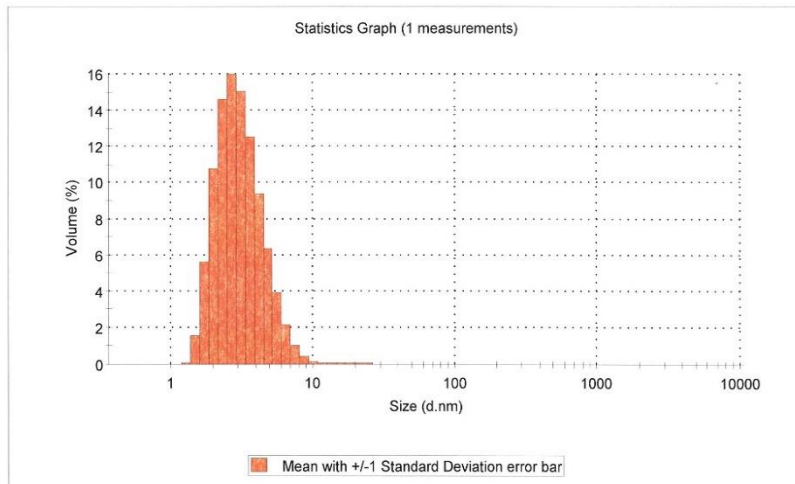
Malvern Instruments Ltd - © Copyright 2008

### Sample Details

**Sample Name:** 16923-06 1  
**File Name:** Ocak-Mayis 2016.dts  
**SOP Name:** mansettings.dat  
**Measurement Date and Time:** 05 Nisan 2016 Salı 12:04:38

**Z-Average (nm):** 9,628921      **Derived Count Rate (kcps):** 124,31368255...  
**Standard Deviation (nm):** 0      **Standard Deviation (kc...)** 0  
**%Std Deviation:** 0      **%Std Deviation:** 0  
**Variance:** 0      **Variance:** 0

Size d.nm	Mean Volume %	Std Dev Volume %	Size d.nm	Mean Volume %	Std Dev Volume %	Size d.nm	Mean Volume %	Std Dev Volume %	Size d.nm	Mean Volume %	Std Dev Volume %
0,4000	0,0		5,615	3,9		78,82	0,0		1106	0,0	
0,4632	0,0		6,503	2,1		91,28	0,0		1281	0,0	
0,5365	0,0		7,531	1,1		105,7	0,0		1484	0,0	
0,6213	0,0		8,721	0,5		122,4	0,0		1718	0,0	
0,7195	0,0		10,10	0,2		141,8	0,0		1990	0,0	
0,8332	0,0		11,70	0,1		164,2	0,0		2305	0,0	
0,9649	0,0		13,54	0,0		190,1	0,0		2669	0,0	
1,117	0,0		15,69	0,0		220,2	0,0		3091	0,0	
1,294	0,1		18,17	0,0		255,0	0,0		3580	0,0	
1,499	1,5		21,04	0,0		295,3	0,0		4145	0,0	
1,736	5,6		24,36	0,0		342,0	0,0		4801	0,0	
2,010	10,8		28,21	0,0		396,1	0,0		5560	0,0	
2,328	14,6		32,67	0,0		458,7	0,0		6439	0,0	
2,696	16,0		37,84	0,0		531,2	0,0		7456	0,0	
3,122	15,1		43,82	0,0		615,1	0,0		8635	0,0	
3,615	12,5		50,75	0,0		712,4	0,0		1,000e4	0,0	
4,187	9,4		58,77	0,0		825,0	0,0				
4,849	6,3		68,06	0,0		955,4	0,0				



# Size Distribution Report by Volume

v2.0



Malvern Instruments Ltd - © Copyright 2008

## Sample Details

**Sample Name:** 16923-06 1 *Hydrophilic*

**SOP Name:** mansettings.dat

**General Notes:** evaporation method

**File Name:** Ocak-Mayis 2016.dts

**Dispersant Name:** Water

**Record Number:** 1340

**Dispersant RI:** 1,330

**Material RI:** 1,49

**Viscosity (cP):** 0,8852

**Material Absorbtion:** 0,00

**Measurement Date and Time:** 05 Nisan 2016 Salı 12:04:...

## System

**Temperature (°C):** 24,9

**Duration Used (s):** 80

**Count Rate (kcps):** 124,3

**Measurement Position (mm):** 4,65

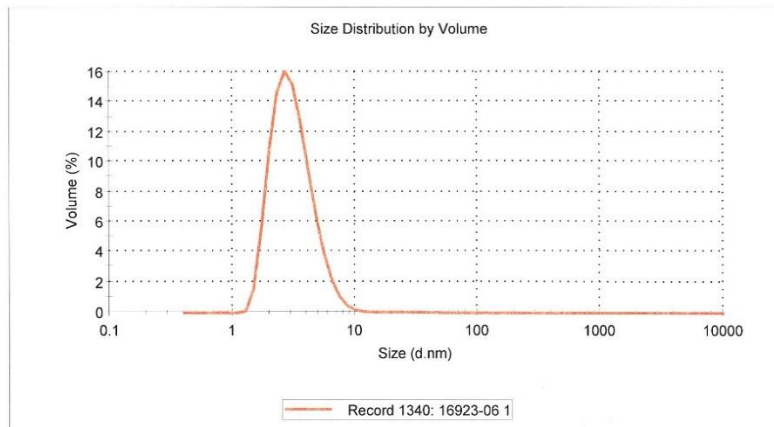
**Cell Description:** Disposable sizing cuvette

**Attenuator:** 11

## Results

	Diam. (nm)	% Volume	Width (nm)
<b>Z-Average (d.nm):</b> 9,629	<b>Peak 1:</b> 23,83	0,3	10,17
<b>Pdl:</b> 0,568	<b>Peak 2:</b> 3,250	99,7	1,319
<b>Intercept:</b> 0,957	<b>Peak 3:</b> 0,000	0,0	0,000

**Result quality** **Good**



- 1% H30 + 1% NaCl



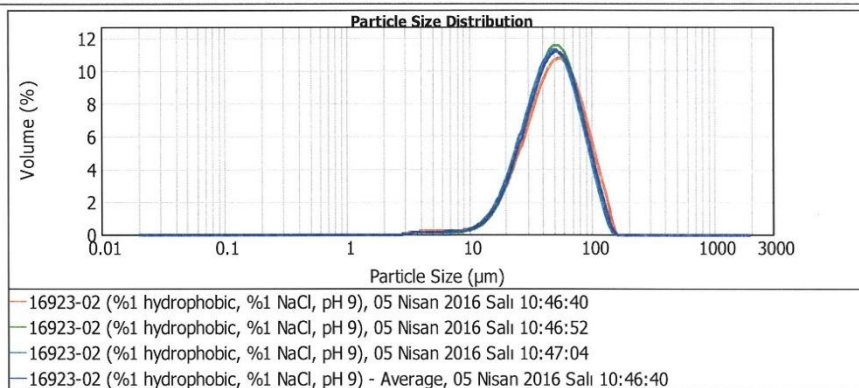
### Result Analysis Report

**Sample Name:** 16923-02 (%1 hydrophobic, %1 NaCl)  
**SOP Name:**  
**Measured:** 05 Nisan 2016 Salı 10:46:40  
**Sample Source & type:** TP AR-GE Merkezi  
**Measured by:** PBA  
**Analysed:** 05 Nisan 2016 Salı 10:46:41  
**Sample bulk lot ref:**  
**Result Source:** Averaged

**Particle Name:** Silica  
**Accessory Name:** Hydro 2000S (A)  
**Analysis model:** General purpose  
**Sensitivity:** Normal  
**Particle RI:** 1.487  
**Absorption:** 0  
**Size range:** 0.020 to 2000.000  $\mu\text{m}$   
**Obscuration:** 3.03 %  
**Dispersant Name:** Water  
**Dispersant RI:** 1.330  
**Weighted Residual:** 0.625 %  
**Result Emulation:** Off

**Concentration:** 0.0163 %Vol  
**Span :** 1.417  
**Uniformity:** 0.436  
**Result units:** Volume  
**Specific Surface Area:** 0.156  $\text{m}^2/\text{g}$   
**Surface Weighted Mean D[3,2]:** 38.505  $\mu\text{m}$   
**Vol. Weighted Mean D[4,3]:** 53.486  $\mu\text{m}$

**d(0.1):** 22.965  $\mu\text{m}$       **d(0.5):** 48.608  $\mu\text{m}$       **d(0.9):** 91.856  $\mu\text{m}$



Size ( $\mu\text{m}$ )	Volume In %	Size ( $\mu\text{m}$ )	Volume In %	Size ( $\mu\text{m}$ )	Volume In %	Size ( $\mu\text{m}$ )	Volume In %	Size ( $\mu\text{m}$ )	Volume In %	Size ( $\mu\text{m}$ )	Volume In %
0.010	0.00	1.096	0.00	11.482	0.54	120.226	1.74	1258.925	0.00		
0.011	0.00	1.259	0.00	13.183	0.54	138.038	0.38	1445.440	0.00		
0.013	0.00	1.445	0.00	15.136	0.90	158.489	0.00	1659.587	0.00		
0.015	0.00	1.660	0.00	17.378	1.44	181.970	0.00	1905.461	0.00		
0.017	0.00	1.905	0.00	19.953	2.22	208.930	0.00	2187.762	0.00		
0.020	0.00	2.188	0.00	22.909	3.23	239.893	0.00	2511.886	0.00		
0.023	0.00	2.512	0.00	26.303	4.47	275.423	0.00	2884.032	0.00		
0.026	0.00	2.884	0.00	30.200	5.85	316.228	0.00	3311.311	0.00		
0.030	0.00	3.311	0.04	34.674	7.26	363.078	0.00	3801.894	0.00		
0.035	0.00	3.802	0.09	39.811	8.54	416.869	0.00	4365.158	0.00		
0.040	0.00	4.365	0.14	45.709	9.52	478.630	0.00	5011.872	0.00		
0.046	0.00	5.012	0.15	52.481	10.04	549.541	0.00	5754.399	0.00		
0.052	0.00	5.754	0.16	60.256	9.98	630.957	0.00	6606.934	0.00		
0.060	0.00	6.607	0.16	69.183	8.17	724.436	0.00	7585.776	0.00		
0.069	0.00	7.586	0.17	79.433	6.62	831.764	0.00	8709.636	0.00		
0.079	0.00	8.710	0.22	91.201	4.93	954.993	0.00	10000.000	0.00		
0.091	0.00	10.000	0.33	104.713	3.26	1096.478	0.00				
0.105	0.00	11.482	0.33	120.226	3.26	1258.925	0.00				

Operator notes:

• 2% H3O

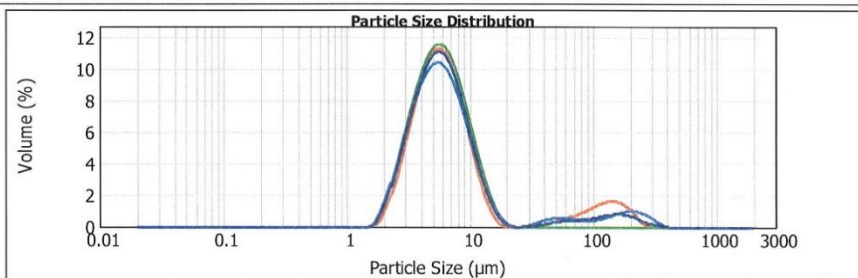


### Result Analysis Report

**Sample Name:** 16923-04 (%2 hydrophobic) - Average  
**SOP Name:**  
**Measured:** 05 Nisan 2016 Sali 11:11:04  
**Sample Source & type:** TP AR-GE Merkezi  
**Measured by:** PBA  
**Analysed:** 05 Nisan 2016 Sali 11:11:05  
**Sample bulk lot ref:**  
**Result Source:** Averaged

<b>Particle Name:</b> Silica	<b>Accessory Name:</b> Hydro 2000S (A)	<b>Analysis model:</b> General purpose	<b>Sensitivity:</b> Normal
<b>Particle RI:</b> 1.487	<b>Absorption:</b> 0	<b>Size range:</b> 0.020 to 2000.000 $\mu\text{m}$	<b>Obscuration:</b> 1.36 %
<b>Dispersant Name:</b> Water	<b>Dispersant RI:</b> 1.330	<b>Weighted Residual:</b> 1.912 %	<b>Result Emulation:</b> Off
<b>Concentration:</b> 0.0008 %Vol	<b>Span :</b> 1.737	<b>Uniformity:</b> 1.94	<b>Result units:</b> Volume
<b>Specific Surface Area:</b> 1.13 $\text{m}^2/\text{g}$	<b>Surface Weighted Mean D[3,2]:</b> 5.332 $\mu\text{m}$	<b>Vol. Weighted Mean D[4,3]:</b> 15.353 $\mu\text{m}$	

d(0.1): 3.028  $\mu\text{m}$       d(0.5): 5.825  $\mu\text{m}$       d(0.9): 13.147  $\mu\text{m}$

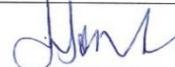
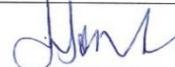
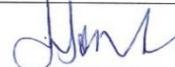


— 16923-04 (%2 hydrophobic), 05 Nisan 2016 Sali 11:11:04  
 — 16923-04 (%2 hydrophobic), 05 Nisan 2016 Sali 11:11:16  
 — 16923-04 (%2 hydrophobic), 05 Nisan 2016 Sali 11:11:28  
 — 16923-04 (%2 hydrophobic) - Average, 05 Nisan 2016 Sali 11:11:04

Size ( $\mu\text{m}$ )	Volume In %	Size ( $\mu\text{m}$ )	Volume In %	Size ( $\mu\text{m}$ )	Volume In %	Size ( $\mu\text{m}$ )	Volume In %	Size ( $\mu\text{m}$ )	Volume In %	Size ( $\mu\text{m}$ )	Volume In %
0.010	0.00	0.105	0.00	1.096	0.00	11.482	0.56	120.225	0.00	1258.925	0.00
0.011	0.00	0.120	0.00	1.259	0.00	13.183	3.10	138.038	0.71	1445.440	0.00
0.013	0.00	0.138	0.00	1.445	0.00	15.136	1.80	158.469	0.72	1659.587	0.00
0.015	0.00	0.158	0.00	1.660	0.01	17.378	0.87	181.970	0.65	1905.461	0.00
0.017	0.00	0.182	0.00	1.905	0.38	19.953	0.30	208.930	0.51	2187.762	0.00
0.020	0.00	0.209	0.00	2.188	1.27	22.909	0.04	239.883	0.31	2511.886	0.00
0.023	0.00	0.240	0.00	2.512	2.52	26.303	0.00	275.423	0.19	2894.032	0.00
0.026	0.00	0.275	0.00	2.884	4.03	30.200	0.01	316.228	0.07	3311.311	0.00
0.030	0.00	0.316	0.00	3.311	5.65	34.674	0.05	363.078	0.01	3801.894	0.00
0.035	0.00	0.363	0.00	3.802	7.22	39.811	0.10	416.869	0.01	4365.158	0.00
0.040	0.00	0.417	0.00	4.365	8.55	45.709	0.20	478.630	0.00	5011.872	0.00
0.046	0.00	0.479	0.00	5.012	9.52	52.481	0.27	549.541	0.00	5754.399	0.00
0.052	0.00	0.550	0.00	5.754	9.98	60.256	0.32	630.957	0.00	6606.934	0.00
0.060	0.00	0.631	0.00	6.607	9.86	69.183	0.35	724.436	0.00	7585.776	0.00
0.069	0.00	0.724	0.00	7.586	9.13	79.433	0.37	831.764	0.00	8709.636	0.00
0.079	0.00	0.832	0.00	8.710	7.88	91.201	0.41	954.993	0.00	10000.000	0.00
0.091	0.00	0.955	0.00	10.000	6.32	104.713	0.47	1096.478	0.00		
0.105	0.00	1.096	0.00	11.482	4.65	120.225	0.56	1258.925	0.00		

Operator notes:

## D. Test Report of the XRF

	<b>TP AR-GE MERKEZİ ÜRETİM TEKNOLOJİSİ MÜDÜRLÜĞÜ ANALİZ RAPORU</b>							
		08-17						
<b>Numune Kodu</b>	: 17.02.078							
<b>Numunenin Üniteye Geliş Tarihi</b>	: 18.08.2017							
<b>Yapılan Analiz(ler)</b>	: Sıvı numunelerde XRF element analizi.							
<b>Analizin Yapıldığı Tarih</b>	: 18.08.2017							
<b><u>XRF ANALİZ SONUÇLARI</u></b>								
Nano çözelti tapa giriş numunesi								
<table border="1"><thead><tr><th>Element</th><th>Konsantrasyon (% ağırlık)</th></tr></thead><tbody><tr><td>Si</td><td>0,5791</td></tr></tbody></table>			Element	Konsantrasyon (% ağırlık)	Si	0,5791		
Element	Konsantrasyon (% ağırlık)							
Si	0,5791							
Nano çözelti tapa çıkış numunesi								
<table border="1"><thead><tr><th>Element</th><th>Konsantrasyon (% ağırlık)</th></tr></thead><tbody><tr><td>Si</td><td>0,5991</td></tr></tbody></table>			Element	Konsantrasyon (% ağırlık)	Si	0,5991		
Element	Konsantrasyon (% ağırlık)							
Si	0,5991							
<table border="1"><thead><tr><th>ANALİZİN YAPILDIĞI ÜNİTE</th><th>YAZAN</th><th>ONAYLAYAN</th></tr></thead><tbody><tr><td>ÜRETİM TEKNOLOJİSİ MÜDÜRLÜĞÜ</td><td> İrem Yaşar AKSU Mühendis</td><td> Selçuk SALDI Ünite Müdürü</td></tr></tbody></table>			ANALİZİN YAPILDIĞI ÜNİTE	YAZAN	ONAYLAYAN	ÜRETİM TEKNOLOJİSİ MÜDÜRLÜĞÜ	 İrem Yaşar AKSU Mühendis	 Selçuk SALDI Ünite Müdürü
ANALİZİN YAPILDIĞI ÜNİTE	YAZAN	ONAYLAYAN						
ÜRETİM TEKNOLOJİSİ MÜDÜRLÜĞÜ	 İrem Yaşar AKSU Mühendis	 Selçuk SALDI Ünite Müdürü						
1/3								

## E. Oil Recovery Test Results

- Recovery Test Results with CC301 Dispersion

Application	Run	Fluid	Time, min	Flow Rate, cc/min	Cum. pumped, cc	Pore volume	Production, cc	Recovery, %OOIP
600 psi CO <sub>2</sub> Injection					0	0.00	0.0	0.0
					22	0.16	4.0	3.2
					50	0.36	8.0	6.4
					250	1.81	25.0	20.1
					500	3.61	31.0	24.9
					980	7.08	33.5	26.9
					1030	7.44	34.1	27.4
					1080	7.80	34.8	27.9
					1100	7.94	35.0	28.1
WAG	1	water	30	0.25	1107.5	8.00	35.0	28.1
		water	30	0.25	1115	8.05	36.0	28.9
		water	30	0.25	1122.5	8.11	40.0	32.1
		water	20	0.25	1127.5	8.14	46.0	36.9
	2	CO <sub>2</sub>	30	0.25	1135	8.20	46.0	36.9
		CO <sub>2</sub>	30	0.25	1142.5	8.25	46.0	36.9
		CO <sub>2</sub>	30	0.25	1150	8.30	46.0	36.9
		CO <sub>2</sub>	20	0.25	1155	8.34	46.0	36.9
	3	water	30	0.25	1162.5	8.39	46.0	36.9
		water	30	0.25	1170	8.45	47.0	37.7
		water	30	0.25	1177.5	8.50	49.0	39.3
		water	20	0.25	1182.5	8.54	50.0	40.1
	4	CO <sub>2</sub>	30	0.25	1190	8.59	50.0	40.1
		CO <sub>2</sub>	30	0.25	1197.5	8.65	50.0	40.1
		CO <sub>2</sub>	30	0.25	1205	8.70	50.0	40.1
		CO <sub>2</sub>	20	0.25	1210	8.74	50.2	40.3
	5	water	30	0.25	1217.5	8.79	50.3	40.4
		water	30	0.25	1225	8.85	51.3	41.2
		water	30	0.25	1232.5	8.90	52.5	42.1
		water	20	0.25	1237.5	8.94	53.5	42.9
	6	CO <sub>2</sub>	30	0.25	1245	8.99	53.5	42.9
		CO <sub>2</sub>	30	0.25	1252.5	9.04	53.5	42.9
		CO <sub>2</sub>	30	0.25	1260	9.10	54.0	43.3
		CO <sub>2</sub>	20	0.25	1265	9.13	54.0	43.3
	7	water	30	0.25	1272.5	9.19	54.0	43.3
		water	30	0.25	1280	9.24	55.3	44.4
		water	30	0.25	1287.5	9.30	55.5	44.5
		water	20	0.25	1292.5	9.33	55.5	44.5

	8	CO <sub>2</sub>	30	0.25	1300	9.39	55.5	44.5
		CO <sub>2</sub>	30	0.25	1307.5	9.44	55.6	44.6
		CO <sub>2</sub>	30	0.25	1315	9.50	55.6	44.6
		CO <sub>2</sub>	20	0.25	1320	9.53	55.7	44.7
	9	water	30	0.25	1327.5	9.59	56.2	45.1
		water	30	0.25	1335	9.64	56.8	45.6
		water	30	0.25	1342.5	9.69	56.8	45.6
		water	20	0.25	1347.5	9.73	56.8	45.6
	10	CO <sub>2</sub>	30	0.25	1355	9.78	56.8	45.6
		CO <sub>2</sub>	30	0.25	1362.5	9.84	56.8	45.6
		CO <sub>2</sub>	30	0.25	1370	9.89	56.8	45.6
		CO <sub>2</sub>	20	0.25	1375	9.93	56.8	45.6
	11	water	30	0.25	1382.5	9.98	56.8	45.6
		water	30	0.25	1390	10.04	57.0	45.7
		water	30	0.25	1397.5	10.09	57.0	45.7
		water	20	0.25	1402.5	10.13	57.0	45.7
12	CO <sub>2</sub>	30	0.25	1410	10.18	57.0	45.7	
	CO <sub>2</sub>	30	0.25	1417.5	10.24	57.1	45.8	
	CO <sub>2</sub>	30	0.25	1425	10.29	57.1	45.8	
	CO <sub>2</sub>	20	0.25	1430	10.33	57.1	45.8	
NWAG	1	Nano	30	0.25	1437.5	10.38	57.1	45.8
		Nano	30	0.25	1445	10.43	57.1	45.8
		Nano	30	0.25	1452.5	10.49	57.3	46.0
		Nano	20	0.25	1457.5	10.52	57.4	46.1
	2	CO <sub>2</sub>	30	0.25	1465	10.58	57.4	46.1
		CO <sub>2</sub>	30	0.25	1472.5	10.63	57.4	46.1
		CO <sub>2</sub>	30	0.25	1480	10.69	57.4	46.1
		CO <sub>2</sub>	20	0.25	1485	10.72	57.4	46.1
	3	Nano	30	0.25	1492.5	10.78	57.4	46.1
		Nano	30	0.25	1500	10.83	57.5	46.1
		Nano	30	0.25	1507.5	10.89	57.5	46.1
		Nano	20	0.25	1512.5	10.92	57.5	46.1
	4	CO <sub>2</sub>	30	0.25	1520	10.98	57.5	46.1
		CO <sub>2</sub>	30	0.25	1527.5	11.03	57.5	46.1
		CO <sub>2</sub>	30	0.25	1535	11.08	57.5	46.1
		CO <sub>2</sub>	20	0.25	1540	11.12	57.5	46.1
	5	Nano	30	0.25	1547.5	11.17	57.5	46.1
		Nano	30	0.25	1555	11.23	57.5	46.1
		Nano	30	0.25	1562.5	11.28	57.5	46.1
		Nano	20	0.25	1567.5	11.32	57.5	46.1
	6	CO <sub>2</sub>	30	0.25	1575	11.37	57.5	46.1
		CO <sub>2</sub>	30	0.25	1582.5	11.43	57.5	46.1
		CO <sub>2</sub>	30	0.25	1590	11.48	57.5	46.1
		CO <sub>2</sub>	20	0.25	1595	11.52	57.5	46.1

Foam	Nano dispersion+ CO <sub>2</sub>	1655	11.95	61.0	48.9
		1845	13.32	70.0	56.2
		2095	15.13	83.5	67.0
		2345	16.93	86.5	69.4
		2595	18.74	88.5	71.0
		2795	20.18	89.0	71.4
		2895	20.90	89.5	71.8
		2995	21.63	89.5	71.8

- **Recovery Test Results with PEG Dispersion**

Application	Run	Fluid	Time, min	Flow rate, cc/min	Cum. pumped, cc	Pore Volume	Production, cc	Recovery, %OOIP
600 psi CO <sub>2</sub> Injection		CO <sub>2</sub>			0	0.00	0	0.00
		CO <sub>2</sub>			22	0.16	0	0.00
		CO <sub>2</sub>			50	0.36	1	1.08
		CO <sub>2</sub>			250	1.81	8	8.61
		CO <sub>2</sub>			500	3.61	13	13.99
		CO <sub>2</sub>			750	5.42	14.5	15.61
		CO <sub>2</sub>			1000	7.22	15	16.14
WAG	1	water	30	0.25	1007.5	7.28	15	16.14
		water	30	0.25	1015	7.33	15.5	16.68
		water	30	0.25	1022.5	7.38	16.1	17.33
		water	20	0.25	1027.5	7.42	16.9	18.19
	2	CO <sub>2</sub>	30	0.25	1035	7.47	16.9	18.19
		CO <sub>2</sub>	30	0.25	1042.5	7.53	16.9	18.19
		CO <sub>2</sub>	30	0.25	1050	7.58	17	18.30
		CO <sub>2</sub>	20	0.25	1055	7.62	17	18.30
	3	water	30	0.25	1062.5	7.67	17	18.30
		water	30	0.25	1070	7.73	17.3	18.62
		water	30	0.25	1077.5	7.78	17.8	19.16
		water	20	0.25	1082.5	7.82	18.4	19.80
	4	CO <sub>2</sub>	30	0.25	1090	7.87	18.4	19.80
		CO <sub>2</sub>	30	0.25	1097.5	7.93	18.4	19.80
		CO <sub>2</sub>	30	0.25	1105	7.98	18.7	20.13
		CO <sub>2</sub>	20	0.25	1110	8.02	19.1	20.56
	5	water	30	0.25	1117.5	8.07	19.3	20.77
		water	30	0.25	1125	8.12	19.7	21.20
		water	30	0.25	1132.5	8.18	20.2	21.74
		water	20	0.25	1137.5	8.21	20.7	22.28
6	CO <sub>2</sub>	30	0.25	1145	8.27	20.8	22.39	
	CO <sub>2</sub>	30	0.25	1152.5	8.32	20.9	22.49	

		CO <sub>2</sub>	30	0.25	1160	8.38	21	22.60
		CO <sub>2</sub>	20	0.25	1165	8.41	21.1	22.71
	7	water	30	0.25	1172.5	8.47	21.3	22.93
		water	30	0.25	1180	8.52	21.6	23.25
		water	30	0.25	1187.5	8.57	21.8	23.46
		water	20	0.25	1192.5	8.61	22.1	23.79
	8	CO <sub>2</sub>	30	0.25	1200	8.67	22.1	23.79
		CO <sub>2</sub>	30	0.25	1207.5	8.72	22.3	24.00
		CO <sub>2</sub>	30	0.25	1215	8.77	22.5	24.22
		CO <sub>2</sub>	20	0.25	1220	8.81	22.5	24.22
	9	water	30	0.25	1227.5	8.86	22.7	24.43
		water	30	0.25	1235	8.92	22.8	24.54
		water	30	0.25	1242.5	8.97	23	24.76
		water	20	0.25	1247.5	9.01	23.1	24.86
	10	CO <sub>2</sub>	30	0.25	1255	9.06	23.1	24.86
		CO <sub>2</sub>	30	0.25	1262.5	9.12	23.2	24.97
		CO <sub>2</sub>	30	0.25	1270	9.17	23.4	25.19
		CO <sub>2</sub>	20	0.25	1275	9.21	23.4	25.19
	11	water	30	0.25	1282.5	9.26	23.4	25.19
		water	30	0.25	1290	9.32	23.4	25.19
water		30	0.25	1297.5	9.37	23.5	25.29	
water		20	0.25	1302.5	9.41	23.5	25.29	
12	CO <sub>2</sub>	30	0.25	1310	9.46	23.5	25.29	
	CO <sub>2</sub>	30	0.25	1317.5	9.51	23.5	25.29	
	CO <sub>2</sub>	30	0.25	1325	9.57	23.6	25.40	
	CO <sub>2</sub>	20	0.25	1330	9.60	23.6	25.40	
NWAG	1	Nano	30	0.25	1337.5	9.66	23.6	25.40
		Nano	30	0.25	1345	9.71	23.6	25.40
		Nano	30	0.25	1352.5	9.77	23.7	25.51
		Nano	20	0.25	1357.5	9.80	23.7	25.51
	2	CO <sub>2</sub>	30	0.25	1365	9.86	23.7	25.51
		CO <sub>2</sub>	30	0.25	1372.5	9.91	23.7	25.51
		CO <sub>2</sub>	30	0.25	1380	9.97	23.8	25.62
		CO <sub>2</sub>	20	0.25	1385	10.00	23.8	25.62
	3	Nano	30	0.25	1392.5	10.06	23.9	25.72
		Nano	30	0.25	1400	10.11	24	25.83
		Nano	30	0.25	1407.5	10.16	24.1	25.94
		Nano	20	0.25	1412.5	10.20	24.3	26.15
	4	CO <sub>2</sub>	30	0.25	1420	10.25	24.3	26.15
		CO <sub>2</sub>	30	0.25	1427.5	10.31	24.4	26.26
		CO <sub>2</sub>	30	0.25	1435	10.36	24.4	26.26
		CO <sub>2</sub>	20	0.25	1440	10.40	24.4	26.26
	5	Nano	30	0.25	1447.5	10.45	24.6	26.48
		Nano	30	0.25	1455	10.51	24.9	26.80

		Nano	30	0.25	1462.5	10.56	25	26.91
		Nano	20	0.25	1467.5	10.60	25.1	27.02
	6	CO <sub>2</sub>	30	0.25	1475	10.65	25.2	27.12
		CO <sub>2</sub>	30	0.25	1482.5	10.71	25.4	27.34
		CO <sub>2</sub>	30	0.25	1490	10.76	25.7	27.66
		CO <sub>2</sub>	20	0.25	1495	10.80	25.7	27.66
		Nano	30	0.25	1502.5	10.85	25.8	27.77
	7	Nano	30	0.25	1510	10.90	26	27.98
		Nano	30	0.25	1517.5	10.96	26.3	28.31
		Nano	20	0.25	1522.5	10.99	26.5	28.52
		CO <sub>2</sub>	30	0.25	1530	11.05	26.6	28.63
	8	CO <sub>2</sub>	30	0.25	1537.5	11.10	26.8	28.85
		CO <sub>2</sub>	30	0.25	1545	11.16	26.9	28.95
		CO <sub>2</sub>	20	0.25	1550	11.19	26.9	28.95
		Nano	30	0.25	1557.5	11.25	27	29.06
	9	Nano	30	0.25	1565	11.30	27.1	29.17
		Nano	30	0.25	1572.5	11.36	27.2	29.28
		Nano	20	0.25	1577.5	11.39	27.3	29.38
		CO <sub>2</sub>	30	0.25	1585	11.45	27.3	29.38
	10	CO <sub>2</sub>	30	0.25	1592.5	11.50	27.3	29.38
		CO <sub>2</sub>	30	0.25	1600	11.55	27.4	29.49
		CO <sub>2</sub>	20	0.25	1605	11.59	27.4	29.49
						1825	13.18	27.4
1200 psi CO <sub>2</sub> Injection		CO <sub>2</sub>			2100	15.16	28.5	30.67
					2500	18.05	28.6	30.78
					2700	19.50	28.6	30.78
Foam		Nano dispersiyon+ CO <sub>2</sub>			2800	20.22	29.9	32.18
					2900	20.94	31.4	33.80
					3000	21.66	32.2	34.66
					3100	22.39	33	35.52
					3200	23.11	33.8	36.38
					3300	23.83	34.2	36.81
					3400	24.55	34.5	37.13

## CURRICULUM VITAE

### PERSONAL INFORMATION

Surname, Name : Safran, Saibe Esra  
Nationality : Turkish (TC)  
Date and Place of Birth : 13 Oct 1984  
Phone : +90 5412531811  
E-mail : e183746@metu.edu.tr

### EDUCATION

Degree	Institution	Year of Graduation
ME	Stevens Ins.of Tech. Chem. Eng.	2010
BS	Ankara Uni. Chemical Eng.	2006
High School	Niksar Daniřment Gazi Lisesi	2002

### WORK EXPERIENCE

Year	Place	Enrollment
2010-Present	TPAO Reserch Center	Senior Engineer
2006-2007	Niksar Su řiřeleme A.ř.	Quality Control Eng.
2005 Temmuz	MKE	Intern Engineering Student

### FOREIGN LANGUAGES

Advanced English

### PUBLICATIONS

- Calıřgan, H.; Karabakal, U.; Babadagli, T.; Turkmenoglu, A.; **Yildirim, S.E.**; Ercan, C; Gozel, M.E. Wettability alteration potential of caustic to improve waterflooding efficiency: a laboratory scale analysis for the Garzan field, Turkey. 20th IPETGAS Ankara. 2015
- Conference Poster: “ Evaluation of scale type in Batı Raman and Garzan field production wells and comparison of possible scale inhibitor performance” (26. National Chemistry Conference, 2012, Muęla)

### HOBBIES

Sports, Designing, Theater